NOBLE METALS IN THE RONDA AND JOSEPHINE PERIDOTITES

by

HARLAN WHEELOCK STOCKMAN

B.S. University of Rochester (1976)

SUBMITTED IN PARTIAL FULFILLMENT

OF THE REQUIREMENTS FOR THE

DEGREE OF

DOCTOR OF PHILOSOPHY

at the

MASSACHUSETTS INSTITUTE OF TECHNOLOGY

Signature of Author.....
Department of Earth and Planetary Sciences
March 15, 1982

Certified by.....
Thesis Supervisor

Accepted by.....
Chairman, Department Committee on Graduate Students

TABLE OF CONTENTS

LIST OF FIGURES

LIST OF TABLES

NOBLE METALS IN THE RONDA AND JOSEPHINE PERIDOTITES

by

HARLAN WHEELOCK STOCKMAN

Submitted to the Department of Earth and Planetary Sciences on March 15, 1982 in partial fulfillment of the requirements for the Degree of Doctor of Philosophy in Geochemistry

ABSTRACT

A sensitive and accurate radiochemical neutron activation technique, based on a rapid tellurium coprecipitation, has been developed for analysis of Au, Pd, Pt, and Ir at the part-per-billion level in ultramafic and mafic rocks. The technique has been used to analyze whole rock samples from the Ronda Ultramafic Complex in Spain, and the Josephine Peridotite in Oregon.

In both the Ronda and Josephine peridotites, which are interpreted as residues after partial melting, Pd and Au abundances correlate positively with abundances of incompatible elements such as Ca and Sc, whereas Ir abundances show no systematic variation with abundances of incompatible elements. Platinum shows a weak positive correlation with incompatible elements in the Ronda peridotites, and possibly in the Josephine peridotites. Overall, Pd, Au, and possibly Pt were enriched in the melts relative to Ir during partial melting of the Ronda and Josephine peridotites. Sulfide was probably the host of the noble metals at temperatures below the silicate solidus, but it is doubtful that the peridotites were saturated with sulfide during extensive (> 1%) partial melting. The average noble metal abundances in the most Ca-and Sc-rich peridotites from both bodies are ca. 10^{-2}x the abundances in C1 carbonaceous chondrites.

In the Ronda mafic layers, which are interpreted as accumulates of partial melts ascending through the mantle, Pd and Au correlate positively with Cr and Ni, and may have

been removed from the partial melts as a consequence of sulfide precipitation. Chromitites from the Josephine Peridotite, also interpreted as accumulates of partial melts, have high Ir contents and high (Ir+Pt)/(Pd+Au), which suggest that chromite precipitation may be important in depleting Ir from partial melts and in fractionating the noble metals.

The Ir-rich Josephine chromitites contain platinum group minerals rich in Ir, Pt, Ru, and Os, which account for at least 30% of the whole rock Ir content. Electron microprobe and scanning electron microscope studies allow two types of chromitite platinum group minerals to be distinguished. Type 1 platinum group minerals are alloys, sulfides, and arsenides which appear to have formed at the same time as the chromitites, possibly by direct precipitation from silicate-sulfide melts, at conditions of relatively high sulfur activity. Type 2 platinum group minerals are alloys which appear to have formed by desulfuration of type 1 sulfides at late-stage conditions of low sulfur activity, possibly during serpentinization. The platinum group mineral-rich chromitites may be sources of some of the platinum group minerals found in placers of the Josephine Peridotite.

Thesis supervisor: Dr. Frederick A. Frey
Title: Professor of Geochemistry

CHAPTER I: INTRODUCTION

The noble metals are the six platinum group elements (Ru, Rh, Pd, Os, Ir, and Pt) and Au. These elements are said to be "noble," because in the metallic state they are relatively inert to corrosion, and are not easily oxidized. The noble metals generally occur in the earth's crust and upper mantle at part-per-billion levels, though Os and Ir may be as low as part-per-trillion levels in basalts and granites, and all the noble metals may reach part-per-million levels in ore deposits (Crocket et al., 1968; Crocket, 1979; Hertogen et al., 1980). Geochemically, the noble metals have been considered to be siderophilic, and to a lesser extent, chalcophilic (Arculus and Delano, 1981). Rhenium is considered to be a noble metal by some cosmochemists (e.g., Chou, 1978); however, Re differs from the noble metals in forming stable oxyanions (e.g., ReO_4^-, $ReO_4^=$; Cotton and Wilkinson, 1972) at relatively low oxygen activities, and Re shows little coherence with the noble metals in terrestrial environments (Noddack and Noddack, 1931).

Most studies of noble metal geochemistry have been restricted to unusual rock types, such as ore deposits (see, e.g., Economic Geology, volume 71, 1976). There are relatively few studies of noble metals in typical crustal and mantle rocks (Crocket, 1979), and the noble metals remain one of the least understood geochemical groups.

I-1: THREE PROBLEMS OF NOBLE METAL GEOCHEMISTRY

The data and interpretations presented in this thesis relate directly to the following three problems of noble metal geochemistry.

Mantle abundances of noble metals

Estimates of mantle noble metal abundances have been important in theories of core-mantle separation and the nature of the earth's core (Chou, 1978; Arculus and Delano, 1981). It has been claimed that the mantle noble metal ratios are "chondritic" (Arculus and Delano, 1981). However, the mantle noble metal abundances are not well-known. Estimates of mantle noble metal abundances have been derived largely from analyses of peridotitic nodules in kimberlites and basanites (Paul et al., 1979; Morgan et al., 1980; Mitchell and Keays, 1981). The nodule analyses show large variations, both in noble metal ratios and absolute abundances; for example, reported averages of nodule analyses vary from 0.5 to 6.2 ppb for Au, and from 0.56 to 1.5 for Pd/Ir (Jagoutz et al., 1979; Paul et al., 1979; Morgan et al., 1980). The variations among individual nodule noble metal analyses are far greater, covering several orders of magnitude (Paul et al., 1979); this large dispersion has been attributed both to mantle heterogeneity (Paul et al., 1979) and to mantle metasomatism and low-temperature alteration (Morgan et al., 1980). Alpine ultramafic bodies may provide better estimates of mantle noble metal abundances,

but there are very few accurate and sensitive noble metal analyses for these rocks (Crocket, 1979).

Mantle-basalt fractionation of noble metals

The noble metal abundance patterns of basalts are quite different from those of mantle peridotites. This point is illustrated in figure I-1, in which chondrite-normalized noble metal abundances of basalts and peridotites have been plotted versus the noble metals arranged in order of decreasing metal melting temperatures. If, as is commonly supposed, basalts are derived by partial melting of the mantle (Ringwood, 1975), some fractionation of the refractory noble metals (Os and Ir) from the less-refractory noble metals (Pd and Au) must have taken place, either during partial melting or during a subsequent process such as fractional crystallization (Hertogen et al., 1980). However, previous studies have not indicated what processes are actually responsible for the observed fractionation.

Formation of platinum group minerals in the mantle

Platinum group minerals (PGMs) are found in placers of mantle-derived alpine ultramafics throughout the world (Cabri and Harris, 1975). The PGMs have apparently been derived from the mantle rocks, but origin of PGMs in the mantle is not well understood. It has been suggested that some PGMs represent inert, "primitive" minerals remaining in the mantle since accretion of the earth (Bird and Bassett, 1980); however, Os isotopic studies on some PGMs

Figure I-1: A comparison of the abundances of noble metals in basalts and mantle peridotites. The range for peridotites is derived from the average of analyses of the Mt. Albert alpine peridotite by Crocket and Chyi (1972), the lherzolite nodule averages of Mitchell and Keays (1980) and Morgan et al. (1980), and the range of Pt values reported for the U.S.G.S. standard PCC-1 (Ahmad et al. 1977). The continental basalt average is from Paul et al. (1979) and Hertogen et al. (1980). The values for W-1, a diabase, are from Ahmad et al. (1977). All abundances are normalized to the C1-chondrite averages of Crocket et al. (1967).

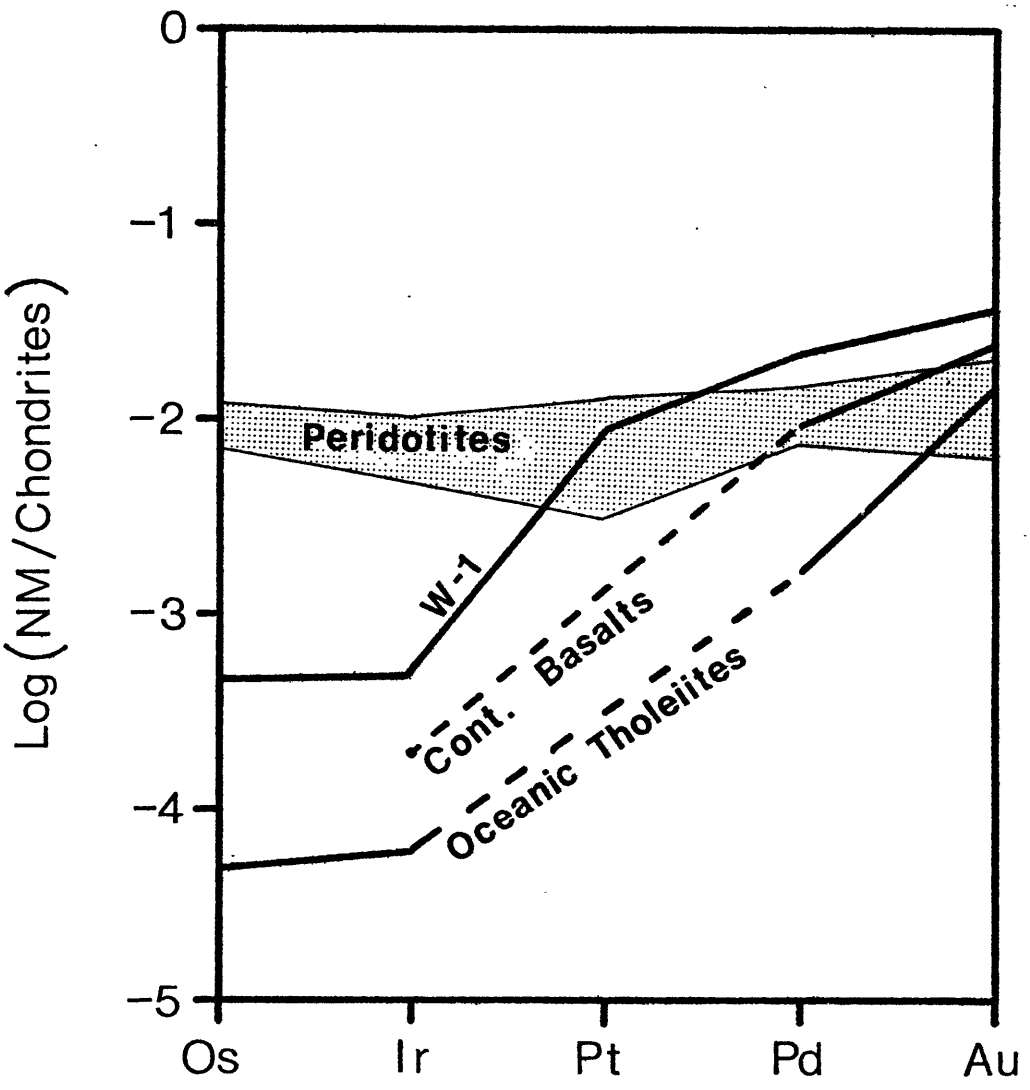
0
-1
-2
-3
-4
-5
Log (NM/Chondrites)
Peridotites
W-1
Cont. Basalts
Oceanic Tholeiites
Os
Ir
Pt
Pd
Au

suggest formation near the time of emplacement of the ultramafic bodies (Allegre and Luck, 1980). Furthermore, the high solubilities of platinum group elements in base metal sulfides suggests that in most mantle rocks the platinum group elements should be dissolved in the base metal sulfides, and should not form discrete PGMs. It is possible that PGMs form under relatively unusual conditions in the mantle, but at present, the conditions for formation of PGMs are not known.

I-2: OBJECTIVE AND PLAN OF THIS WORK

The objective of this thesis is to obtain information toward the solution of the three problems outlined in section I-1. This information consists of noble metal analyses and mineralogical studies of rocks from two large alpine ultramafic bodies; the Ronda Ultramafic Complex in Spain, and the Josephine Peridotite in Oregon. These bodies are interpreted to contain residual peridotites remaining after partial melting of the mantle, as well as accumulates or precipitates of the partial melts (Obata, 1980; Dick, 1977).

This thesis contains 5 chapters. Chapter II details the development of an analytical technique suitable for analyses of noble metals at the part-per-billion level. Whole-rock noble metal analyses for the Ronda and Josephine bodies are presented, along with analyses of other elements in Chapter III, and the data are interpreted in terms of partial melting and fractional crystallization processes in

the mantle. Chapter IV contains a detailed mineralogical description of the first reported occurrence of PGMs *in situ* in the Josephine Peridotite, and some speculations on the origin of these minerals. Chapter V provides a summary and overview of this study.

The remainder of Chapter I is devoted to a review and discussion of the geochemical properties of the noble metals.

I-3: GEOCHEMICAL BEHAVIOUR OF NOBLE METALS IN THE MANTLE

Several attempts have been made to predict the geochemical behaviour of the noble metals on the basis of crystal chemical and thermodynamic arguments (Crocket, 1969; Keays and Crocket, 1970; Hertogen *et al.*, 1980; Arculus and Delano, 1981). At present, there is no consensus in the literature as to what factors control noble metal geochemistry. This section contains a review of the crystal chemical properties of noble metals and the stability of noble metal compounds, as well as some speculations about the behavior of noble metals under mantle conditions.

Electron configurations and oxidation states

The noble metals are fourth and fifth row transition elements, so the outer electrons of noble metal ions are d electrons. The earth's mantle is probably composed of oxides (including silicates) and minor sulfides, hence the electron configurations and oxidation states of noble metals in oxides and sulfides are relevant to mantle noble metal

geochemistry. In noble metal oxides and sulfides, the common outer electron configurations and oxidation states are d^4 (Ru^{+4}, Os^{+4}), d^5 (Ru^{+3}, Os^{+3}, Rh^{+4}, Ir^{+4}), d^6 (Ru^{+2}, Os^{+2}, Rh^{+3}, Ir^{+3}, Pt^{+4}), d^7 (Rh^{+2}, Ir^{+2}, Pt^{+3} (rare)), d^8 (Rh^{+1}, Pd^{+2}, Pt^{+2}, Au^{+3}) and d^{10} (Au^{+1}) (Shannon and Prewitt, 1969; Jellinek, 1972). The noble metals are distributed among a few types of crystal sites in oxides and sulfides; virtually all the d^4, d^5, d^6, and d^7 ions are found in relatively symmetrical octahedral sites; the d^8 ions are found in square planar (Pd^{+2}, Pt^{+2}, Au^{+3}) or square pyramidal (Rh^{+1}) sites; and Au^{+1} (d^{10}) is found in linear coordination (Shannon and Prewitt, 1969; Wold, 1971; Jellinek, 1972; Muller and Roy, 1974). Some noble metals (Pd, Rh, and Pt) form metal-rich chalcogenides* with short metal-metal bonds; these compounds are probably characterized by metallic bonding, and it is doubtful that meaningful oxidation states can be assigned to the noble metals in metal-rich chalcogenides (Jellinek, 1972).

The preferences of the noble metals for different coordinations and oxidation states may be a fundamental cause of noble metal fractionation during partial melting. The elements Os, Ru, and Ir show the strongest preference for octahedral coordination; Pt and Rh show a lesser preference for octahedral coordination; and Pd and Au show a

---

* Chalcogenides are compounds of a metal with S, Se, Te, and Po.

strong preference for distorted, or unusual site geometries. Octahedral sites are abundant in the solid silicates, oxides, and sulfides which might contain noble metals in solid solution in the mantle (e.g., olivine, spinel, perovskite, and the pyrrhotite monosulfide solid solution), but the distorted or unusual site geometries are probably much more abundant in partial melts (see Burns and Fyfe, 1966 for an analogous argument applied to first row transition elements). Hence, partial melting may provide a fractionation of the noble metals such that the elements preferring distorted sites (Pd, Au, and to a lesser extent, Pt and Rh) are enriched in the melts over the elements preferring octahedral coordination.

Relative importance of silicates, oxides, sulfides, alloys, and noble metal minerals as carriers of noble metals in the mantle

There are few data on the solid solution of noble metals in silicates and oxides. The only reported natural noble metal oxides are PdO (Genser et al., 1938; considered uncertain by Cabri, 1972) and RuO_2 tentatively identified in meteorites (El Goresy et al., 1978), and the noble metals are generally considered oxyphobic (Vermaak and Hendriks, 1976). Crocket (1969) has summarized some older literature data on the occurrence of high (ppm level) platinum group element contents in oxides from pegmatites; it is not known if the platinum group elements occur in these minerals as solid solution or as PGM inclusions.

Crocket (1979) has argued that the constant orthopyroxene/plagioclase/chromite partition coefficients reported by Gijbels et al. (1974) for Os, Ir, and Ru in the Bushveld Complex suggest solid solution in these minerals; however, close examination of the data set of Gijbels et al. indicates that the reported constancy has little basis. Gijbels et al. (1974) analyzed very few sets of coexisting orthopyroxene, plagioclase, and chromite, and discarded most of these data as "anomalous"; the reported partition coefficients appear not to be derived from analyses on coexisting minerals, but rather from a computer model involving many ad hoc assumptions. Mitchell and Keays (1981) found that mantle silicates and oxides (olivine, pyroxene, garnet, and spinel) can account for no more than ca. 30% of the noble metal content of mantle nodules, and infer that these minerals are not the major carriers of noble metals in the mantle.

Ionic radii for the noble metals in oxides are poorly known. Based on data for synthetic noble metal oxides, the lower valence noble metal ions seem to be large (e.g., 1.00Å for Pd^{+2} and 1.49Å for Au^{+1} in 6-fold coordination; Muller and Roy, 1974) and on the basis of ionic radius alone, these ions might be expected to substitute for Ca^{+2} and K^{+1} (1.14Å and 1.52Å in 6-fold coordination, respectively; Muller and Roy, 1974) in oxides and silicates. The ionic radii of Pt^{+4}, Rh^{+4}, Ir^{+4}, Ru^{+4}, and Os^{+4} (0.77, 0.755, 0.76, and 0.77Å, respectively; Muller and Roy, 1974) are similar to the radii

of Ti^{+4} and Cr^{+3} in octahedral coordination (0.745 and 0.755Å; Muller and Roy, 1975), which suggests the possibility of solid solution of these noble metal ions in perovskite and spinel. Synthetic solid solutions of $CaIrO_3$ in $CaTiO_3$ (perovskite) are known (Griffith et al., 1978), as are some spinels of the form Mg_2PtO_4 (Muller and Roy, 1974). However, high oxygen fugacities are generally required to maintain noble metals in the +4 state in oxides. RuO_2 is one of the most stable noble metal +4 oxides, yet it decomposes to metal at log $F(O_2)$ = -1.3 at ca. 1,200C (calculated from data in Bergmann et al., 1970). In contrast, the oxygen fugacity of the mantle is thought to be less than or equal to the quartz-fayalite-magnetite buffer (log $f(O_2)$) = -8.5 at 1,200C; Arculus and Delano, 1981). The noble metal oxides may be more stable with respect to reduction when dissolved in mantle major element oxides (due to lowered activities), but at present the possibility of the solid solution remains moot.

In contrast to the noble metal oxides, noble metal sulfides are quite stable, and a large number of synthetic and natural noble metal sulfides* are known (Wold, 1971; Jellinek, 1972; Muller and Roy, 1974; and Cabri, 1976). In addition, the noble metals have substantial solubilities in Fe, Ni, and Cu sulfides at high temperatures. At least

---

* "Sulfide" is here used to include compounds with Se, Te, As, and Sb.

0.16 wt.% Pd and 1.1 wt.% Rh (Distler et al., 1977) and up to 10 wt.% Ru (Knop et al., 1976) may be dissolved in pentlandite at temperatures above 700C. Sulfur-rich pyrrhotites can hold up to 2.2 wt.% Pd, 9.8 wt.% Rh, 8.7 wt.% Ir, 2.1 wt.% Ru, and 0.5 wt.% Os at 760C before becoming saturated with discrete PGMs (Malevskiy et al., 1977). The solubilities of the platinum group elements in metal-rich pyrrhotites (e.g., troilite) may be much lower (Malevskiy et al., 1977), but appear to be at least 0.01 wt.% at 985C (Noddack et al., 1940). There are few unambiguous experimental data on the solubility of Au in Fe sulfides, but extensive solid solutions of Au_2S in Cu_2S are known (Atterer et al., 1954). About 1 wt.% Pt is soluble in Fe sulfide melts at 1,000C, and PdS and FeS melts are totally miscible at 1,000C (Skinner et al., 1976).

Given the high solubilities of the noble metals in solid sulfides and sulfide melts, a relatively small mantle sulfide content would be adequate to contain the noble metal content of the mantle at high temperatures, and to prevent the formation of noble metal minerals such as Pt-Fe or Os-Ir-Ru alloys. Typical mantle rocks contain 10ppb or less of each noble metal (Crocket, 1979); a reasonable minimum solubility for each noble metal in sulfide at high temperatures is 0.01 wt.%, hence 0.01 wt.% sulfide in the mantle would be adequate to contain the typical mantle noble metal content. A sulfide content of 0.01 wt.% is quite reasonable, and probably low for most mantle rocks

(MacLean, 1969); peridotite nodules average ca. 100ppm S (Morgan et al., 1980), which is equivalent to ca. 0.027% sulfide.

All the noble metals have high solubilities in Fe-Ni and Cu alloys at temperatures above 800C (Koch and Banse, 1949; Banse et al., 1951; Atterer et al., 1958; Bergmann et al., 1970; Raub and Raub, 1978; Griffith and Raub, 1980). Noddack et al. (1940) find that Fe metal/FeS partition coefficients for the platinum group elements are 10-20, and Jones and Drake (1981) find that the Fe metal/sulfide melt partition coefficients for Ir may be much greater than 1, so the platinum group elements should be enriched in any mantle base metal alloys over mantle sulfides. Base metal alloys are not known from unserpentinized alpine peridotites, but have been found in mantle nodules from kimberlites (Haggerty, 1975). However, the occurrences of base metal alloys in mantle nodules are very rare, whereas sulfides are common in the nodules (Haggerty, 1975; Bishop et al., 1975; Morgan et al. 1980); thus sulfides are probably more important as carriers of noble metals in the upper mantle.

The role of base metal sulfides as hosts of noble metals in the mantle may be altered by partial melting. Sulfur has a substantial solubility in silicate melts at high pressures and temperatures (>0.2 wt.% above 1,400C and 1 atm; Shima and Naldrett, 1975; Mysen and Popp, 1980), so that the mantle sulfide content should eventually be

consumed during partial melting. If the noble metal (base metal sulfide)/(silicate melt) partition coefficients were sufficiently high, the noble metal concentration of the sulfide would increase as the amount of sulfide decreased, and the sulfide might eventually become saturated with noble metal minerals, particularly refractory minerals such as Os-Ir-Ru alloys. At the same time, the silicate melt may become an important host of the noble metals which prefer distorted sites (i.e., Pt, Pd, and Au); the (base metal sulfide)/(silicate melt) partition coefficients for Pt and Pd are very high (>1,000; Naldrett and Duke, 1980), but silicate melts may be much more abundant than base metal sulfides during partial melting.

Summary: noble metals in the mantle

Crystal chemical considerations suggest that during melting of the mantle, a fractionation may occur such that Pd, Au, and possibly Pt and Rh are enriched in the melt phase relative to Os, Ir, and Ru. Solid solution of some noble metals in mantle oxides may be possible, though it is questionable whether the solid solutions would be stable at mantle oxygen fugacities. The high solubilities of noble metals in sulfides suggest that much of the mantle noble metal content may be in sulfides. Because of the high solubilities of noble metals in mantle sulfides, the existence of discrete noble metal minerals in the mantle is probably limited to rocks with relatively high noble

metal/sulfide ratios, i.e., rocks in which the sulfides are saturated with noble metal minerals. In particular, PGMs may form if the mantle sulfide content is depleted during partial melting.

CHAPTER II: DEVELOPMENT AND DESCRIPTION OF AN ANALYTICAL TECHNIQUE FOR Au, Pd, Pt, AND Ir

II-1: INTRODUCTION

A major purpose of this work is the examination and interpretation of noble metal variations in alpine ultramafic and associated mafic rocks. The noble metal contents of these rocks are typically very small, in the part per billion (ppb) range, so the technique employed for noble metal analyses must be very sensitive. As part of this work, a sensitive and accurate radiochemical neutron activation technique, based on classical tellurium coprecipitation methods (Feigl, 1949; Rodden, 1950; Marhenke and Sandell, 1963), was developed for analysis of Au, Pd, Pt, and Ir in rocks. Several noble metal analysis techniques may be found in the literature (see the review by Beamish and van Loon, 1972; Nadkarni and Morrison, 1974; Ahmad et al., 1977; Hoffman et al., 1978; and Page et al., 1980); however, most of these techniques involve lengthy chemical procedures and specialized equipment, or simply fail to meet the requirements of the present study.

This chapter comprises a brief description of the Te-coprecipitation technique, an evaluation of how well the technique is suited for analyses of rocks, and a detailed description of the use and development of the procedure.

II-2: BRIEF DESCRIPTION OF THE RADIOCHEMICAL TELLURIUM COPRECIPITATION TECHNIQUE

The analytical technique developed and used in this work is a carrier-based, radiochemical neutron activation technique involving a rapid group separation of Au, Pd, Pt, and Ir, followed by high-resolution Ge(Li) and intrinsic Ge spectroscopy of γ-and x-radiations. A 0.3 - 0.5g sample of rock powder is irradiated in a thermal neutron flux of 8×10^{12} neutrons/cm^2 sec for 6 hours, then fused with carriers in an Na_2O_2-NaOH flux. The fusion cake is dissolved in dilute HCl, and the carriers and activated noble metals are coprecipitated in 3mg. of Te, using Sn^{+2} as a reductant. The Te-noble metal coprecipitate is washed and packaged in a compact counting form, then counted for 2,000 - 50,000 seconds on the semi-conductor detectors. Radiochemical processing of a pair of samples is generally accomplished within 1.5 hours. After the primary activities have been counted and allowed to decay, the samples are re-irradiated for 4 minutes at 8×10^{12} neutrons/cm^2 sec, and the relative yields on the carriers in the samples and standards are determined by Ge(Li) and intrinsic Ge spectroscopy. The absolute yield of the radiochemical procedure, as determined by radioactive tracer experiments, is ca. 90-100% for Au, Pd, and Pt, and 60% for Ir. Typical detection limits* for analysis of a 0.5g sample of

---

* Defined as L_D of Currie (1968).

peridotite are: 0.01 - 0.02ppb Au; 0.1 - 0.4ppb Pd; 1-2 ppb Pt; and 0.02ppb Ir.

II-3: EVALUATION OF THE TECHNIQUE

Accuracy: analyses of standard rocks

Abundances of Au, Pd, Pt,* and Ir in the standard rocks PCC-1 and W-1, obtained in the present study, are given in table II-1 along with values reported in the literature. The values obtained in this study fall within the range of reported values, though there is obviously considerable disagreement among the literature analyses. Values of Pd obtained in this study are on the low side of reported values; however, the value of 9.8 ± 1.5 - 1.8ppb for W-1 is within error of the 11.5 ± 1.0ppb value obtained by Crocket *et al.* (1968) in a careful study involving 17 replicate analyses. The value of 4.7ppb for Au in W-1 obtained in this work is in good agreement with the literature values, if the single high literature value is excepted. Of the literature values for Ir in PCC-1, the majority is in the range 5-7ppb, in agreement with the value of 6.4 ± 1.1 - 1.2ppb obtained in this study; one of the lower literature values (3.5ppb, from Nadkarni and Morrison, 1974) was obtained by a method involving no yield determination, and may be incorrect. The Ir value obtained

---

* Pt was not determined in W-1 in this study due to poor counting statistics.

TABLE II-1: REPLICATE ANALYSES OF U.S.G.S. STANDARD ROCKS

	PCC-1		W-1	
	this work	literature[a]	this work	literature[a]
Pd	3.6, 3.7, 3.8 4.3, 5.5 $\bar{x}$ = 4.2 ± (0.8, 0.7)[e]	3.0, 4.4[b], 4.7[c], 5.9, 6.0, 6.3 7, 13[d]	8.2, 9.2, 12 $\bar{x}$ = 9.8 ± (1.8, 1.5)	9[f], 9.2[g], 10.1[b], 11.5 12.2[c], 14, 15.8, 16, 17.7, 19.3, 25[d]
Au	0.67, 0.68, 0.88 0.92, 0.95, 1.07 $\bar{x}$ = 0.86 ± (0.16, 0.15)	0.63, 0.67, 0.73, 0.73, 0.8, 0.8, 1.3, 1.42, 1.6, 3.0, 3.14, 3.2, 3.4	4.21, 4.47 5.47 $\bar{x}$ = 4.7 ± (0.7, 0.5)	3.6, 3.7, 4.2 4.6, 4.6[h], 4.7 4.8, 4.9[i], 5.0[j] 5.8, 8.5[k]
Ir	5.00, 5.60, 5.85 6.08, 7.62, 8.1 $\bar{x}$ = 6.4 ± (1.2, 1.1)	2.1, 2.6-3.6, 3.5, 5, 5.1, 5.2, 5.8, 5.7, 6.0, 6.6, 6.65, 6.7, 7.1	0.34, 0.38 $\bar{x}$ = 0.36	<0.05, 0.26, 0.26, 0.28, 0.30, 0.34, 2.3
Pt	5, 6, 7, 10, 12 $\bar{x}$ = 8 ± (2.7, 2.4)	3.5, 4.8, 5.1, 5.7[b], 5.8[b], 8[d], 13.5		

a) Literature values without superscripts are from compilation by Ahmad et al. (1977).

b) Page et al. (1980).

c) Rowe and Simon (1971).

d) Unreferenced value from Flanagan (1973).

e) First and second vlaues in parentheses are standard deviations with N-1 and N degrees of freedom, respectively.

f) Grimaldi and Schnepfe (1967).

g) Sarma et al. (1965).

h) Baedecker and Ehmann (1965), avg. 3 analyses.

i) Hamaguchi et al. (1961).

j) Shcherbakov and Perezhogin (1964).

k) Vincent and Crocket (1960).

for W-1 in this study is in reasonable agreement with the majority of literature analyses. The value for Pt in PCC-1 obtained in this study is in the range of literature analyses, but is on the high end.

It is difficult to explain the large range of literature abundances for Au in PCC-1. Some of the range may be due to differences in the techniques used by different analysts. However, techniques which seem to be comparable on the basis of analyses of other standard rocks fail to give comparable Au analyses for PCC-1. For example, analyses of Au in W-1 obtained in this study and by Ahmad et al. (1977) are in good agreement (4.7±0.7ppb, both studies), and agree with the majority of literature analyses (table II-1), which suggests that the techniques used in the two different studies should give comparable results; yet the PCC-1 Au analyses obtained in the same two studies are very different (0.86±0.16ppb, this study; 3.0±0.3ppb, Ahmad et al., 1977). It is possible that the differences among the PCC-1 Au analyses may be due to real differences in the Au contents of the aliquants of PCC-1 distributed by the U.S.G.S., but this possibility is difficult to test.

Precision

Based on replicate analyses of W-1 and PCC-1, the average precision* of the Te-coprecipitation technqiue is

---

* Precision is here defined as the ratio of the standard deviation to the mean of replicate analyses.

ca. ±16% for Au, Pd, and Ir; this precision compares favorably with the average precisions reported in the literature (see, for example, the compilation of literature values in Ahmad et al., 1977). The most precise noble metal techniques to date appear to be that of Ahmad et al. (1977), with an average precision of ±6% for analysis of Au, Pd, Pt, and Ir in W-1 and PCC-1, and that of Crocket et al. (1967), with an average precision of ±13% for replicate analyses of Au, Pd, and Ir in W-1; many noble metal analysis techniques give precisions worse than ±20%. The average precision of the Te-coprecipitation technique for Pt is rather poor, ca. 30-35%, though poor precision is fairly typical for Pt analyses at ppb levels. The cause of the poor precision for Pt is not known, but may be related to sample heterogeneity (see, e.g., Chyi and Crocket, 1976).

As previously stated, an objective of this study is to evaluate correlations of noble metal contents with other geochemical variables in ultramafic rocks. With a precision of ±16%, it should be possible to resolve Au, Pd, and Ir variations of 30% at the 95% confidence level; with a precision of 30-35%, it should be possible to resolve Pt variations of 60-70% at the 95% confidence level. As these variations are relatively small compared with those found in single alpine ultramafic bodies (Crocket and Chyi, 1972; and chapter III, this work), the Te-coprecipitation technique is appropriate for the study of noble metal variations in alpine ultramafics.

Detection limits

With the Te-coprecipitation technique, it is possible to obtain detection limits of 0.01 - 0.02ppb Au, 0.1 - 0.4ppb Pd, 1-2 ppb Pt, and 0.02ppb Ir for an analysis of 0.5g of ultramafic rock. These limits compare favorably with those reported for other techniques. Crocket and Teruta (1977) report limits of 0.05ppb Au, 0.1 - 0.2ppb Pd, 20ppb Pt, and 0.01ppb Ir for a radiochemical technique involving extensive radiochemical separations and β^- counting for Pd. Hoffman et al. (1978) report detection limits of 0.1ppb Au, 5ppb Pd, 5ppb Pt, and 0.1ppb Ir for an instrumental neutron activation technique involving fire assay preconcentration. Page et al. (1980) report "sensitivities" of 0.1ppb Pd and 0.8ppb Pt for a sophisticated atomic absorption technique. Haffty and Riley (1968) report detection limits of 4ppb Pd and 10ppb Pt for a fire-assay spectrographic technique.

Simplicity

When compared with virtually all other noble metal analysis techniques, the Te-coprecipitation technique is extremely simple. Most radiochemical neutron activation techniques with high sensitivity involve extensive radiochemical purification steps or involve exotic reagents; thus, the method of Crocket et al. (1968) requires ca. 1 1/2 days for radiochemical processing of a set of 1-12 samples (pers. comm. J.H. Crocket, 1978), and the method of

Ahmad et al. (1977) involves several organic reagents which are not available from chemical supply houses. Non-radiochemical methods, such as fire assay pre-concentration methods, require exhaustive blank control and extreme precautions against contamination.

Another simple radiochemical group separation technique, based on a noble metal-selective chelating resin, has been reported by Nadkarni and Morrison (1974). This technique was investigated as part of the present study, but was abandoned after repeated failures to reproduce the quantitative yields and selectivity claimed by Nadkarni and Morrison. Tracer experiments indicated that the Ir yield of the resin was highly variable, and generally less than 80%, not the ca. 100% value reported in the literature; in addition, the claim that all the noble metals could be stripped from the resin with thiourea proved incorrect. Other difficulties with the method proposed by Nadkarni and Morrison involved the absorption of large amounts of activated Cu, Na, Sc, and Cr on the resin, causing high Compton background in Ge(Li) spectra; and the lack of a procedure for determining the yield of the radiochemical separation of noble metals.

Possible improvements in the Te-coprecipitation method

It is possible that the precision of the Te-coprecipitation method could be improved through more careful control of the experimental conditions. Flux

variations across the irradiation container were not usually monitored in this study. In order to estimate the error due to flux variations, iron wire flux monitors were included in one irradiation; the average flux variation for this irradiation was 3% of the main flux, and the largest variation was 6%. Thus, the inclusion of a small Fe-wire flux monitor in each sample, and subsequent flux corrections might improve precision somewhat. In addition, differences of 5% were observed for Ir analyses made by counting the same sample on different detectors in different geometries; hence, it is possible that a stricter control of the counting geometries might result in a further improvement in the precision. However, because Au and Ir are determined in the same geometry, and against the same standard, geometry and flux variations should cause correlative errors in analyses for the two elements. Yet, the correlation of Au and Ir in replicate analyses of PCC-1 is quite weak (corr. coefficient = 0.41), which suggests that most of the imprecision in analyses of these elements is not be due to flux and geometry effects. Differences among the synthetic standards used for analyses have also been considered as a possible cause of imprecision; however, repeated cross-checks of the standards by instrumental neutron activation have failed to indicate any differences greater than the ±3% uncertainty due to counting statistics.

II-4: DETAILED ANALYTICAL PROCEDURE

A) Stock Solutions

Carriers

Begin preparation of stock solution containing 0.500mg/ml Pt by weighing 0.2265g of ammonium hexachloroplatinate into a 250ml erlenmeyer flask containing ca. 100ml of pre-mixed 2M HCl. Warm the solution gently on a hot plate, swirling to dissolve the Pt salt; allow the solution to cool, and transfer quantitatively to a 200ml volumetric, using 2M HCl, not water,* to rinse the erlenmeyer. Bring to volume with 2M HCl, not water. Rapidly suction filter the solution through a pre-weighed piece of 1cm diameter acid-resistant filter paper in a Hirsch funnel. Transfer the solution to a polyethylene bottle with a tight-fitting cap, then rinse, dry, and weigh the filter paper to verify that no more than 1% of the salt remained undissolved. Prepare a solution containing ca. 0.200mg/ml Ir by weighing 0.0914g of ammonium hexachloroiridate into a 250ml erlenmeyer containing ca. 100ml of 2M HCl, and proceed as for the Pt salt.

Begin preparation of a stock solution containg 0.700mg/ml Pd by weighing 0.1400g of Pd sponge into a 250ml beaker. Add 15ml of aqua regia to the beaker, and warm the

---

* A gelatainous precipitate may form when the solutions are diluted with distilled H_2O rather than 2M HCl.

solution very gently on a hotplate until the effervescence subsides. Evaporate the solution gently on a hotplate, under a stream of filtered air, and swirl the beaker occasionally, until a thick syrup is formed at incipient dryness. Add 2ml conc. HCl and bring the solution to incipient dryness; repeat five times (this procedure is required for the destruction of unstable Pd^{+4} - NO_3 complexes). Dissolve the syrup in ca. 10ml conc. HCl, then quantitatively transfer to a 200ml volumetric flask, using pre-mixed 2M HCl to rinse the beaker. Bring to volume with pre-mixed 2M HCl, and filter (as with Pt and Ir solutions) so as to check for complete dissolution of Pd, and to remove any organic dust material which might induce precipitation of Pd metal. Transfer the Pd solution to a tightly-capped plastic bottle.

The Au stock solution containing 0.500mg/ml Au is prepared by weighing 0.100g of Au sponge into a 250ml beaker and proceeding as for Pd; however, special care must be taken never to heat the Au solutions too rapidly, or to bring the solution to complete dryness, as precipitation of Au metal (insoluble in HCl) will result. In addition, the final Au stock solution must be stored in a dark place to prevent photoreduction.

Prepare a carrier solution containing 0.125mg/ml Pt, 0.0500mg/ml Ir, 0.175mg/ml Pd, and 0.125mg/ml Au by pipetting 25ml of each stock solution into a plastic bottle.

Tellurium solution

Begin preparation of a stock solution containing 1.0mg/ml Te by weighing 0.10g of Te metal powder into a 250ml beaker. Add 5ml HCl and 5ml HNO_3, allow the effervescence to subside, then bring the solution to incipient dryness. Add ca. 2-5ml conc. HCl to the white-yellow Te chloro-nitrate precipitate, and bring to incipient dryness; repeat five times (after 2 or 3 times the ppt. will disappear, to be replaced by an orange-yellow syrup). Dissolve the syrup in 10ml conc. HCl, and bring to 100ml. with distilled H_2O.

Stannous chloride solution

Begin preparation of a 1.0 M stannous chloride solution by weighing 22.5g of stannous chloride dihydrate into a 250ml beaker. Add 16ml conc. HCl and warm to dissolve the salt. Bring to 100ml with distilled HCl (the resulting solution is ca. 2M in HCl). Store in a tightly stoppered amber bottle. Make fresh solution every 2 months.

Lithium chloride solution

Prepare a 10mg/ml solution of LiCl by dissolving 1g of the salt in 100ml of distilled H_2O.

Dilute acids

Prepare ca. 500ml of 2:1 (v/v) HCl:H_2O (ca. 8N) and ca. 1000ml of 1:11 (v/v) HCl:H_2O (ca. 1N). These acids are used only during radiochemical processing.

B) Preparation of sample crucibles and standard beakers

Begin preparation of crucibles (for receipt of irradiated samples) by coating the insides of 20ml Ni crucibles ca. 1/2 way up with an extremely thin coating of EPOXY-PATCH epoxy, using a Q-tip for application. Heat the crucibles on a hot plate to dry the epoxy, then repeat the coating procedure two times (the coating is necessary to prevent the plating of the noble metals onto the crucible walls when carrier is added as an acid solution; however, if the coating is too thick, an explosion will result when Na_2O_2 is later heated in the crucible). Add a few milligrams of NaCl to the bottom of each cooled crucible, and pipet 1ml of the Au-Pd-Pt-Ir carrier solution into each crucible, taking care not to touch the pipet to the uncoated metal. Gently evaporate the solutions to dryness.

Prepare beakers to receive the irradiated Pt-Pd and Au-Ir standards by pipetting 1ml of the carrier solution into each of two 250ml beakers. Add a few milligrams NaCl and 2 drops HNO_3 to each beaker and cover with parafilm. Label each beaker.

On the day before radiochemical processing, place 10 pellets of NaOH into each crucible (along with 0.3g Fe_2O_3 if siliceous rocks are to be processed) and dry in an oven at ca. 100C overnight.

C) Preparation of standards

Preparation of poly vials

Clean ca. 40 2/5 dram fliptop polv vials (to prepare 20 Pt-Pd and 20 Au-Ir standards) by soaking them in a 2:1 (v/v) $HCl:HClO_4$ mixture. Rinse the vials with water, then distilled water, then pure acetone, then dry the vials at ca. 70C for a few minutes in an oven. Allow the vials to cool. Add spectroscopically pure SiO_2 powder to each vial to fill to ca. 1/2 capacity.

Standard solutions

Prepare a Au-Ir standard solution containing 500 ng*/ml Au and 200ng/ml Ir by pipetting 1ml each of the Au and Ir stock solutions into a 1,000ml volumetric flask containing ca. 500ml of pre-mixed 2M HCl; bring the solution to volume with 2M HCl. Prepare a Pt-Pd standard solution containing 5,000ng/ml Pt and 7,000ng/ml Pd by pipetting 1ml each of the Pt and Pd stock solutions into a 100ml volumetric flask containing ca. 50ml pre-mixed 2M HCl; bring the solution to volume with 2M HCl.

Standard solutions should be prepared fresh immediately before buretting into the poly vials.

Preparation of standards

Prepare each individual Au-Ir standard, containing 150ng Au and 60.0ng Ir, by delivering (via a microburet) 0.300ml of the Au-Ir standard solution into a pre-weighed

---

* ng = nanogram, or 10^{-9} grams.

vial (weight including silica powder). Quickly weigh each vial after delivering the Au-Ir solution. After preparing ca. 20 standards, calculate the mean weight of the solutions delivered to the vials. Discard any standards with solution weights deviating from the mean by more than 0.5%. Place the remaining standards in an oven at ca. 70C and dry the standard solution onto the SiO_2 powder. Seal the vials with a soldering iron. Verify that the vials are airtight by squeezing each one gently, with pliers, under water; discard any vials which leak. Lable the remaining vials with an indelible felt-tip pen.

Prepare Pt-Pd standards containing 1,500ng Pt and 2,100ng Pd each by delivering 0.300ml aliquots of the Pt-Pd standard solution into pre-weighed poly vials (containing SiO_2), and proceed as for Au-Ir standards.

D) Preparation of samples

Thoroughly clean all work surfaces, including the microbalance pan, before preparing the samples.

Prepare sample tubes by cutting 4cm lengths of 0.5-0.6cm inner diameter thin-wall polyethylene tubing ("Intramedic" brand), then seal one end of each tube by gently melting the end over a bunsen burner and squeezing it with pliers. Clean the tubes with $HCl-HClO_4$, then water, distilled water, and pure acetone. Label each tube with an indelible felt-tip pen. Weigh ca. 0.5g of ultrabasic rock powder, or 0.3g of a more siliceous rock powder, into each tube. Seal the open end of each tube by gently melting it

and squeezing it with pliers. Verify that the sample tubes are airtight by squeezing them under water with pliers. Rinse off the tubes with distilled water and dry them.

E) Irradiation

Irradiate 4 rock powder tubes and 2 standard vials (Au-Ir and Pt-Pd), sealed in plastic bag and placed in a "rabbit" (plastic irradiation cannister), for 6 hrs. at a thermal neutron flux of $8x10^{12}$ neutrons/cm^2 sec. Cool the samples for 12 to 18 hrs. After the decay period, the most active species in ultramafic rocks will be 56Mn, followed by 24Na. The most active species in the standards will be 31Si (β decay only), followed by 198Au (γ + β) and possibly 82Br and 80mBr (from the HCl); the standard dose rates will be negligible compared to the sample dose rates. Dose rates (γ + β) at 1 meter from the rabbit will be from 2mR/hr to 15mR/hr.

F) Radiochemistry: samples

Process the samples behind 2"-4" of Pb bricks in a drawing hood. Never directly touch the active samples.

The procedure below describes processing of a single sample. In practice, two samples may be processed simultaneously in 1.5 hours.

Sample transfer and fusion

Tap the sample tube gently against a Pb brick so as to bring all the rock powder to one end (use tongs to hold the

tube). Snip the end of the tube off with scissors and pour the rock powder evenly over the NaOH pellets (and carriers) in the Ni crucible. If the sample tubes have been constructed properly, much less than 1% of the powder sticks to the tube. Add ca. 6g of fresh yellow Na_2O_2 to the crucible. Gently tap the crucible to even out the Na_2O_2. Heat the crucible over a low meeker burner flame ca. 5 min., or until the fusion mixture has nearly melted. Turn up the meeker flame until the mixture is totally melted and is at dull red heat (ca. 600C; at higher temperatures, insoluble Ni oxides form and the crucible corrodes rapidly; using dull red heat, a crucible will last through 10 fusions). Continue heating the crucible for 5-10 min., swirling the mixture occasionally. Place the crucible on a Pb brick to speed cooling. After ca. 3 min., a "ding" will be heard as the fusion cake cracks, and the cake may be leached as follows.

Leaching the fusion cake

Immediately after the ca. 3 min. cooling period, place the crucible on its side in a 250ml beaker containing 60ml of distilled H_2O and 3 silicate boiling chips; cover immediately with a watch glass. After the effervescence has subsided, rinse the watch glass off into the beaker with ca. 5ml of 2:1 $HCl:H_2O$. Rinse the inside and outside of the crucible to dissolve any remaining black oxides, then add

the rinsings to the beaker. The solution is now ca. 2.1M* in H^+ and ca. 3.8M in Cl^-. Replace the watch glass, set the beaker on a hot plate, and boil the solution gently for 10 min. in order to convert H_2O_2 (produced by the reaction of Na_2O_2 and H_2O) to H_2O and O_2. The solution should be clear, without traces of colloidal silica or undissolved rock. Solutions of peridotites will be green (partly due to Ni^{+2} from dissolution of the crucible); solutions of more Fe-rich siliceous rocks will be yellow green (from Fe^{+3}), and solutions of chromitites will be orange (from dichromate). After boiling, filter the solution through a fast, acid-resistant filter paper (e.g. S+S 595), and collect the solution in a 250ml erlenmeyer flask containing 3 silicate boiling chips; rinse the beaker and filter paper with ca. 40ml of 1:11 HCl and add the rinsings to the erlenmeyer.** Add 2ml Te solution to the erlenmeyer, and place the flask on a hot plate to boil. The solution volume should be ca. 140-150ml.

Te precipitation

When the solution in the erlenmeyer is at a rolling (but not violent) boil, add ca. 10-15ml of Sn^{+2} solution,

---

* Accounting for neutralization of alkali from Na_2O_2, NaOH.

** This filtration step is a precaution intended to remove any unseeen traces of undissolved silica gel, rock powder, or Ni oxide before Te precipitation. If complete dissolution is always achieved, the filtration step can be eliminated.

dropwise at first; a black cloud of tellurium will precipitate (the amount of Sn^{+2} solution necessary to precipiate the Te from chromitite solutions may be slightly more than 15ml; and with chromitite solutions it may be difficult to see the precipitate, as reduction of Cr^{+6} to Cr^{+3} makes the solution very deep green). Boil the solution ca. 5-10 min. until the Te is well coagulated, then add 1ml Te solution, and boil again for 5-10 min., once again until the precipitate is well coagulated.

Filtering and washing the precipitate

Place a 4.2cm diameter circle of acid-resistant filter paper (e.g. S+S 595) in 300ml capacity pyrex Millipore filter holder. Place the holder on a large (2,000ml) side arm filter flask attached to an aspirator. Verify that the filter holder does not leak by passing a small amount of water through it. Pour the contents of the erlenmeyer flask (containing the Te precipitate) into the filter holder reservoir; rinse the flask with ca. 10-20ml of 1:11 $HCl:H_2O$ and transfer the rinsings to the reservoir. Apply the suction (do not apply suction before adding the contents of the flask, as an uneven precipitate will result). Rinse down the sides of the reservoir with 1:11 $HCl:H_2O$ and filter 10ml of hot 1:11 $HCl:H_2O$ (ca. 70C) through the precipitate ca. 10 times. Break down the filter apparatus and transfer the paper and precipitate to a tray outside the hood. The dose rate from the precipitate will be very low.

Counting form

Fold the paper in half, with the Te on the inside, then fold again (i.e., quarter the paper). Place the quartered paper in a 1" by 1 1/2" polyethylene counting envelope; seal and label the envelope. Wrap the envelope in one layer of polyethylene film, center it on the counting block (figure II-1), and tape down the cover of the counting block.

G) Radiochemistry: Standards

The procedure below describes the processing of an individual standard. In practice, both standards (Au-Ir and Pt-Pd) can be processed simultaneously. Standards should always be processed after samples (and preferably in a separate room) to avoid cross-contamination.

Equilibration with carriers

Tap the standard vial several times to bring all the SiO_2 powder to one end. Place the vial in the pre-drilled lead brick holder and saw off the vial top with a scalpel. Empty the SiO_2 powder into the standard beaker (containing carriers and a few drops HNO_3). Add 1ml of aqua regia to the vial, then pour the vial aqua regia into the beaker; repeat 2 times, then add another 1ml aqua regia to the vial and set the vial aside. Add 1ml LiCl solution to the beaker (to help prevent metal reduction upon drying), and gently warm the beaker on a hot plate until the effervescence subsides. Add the contents of the vial to the beaker, and

FIGURE II-1: Positioning of the Te precipitate on the plexiglas sample holder. The silhouette of the precipitate shows through the quartered filter paper; the three corners of the silhouette are aligned on the cross hairs of the holder, and the sample bag and cover are taped tightly in place. The dimensions of the plexiglas holder should be such that the holder fits snugly in the counting tower. The cross hairs are positioned so that the precipitate centers on the detector axis.

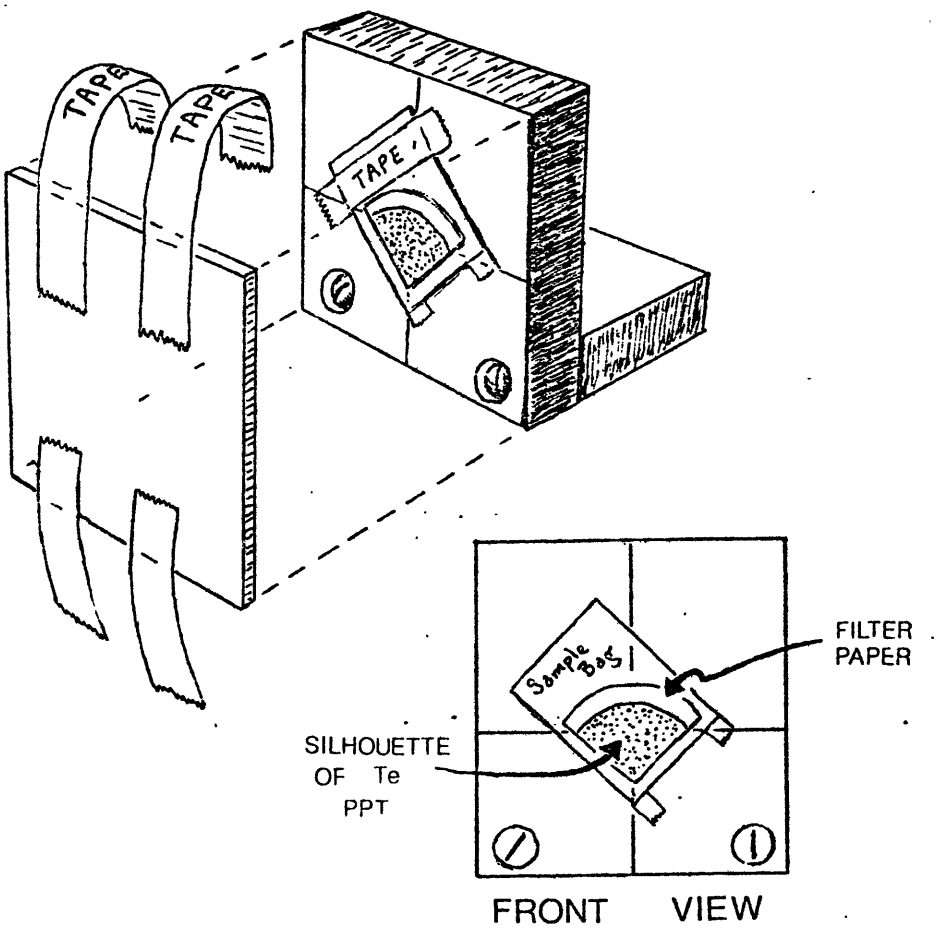
TAPE
TAPE
TAPE
Sample Bag
FILTER PAPER
SILHOUETTE OF Te PPT
FRONT VIEW

again warm until the effervescence subsides. Bring the contents of the beaker to incipient dryness. Add 2ml conc. HCl to the beaker and bring to incipient dryness; repeat 5 times (the repeated addition of HCl transforms the noble metal nitrates to chlorides). Add 10ml conc. HCl, then 90ml 1:11 (ca. 1M) HCl:H_2O. Filter the contents of the beaker through a fast filter paper into a 250ml erlenmeyer flask containing 3 silicate boiling chips. Rinse the beaker, filter paper, and SiO_2 with ca. 40ml 1:11 HCl:H_2O, adding the rinsings to the flask. Add 2ml Te solution to the flask and set the flask on a hot plate to boil. The solution volume should be ca. 140-150ml. Discard the filter paper and SiO_2 to active waste storage.

Te precipitation

When the solution is at rolling boil, add 10ml of the Sn^{+2} solution, dropwise at first. Boil the solution 5-10 minutes to coagulate the precipitate, then add 1ml Te solution, boil to coagulate the precipitate, and continue processing the standard exactly as the samples were processed.

H) Counting

Count the samples for 22 KeV AgKα x-ray (from 109 Pd decay) on an intrinsic Ge low energy photon spectrometer (effective diamter ca. 1.5 cm., effective thickness ca. 0.5mm., resolution ca. 0.6 KeV FWHM at 60 KeV) connected to a multichannel analyzer. Using the low

energy spectrum of 241 Am (26.4 KeV γ-ray and NpL x-rays at 13.9 and 17.1 KeV), adjust the amplifier gain to give 4 or 5 channels/KeV. Count the samples for 2,000-10,000 seconds, and the Pt-Pd standard for 1,000 seconds. The samples should be counted flush against the detector end cap. Dead times will be 0% for samples and ca. 1/2% for the standard.

Count the samples for the 88 KeV 109 Pd γ-ray, the 158 KeV 199 Au (Pt) γ-ray, the 328 KeV 194 Ir γ-ray, the 317 KeV 192 Ir γ-ray, and the 412 KeV 198 Au γ-ray on a large Ge(Li) detector (active volume 30-56cm^3, resolution ca. 2 KeV FWHM at 1,000 KeV) connected to a multichannel analyzer. Using the 59.6 KeV peak of 241 Am and the 661.6 KeV peak of 137 Cs, adjust the amplifier gain to yield 2 channels/KeV. Count the samples for 5,000-50,000 seconds; long counts are necessary for determining Pt via 199 Au. Count the standards for 1,000 seconds or more. The samples should be flush against the detector end cap. Dead times will be 0% for most samples, 1 1/2% for the Pt-Pd standard, and 3% for the Au-Ir standard.

I) Re-irradiation

Packaging samples for re-irradiation

After a suitable decay time (greater than 18 days), package the samples for re-irradiation. Up to four sample-standard sets (each set consisting of four samples and two standards) may be irradiated and processed at the same time. For each set, stack the sealed envelopes so that

the filter papers are directly on top of one another, and tape the set together with mylar tape. Two sets may be placed in each 1" diameter by 3" low flux rabbit.

Re-irradiation

Irradiate the Te precipitates in a flux of 8×10^{12} n/cm^2 sec for 4 minutes. Immediately after irradiation, the samples will contain numerous short-lived active species (38 Cl, 131 Te, 192m$_1$ Ir, 109m Pd), and should be cooled for 12-18 hrs. After cooling, the most active species will be 198 Au, with a $\gamma + \beta$ dose rate of <0.05 mR/hr at 1 meter per set of 6 Te precipitates.

Counting re-irradiated samples

Place each 1" x 1 1/2" sample envelope in a 1 1/4" x 2" counting envelope, and center the sample on the counting block as per figure II-1. Count the samples 5-10cm from the Ge(Li) detectors for 109 Pd, 194 Ir, and 198 Au, and 2-5cm from the LEPS for 109 Pd via the 22 KeV x-ray. The Pt relative yields are determined from the 198 Au 412 KeV peaks in the samples and Pt-Pd standard. Counts of 1,000sec give adequate counting statistics (±0.5%) for 194 Ir and 198 Au on the Ge(Li) detectors and for 109 Pd on the LEPS, but longer counts (ca. 4,000sec) are needed if Pd yields are to be determined with the 88 KeV 109 Pd peak on the Ge(Li) detectors. Dead times should be ca. 5% and uniform on the Ge(Li) detectors, and ca. 1 1/2% and uniform on the LEPS.

J) Data Reduction

Basic Equation

Calculate the concentration of each noble metal in each sample using the formula:

$$\text{ppb NM} = \frac{w}{W} \cdot \frac{N_{SAMP}}{N_{STD}} \cdot \frac{(TCF)}{(TCF)'} \cdot \frac{N'_{STD}}{N'_{SAMP}}$$

where w is the weight of the NM in the standard in nanograms, and W is the rock sample weight in grams; N_{SAMP} and N_{STD} are the net counts in the chosen γ- or x-ray peak in the sample and standard, respectively, as counted after the first irradiation; TCF is a time-correction factor for N_{SAMP} and N_{STD}, which corrects for differences in counting time and exponential decay of the isotopes; N'_{STD} and N'_{SAMP} are the net counts in the standard and sample peaks after re-irradiation for yield determination; and (TCF)' is a time correction factor for N'_{STD} and N'_{SAMP}.

Calculating net counts in peaks

Calculate the net counts in the γ- and x-ray peaks from the multi-channel analyzer outputs, using the formula:

$$N_{NET} = N_{GROSS} - \frac{n}{2b}(N_{H\ BACK} + N_{L\ BACK})$$

where N_{GROSS} is the number of counts in the gross peak of n channels, $N_{H\ BACK}$ is the number of counts in b channels of background on the high energy side of the peak, and $N_{L\ BACK}$ is the number of counts in b channels symmetrically disposed on the low energy side of the peak. For the 22 and 88 KeV

109 Pd radiations, and the 158 KeV 199 Au(Pt) radiation, a 4-channel peak (n = 4) contains 90% or more of the total number of counts in the "full" net peak ($n \to \infty$). For the higher energy radiation from 192 Ir, 194 Ir, and 198 Au, 6-8 channel peaks (n = 6-8) contain more than 95% of the full peaks.

Counting statistics errors

The relative counting error S (Liebhafsky et al., 1972) for the estimation of N_{NET}, is given by:*

$$S = \frac{\sqrt{N_{GROSS} + \frac{n}{2b}(N_{H\ BACK} + N_{L\ BACK})}}{N_{NET}}$$

The combined counting error for the estimation of concentration, including contributions from N_{NET} of the sample, standard, and yield determinations is:

$$S_C = \sqrt{S_{STD}^2 + S_{SAMP}^2 + S'^2_{STD} + S'^2_{SAMP}}$$

where the primed errors are those calculated for yield determination counts.

---

* This formula overestimates S for $2b > n$, and underestimates S for $2b < n$, but the error is generally small.

Time correction factors

The time correction factor TCF is given by:

$$TCF = \frac{\exp(-\lambda t_B) - \exp(-\lambda t_A)}{\exp(-\lambda t_2) - \exp(-\lambda t_1)}$$

where t_A and t_B are the starting and ending times for the count of the standard, t_1 and t_2 are the starting and ending times for the count of the sample, and λ is the decay constant, i.e.:

$$\lambda \equiv \ln 2/(\text{half-life})$$

When:

$$t_B - t_A = t_2 - t_1$$

then

$$TCF = \exp(\lambda(t_1 - t_A))$$

The factor TCF' is completely analogous to TCF, with the starting and ending times for counts made after the second irradiation being used in the equation.

II-5: NOTES ON THE DETAILED PROCEDURE AND DEVELOPMENT OF THE TECHNIQUE

Fusions

Reviews of fusions suitable for noble metal analyses are given by Hillebrand et al. (1953) and Walsh and Hausman (1963). Fusions suitable for dissolving chromite are given by Hartford (1963). Fusion mixtures of Na_2CO_3,

Na_2O_2, and NaOH were investigated in this study. The best mixture found for decomposing 0.5g of ultramafic rock consists of 6g of Na_2O_2 and 0.5g NaOH (ca. 10 pellets); this mixture melts at a low temperature, is highly fluid at dull red heat, and attacks refractory minerals readily. A similar fusion mixture is recommended by Nadkarni and Morrison (1974).

Pyroxenites and siliceous rocks, while readily decomposed by the Na_2O_2 - NaOH mixture, may yield a troublesome SiO_2 gel when the fusion cake is dissolved in acid. Formation of the gel can be suppressed by reducing the sample weight to 0.3g. The addition of 0.3g Fe_2O_3 or $CuSO_4$ to the fusion mixture also seems to aid in suppressing gel formation; the usefulness of the added compounds was determined empirically, after testing fusion mixtures with added oxides, carbonates, and sulfates of Cu, Mn, and Fe. The added $CuSO_4$ has the undesirable side effect of causing the fusion mixture to sputter during melting, and is not recommended.

Fusions are best performed in Ni rather than Zr crucibles for three reasons; first, Zr crucibles yield an insoluble zirconia precipitate which must be removed after fusion; second, Zr crucibles corrode just as rapidly as Ni crucibles at red heat, and hence are of no advantage; and third, Ni crucibles are 1/4th as expensive as Zr crucibles.

Regulating acidity for Te coprecipitation

According to Beamish and van Loon (1977), Te coprecipitation is best done in 1-6M HCl. In this study, it was found that several important factors are strongly dependent on acidity in the range required for Te precipitation. Co-precipitation of Cu, often the major source of Compton background in the noble metal spectra, is suppressed by high acidities. Tracer experiments indicate that at 2.0 M H^+, ca. 1.2% of the sample Cu is coprecipitated with the Te, while at 3.2 M H^+, only 0.025% of the sample Cu is coprecipitated. Unfortunately, high acidities have two negative effects; Ir yields are lowered at acidities much above 2 M H^+, and very acid samples seem to clog the filtration apparatus, perhaps because the Te does not coagulate and passes into the filter paper.

Ir and Au carriers and self-shielding

Gijbels et al. (1971) have discussed the effects of Ir carrier levels on self-shielding during yield determinations by re-irradiation; Beamish and van Loon (1972) have reviewed self-shielding effects in Au. Re-irradiation self-shielding effects were minimized in the present study by using small amounts of Ir and Au carriers (e.g. 50µg Ir carrier/sample for the present study, vs. 10,000µg/sample used by Gijbels et al.). At these low carrier levels, the calculated neutron flux absorption across a stack of 12 Te precipitates on filter paper (as packaged for re-irradiation) is only 0.1%, and may be neglected.

In the present study, Pt was added to the samples only as an additional, non-isotopic carrier for Ir; as Pt was determined via 199 Au, Pt carrier was not actually needed for Pt analyses.

Sample size taken for analysis

It has been contended that, due to the presumed inhomogeneous distribution of noble metals in rocks, large (> 20g) samples are required for representative noble metal analysis (Green et al., 1970; Hoffman et al., 1978); it follows that techniques employing small (≤ 0.5g) samples, such as radiochemical neutron activation, should not give representative results. In my opinion, this contention has not been justified. Green et al. base the argument for large samples on the observation that they obtained high and irreproducible Au analyses for PCC-1 (1.42 and 3.14ppb, as compared with 0.8 ± 0.2ppb for the majority of literature analyses) when using 20-50g samples. Green et al. contend that the high values and poor precision are probably due to the inclusion of a few, Au-rich particles in the 20-50g samples; sampling of such particles would be highly improbable in the small samples normally used in analysis. Green et al. recommended the use of 200g samples for Au analysis, though they did not actually analyze any samples of this size. However, Ahmad et al. (1977) have also obtained high Au values for PCC-1 (3.0ppb), but with good precision (10%) and with small (0.4g) samples; thus the interpretation of Green et al. is in doubt.

It is extremely difficult to predict a priori the sample size needed for representative noble metal analyses. If it is reasonable to assume that a given noble metal is contained entirely in single mineral in the rock sample, the theory of sampling errors (Gaudin, 1939) may be used to predict the size sample needed to meet a specified sampling error, by the equation:

$$W \approx 1.9 \times 10^4 \frac{\rho r^3}{(\%\ \text{error})^2\ w}$$

where W is the mass of the sample in grams, ρ is the density of the phase containing the noble metal, r is the average radius in cm. of a particle of the noble metal-containing phase, w is the mass fraction of that phase in the sample, and (% error) is the permissible error in % of the mean. As an example, the size of a sample needed to obtain Pd analyses to ±5% can be calculated on the assumption that all the Pd is present in sulfides. A typical alpine ultramafic rock contains ca. 0.02 wt.% sulfide in particles averaging 20μ radius (0.002cm) or less, with an average density of 4.5g/cm^3. Substituting these values into the equation, W is calculated as ca. 0.14g., which is a reasonable size for radiochemical analyses.

Counting form and x-ray absorption

Absorption effects may be important in the determination of Pd via the 22 KeV AgKα x-ray. The linear absorption coefficient of the Te-noble metal precipitate at 22 KeV is large (ca. 140cm^{-1}; calculated from data in

Liebhafsky et al., 1972), so the counting form of the precipitate must be kept thin and reasonably uniform. A totally uniform distribution of the precipitate over the 2.5cm^2 area of the quartered filter paper results in an effective thickness of 3 x 10^{-4}cm, and an absorption of ca. 2% of the 22 KeV x-ray. An extremely non-uniform distribution, with the precipitate in clumps over only 10% of the quartered paper, results in ca. 20% absorption of the x-ray. If the distributions of the precipitate for standards and samples are very different, an absorption error is introduced into the pre-yield determination of Pd in the samples. However, the nature of the yield determination by re-irradiation has the effect of cancelling out absorption errors. The concentration of Pd in the sample is related to measured activities and absorption factors by:

$$\text{Pd in sample} \propto \frac{N_{SAMP}}{N_{STD}} \cdot \frac{(1-A_{STD})}{(1-A_{SAMP})} \cdot \frac{N'_{STD}}{N'_{SAMP}} \cdot \frac{(1-A'_{SAMP})}{(1-A'_{STD})}$$

where N_{SAMP} and N_{STD} are the measured counts in the sample and standard x-ray peaks after the first irradiation; N'_{SAMP} and N'_{STD} are the counts in the sample and standard x-ray peaks after re-irradiation for yield determination; A_{STD} and A_{SAMP} are the fractions of the x-rays absorbed in the standard and sample after the first irradiation; and A'_{STD} and A'_{SAMP} are are the fractions of the x-rays absorbed in the counts after re-irradiation. Since the distribution of

the precipitate on the filter paper does not change from before to after re-irradiation, and since the counts before and after re-irradiation are made in similar geometries,

$$A_{SAMP} \approx A'_{SAMP} \text{ and } A_{STD} \approx A'_{STD}$$

and the absorption factors drop out.

When to re-irradiate

Before the samples and standards can be submitted for re-irradiation, the original activities of 109Pd, 194Ir, and 198Au must have decayed to a level which will be insignificant compared with the activities which will be induced in the carriers during re-irradiation. The activity of 198Au in the Au-Ir standard is the most important activity to consider, as 198Au is the longest-lived isotope used for yield determination, and as the original activity of 198Au is tvpically highest in the Au-Ir standard. The ratio, R, of the activity of 198Au induced in the carrier of Au-Ir standard during re-irradiation, to the activity remaining from the original activation, is approximately given by:

$$R \approx \frac{(\mu g \text{ Au in carrier})}{(\mu g \text{ Au in orig. standard})} \cdot \frac{\Delta t_{REIRR}}{\Delta t_{IRR}} \cdot 2^{(T/t_{1/2})}$$

where Δt_{REIRR} and Δt_{IRR} are the lengths of the re-irradiation and original irradiation periods, respectively, T is the number of days between the original

irradiation and re-irradiation, and $t_{1/2}$ is the half-life of 198 Au (2.65 days). The optimal Δt_{REIRR} is ca. 4 min. at a flux of 8 x 10^{12}n/cm^2 sec; this time produces Pd and Ir activities sufficient to give good counting statistics in 1,000sec LEPS and Ge(Li) detector counts, yet produces 198 Au activities low enough to give deadtimes less than 5% at reasonable distances (5-10cm) from the detectors. The optimal Δt_{IRR} is 6hrs at 8 x 10^{12}n/cm^2 sec; the carrier contains ca. 125µg Au, and the original standard contained 150 x 10^{-3}µg Au. Substituting these values,

$$R \approx (9.3) \cdot 2^{(T/t_{1/2})}$$

The 198 Au activity remaining from the original irradiation is defined as "insignificant" when $R \geq 1{,}000$. To meet this criterion, T must be 18-19 days. Hence, the samples and standards should not be re-irradiated until 18-19 days after the original irradiation.

An additional constraint on re-irradiation is that all counts on the original activities must be completed before re-irradiation. For most ultramafic rocks, the last count is well within 19 days; however, for mafic rocks with < 0.5ppb Ir, Ir may be determined by counting 192 Ir as much as 30-60 days after irradiation, and re-irradiation must be delayed until this count is completed.

Choice of radiations

The nuclear characteristics and decay radiations of the noble metals have been reviewed by Crocket et al. (1968), Gijbels (1971), and Nadkarni and Morrison (1974). Additional nuclear data may be found in Lederer and Shirley (1978).

The important reaction for Pd determination is:

$$^{108}\text{Pd}(n,\gamma)\,^{109}\text{Pd} \xrightarrow[\beta^-]{13.5\text{hr.}} {}^{109}\text{mAg} \xrightarrow{40\text{ sec.}} {}^{109}\text{Ag}$$

Decay of 109 m Ag gives an 88 KeV γ-ray with poor yield (5%), and internal conversion AgK x-rays with good yield (ca. 50%). Pd determinations via the 22 KeV Ag Kα x-ray on a LEPS detector are very sensitive, as the thin LEPS detector picks up little Compton background from high energy radiations. The above reaction suffers two primary interferences:

$^{235}\text{U}(n,f)\,^{109}\text{Pd}$ and

$$^{108}\text{Cd}(n,\gamma)\,^{109}\text{Cd} \xrightarrow[\text{EC}]{450\text{ days}} {}^{109\text{ m}}\text{Ag}$$

The first reaction generates very little 109 Pd (Gijbels, 1971 calculates the equivalent of 0.025 ppb Pd for 100ppb U) and is completely negligible in ultramafic rocks, which contain much less than 100ppb of U. The second reaction is normally unimportant, because Cd activates very poorly compared with Pd, and is not coprecipitated by Te.

Contamination of the sample by 109Cd could be detected by following the decay of the 22 and 88 KeV radiations, as the half-life of 109Cd is much longer than the half-life of 109Pd; ca. one fourth of the samples analyzed in this study were checked for 109Cd contamination in this manner, and no contamination was ever found. A secondary interference arises from the production of Pb x-rays by interaction of γ-rays with the detector shielding; the 87.3 KeV Pb Kβ2 x-ray may swamp the 88 KeV 109 Pd γ-ray. However, the Pb x-rays may be reduced by a factor of 100 by lining the detector cave with 0.23cm of Cd, or 1.24cm of Fe (calculated from x-ray absorption coefficients given in Liebhafsky et al., 1972).

Where it has been possible to obtain Pd analyses by both the 22 and 88 KeV radiations, the results have agreed within the uncertainty of counting statistics (table II-2).

TABLE II-2: A COMPARISON OF Pd ANALYSES (ppb) OBTAINED BY DIFFERENT RADIATIONS

Sample	88 KeV γ-ray on Ge(Li) detector	22 KeV x-ray on LEPS
A-DEEP GORGE (chromitite)	51.0±1.3	49.7±1.0
R131	5.7±0.5	5.9±0.3
R224	4.5±0.4	4.8±0.2
R501	5.6±0.5	6.0±0.3
R717	6.3±0.5	5.8±0.3

The important reactions for Pt determination are:

$$^{196}\mathrm{Pt}\,(n,\gamma)\,^{197}\mathrm{Pt} \xrightarrow[\beta^-]{19\ \mathrm{hrs}} {}^{197}\mathrm{Au}$$

$$^{198}\mathrm{Pt}\,(n,\gamma)\,^{199}\mathrm{Pt} \xrightarrow[\beta^-]{20\ \mathrm{min.}} {}^{199}\mathrm{Au} \xrightarrow[\beta^-]{3.15\ \mathrm{days}} {}^{199}\mathrm{Hg}$$

The first reaction produces a 77 KeV γ-ray, and was used by Nadkarni and Morrison (1974) for Pt determinations in a noble metal group separation technique. However, the 77 KeV radiation is not recommended here, as it is commonly swamped by Pt Kβ x-rays generated by decay of 192 Ir. The second reaction produces a 158 KeV γ-ray via 199 Au decay, which may be used for Pt determination. However, the interfering reaction:

$$^{197}\mathrm{Au}\,(n,\gamma)\,^{198}\mathrm{Au}\,(n,\gamma)\,^{199}\mathrm{Au} \xrightarrow[\beta^-]{} {}^{199}\mathrm{Hg}$$

also produces 199 Au. At the fluxes and irradiation times employed in this study, irradiation of 1ppb Au produces almost as much 199 Au as irradiation of 1ppb Pt. Platinum determinations via 199 Au require that separate Au and Pt standards be irradiated with the samples, so that an estimate may be made of the contributions of each reaction. Secondary interferences also affect the determination of Pt via 199 Au. Activated Te, which is obviously coprecipitated

with the noble metals, produces a 158 KeV γ-ray via the reaction:

$$^{122}Te\ (n,\gamma)\ ^{123m}Te \xrightarrow[IC]{117\ days} {}^{123}Te$$

At the irradiation conditions and decay times used in this study, 1ppb of Pt produces more than 100x as many 158 KeV γ-rays as 1 ppb of Te (this was determined both by calculations from nuclear data, and by irradiating Te and Pt and comparing the 158 KeV peak heights). Tellurium is less abundant than Pt in peridotites (see, e.g., abundance data in Morgan et al., 1980, and Crocket, 1979), so the interference can normally be ignored within the accuracy of the Pt determinations. Since the half-life of 123m Te is much longer than the half-life of 199Au, a correction for the Te interference could be made by re-counting the smaple after ca. 30 days (i.e., after the 199Au has decayed away); this procedure was not used in the present study. A more significant interference is the broad backscatter peak at 160 KeV produced by the intense 412 KeV 198 Au peak; this interference is best dealt with by maximizing the dimensions of the cave, and by using as high atomic number shielding material as is possible.

Gold is determined via:

$$^{197}Au\ (n,\gamma)\ ^{198}Au \xrightarrow[\beta^-]{2.65\ days} {}^{198}Hg$$

Decay of 198 Au produces an intense 412 KeV γ-ray which suffers no significant interference in normal determinations. However, in chromitites with very high Ir/Au (>1,000), a weak 192 Ir peak at 417 KeV may cause minor interference.

The important reactions for Ir are:

$$^{191}\mathrm{Ir}\,(n,\gamma)\,^{192}\mathrm{Ir} \xrightarrow[\beta^-]{74\ \text{days}} {}^{192}\mathrm{Pt}$$

$$^{193}\mathrm{Ir}\,(n,\gamma)\,^{194}\mathrm{Ir} \xrightarrow[\beta^-]{19\ \text{hrs}} {}^{194}\mathrm{Pt}$$

The first reaction can be used for very sensitive Ir determinations after long, high-flux irradiations and long decay times. At the fluxes and irradiation times utilized in this study, the second reaction provides the most intense Ir peaks immediately after irradiation. The 317 KeV 192 Ir γ-ray may suffer interference from the 320 KeV γ-ray of 51 Cr when small amounts of Cr are coprecipitated with the Te; however, this interference is usually small, even with chromitites. Coprecipitated Cu may cause a broad backscatter peak under the 317 KeV 192 Ir and 328 KeV 194 Ir peaks, due to backscatter of the 64 Cu 511 KeV β^+ annihilation peak; as 64 Cu has a short half-life (ca. 13hrs), this interference is best dealt with by determining Ir via 192 Ir after a suitable decay.

Table II-3 is a comparison of Ir analyses by the 317 KeV 192Ir and 328 KeV 194Ir peaks. For samples R131, 8/16-3, and 8/24-3, analyses by the two different radiations differ by amounts larger than the error predicted by counting statistics (though the maximum discrepancy is only 4.5%); for these three samples, the analyses by the 317 KeV peak are probably slightly in error due to interference from the 320 KeV 51Cr peak and the subsequent over-estimation of the 317 KeV peak background.

TABLE II-3: A COMPARISON OF Ir (ppb) ANALYSES OBTAINED BY DIFFERENT RADIATIONS

Sample	317 KeV 74 day 192Ir	328 KeV 19 hr. 194Ir
R131	5.60 ± 0.10	5.79 ± 0.10
R501	4.56 ± 0.04	4.53 ± 0.03
8/16-3 (chromitite)	137 ± 0.4	143 ± 0.4
8/24-3 (chromitite)	259 ± 0.5	270 ± 0.5

Tables II-4 and II-5 summarize the noble metal and non-noble metal features of the LEPS and Ge(Li) spectra, as well as typical counting times. Sample spectra are given in figure II-2.

TABLE II-4: NOBLE METAL SPECTRA AND COUNTING TIMES

Isotope	$t_{1/2}$	Energy (KeV)	Relative Intensity*	When counted (hrs after radiochem)	Detector	Count length (Kiloseconds)
109 Pd	13.5 hrs	22	100	0 - 12	LEPS	2 - 10
		25 } x-rays	20	-	LEPS	-
		88	-	0 - 12	Ge(Li)	10 - 20
197 Pt	19 hrs	77.4	-	-	Ge(Li)	-
199 Au	3.15 days	158.4	100	24 - 48	Ge(Li)	20 - 50
		208.2	20	-	Ge(Li)	-
198 A	2.65 days	411.8	100	0 - 48	Ge(Li)	5 - 50
		675.9	1	-	Ge(Li)	-
194 Ir	19 hrs	29.4	-	-	LEPS	-
		328.5	100	0 - 24	Ge(Li)	5 - 50
		645.3	8	-	Ge(Li)	-
192 Ir	74 days	65 - 78 (x-rays)	-	-	Ge(Li)	-
		295.9	30	-	Ge(Li)	-
		308.4	30	-	Ge(Li)	-
		316.5	100	24 hrs to 60 days	Ge(Li)	20 - 50
		468.1	50	24 hrs to 60 days	Ge(Li)	20 - 50
		604.1	-	-	Ge(Li)	-

* Most intense peak of each isotope taken as 100.

TABLE II-5: IMPORTANT NON-NOBLE METAL FEATURES OF SPECTRA

Isotope	$t_{1/2}$	Energy, KeV	Comments
51 Cr	28 days	320.1	Weak in most ultramafics; may be as high as Ir peaks in chromitites.
56 Mn	2.6 hrs	846.8 1,811 2,110	May be as strong as Au, Ir peaks immediately after processing.
59 Fe	45 days	1,099.3 1,291.6	Generally weak.
64 Cu	13 hrs	511	May be 1-10x Au peak height immediately after radiochemical processing.
76 As	27 hrs	599.1	Strong in sulfur-rich rocks.
75 Se	120 days	264.6 279.5	Weak. Observed only in sulfur-rich rocks after long decays.
(110M+110)Ag	253 days	657.6 884.5	Ditto.
Cd x-rays	-	23, 26	Seen only if Cd shielding is used on the detector.
Pb x-rays	-	73, 75, 85, 87	From excitation of detector Pb shielding.
U-Th series background	-	80-100	Internal conversion x-rays; may contribute to erratic background in poorly shielded systems.
Backscatter "peaks"	-	≈ 160	Broad peak from 412 KeV 198 Au.
		≈ 300	Broad shelf from 511 KeV 64 Cu.

FIGURE II-2: Noble metal spectra for R501, a lherzolite from the Ronda Ultramafic Complex. The sample weight was 0.513 grams, and the noble metal abundances are 5.8 ppb Pd, 1.25 ppb Au, 4.53 ppb Ir, and 9.6 ppb Pt. The sample was irradiated for 6 hrs. at 8×10^{12} neutrons/cm^2 sec. The LEPS spectrum was taken for 6,000 seconds, beginning *ca.* 16 hrs. after irradiation, and the Ge(Li) spectrum was taken for 40,000 seconds, beginning *ca.* 24 hrs. after irradiation. The largest non-noble metal peak in the spectrum was the 511 KeV annihilation peak (from Cu), which was *ca.* 70,000 counts high.

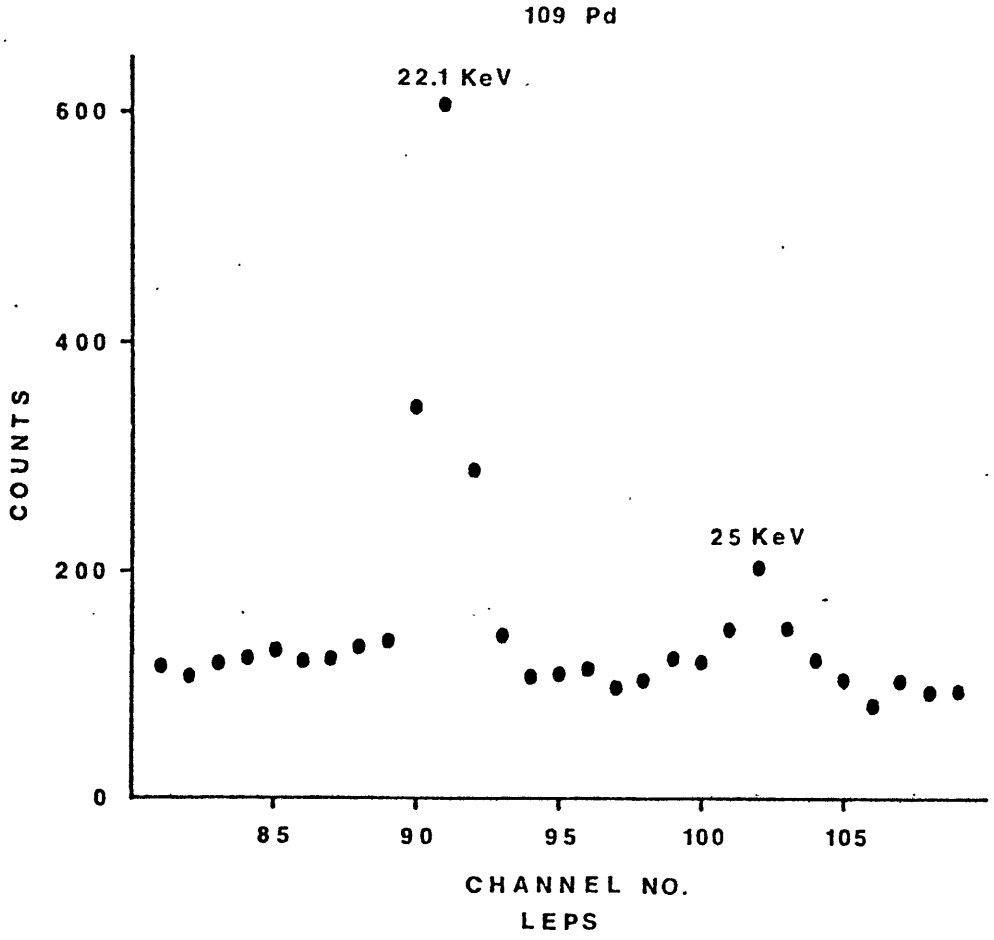
109 Pd
22.1 KeV
25 KeV
600
400
200
0
COUNTS
85
90
95
100
105
CHANNEL NO.
LEPS

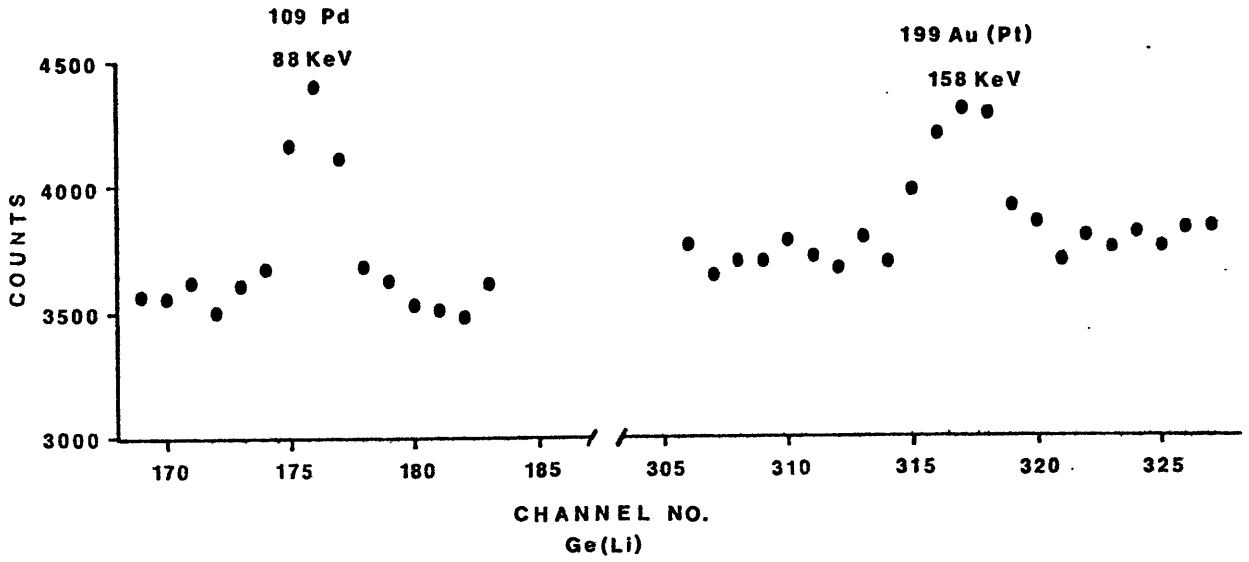
109 Pd
88 KeV
199 Au (Pt)
158 KeV
4500
4000
3500
3000
COUNTS
170
175
180
185
305
310
315
320
325
CHANNEL NO.
Ge(Li)

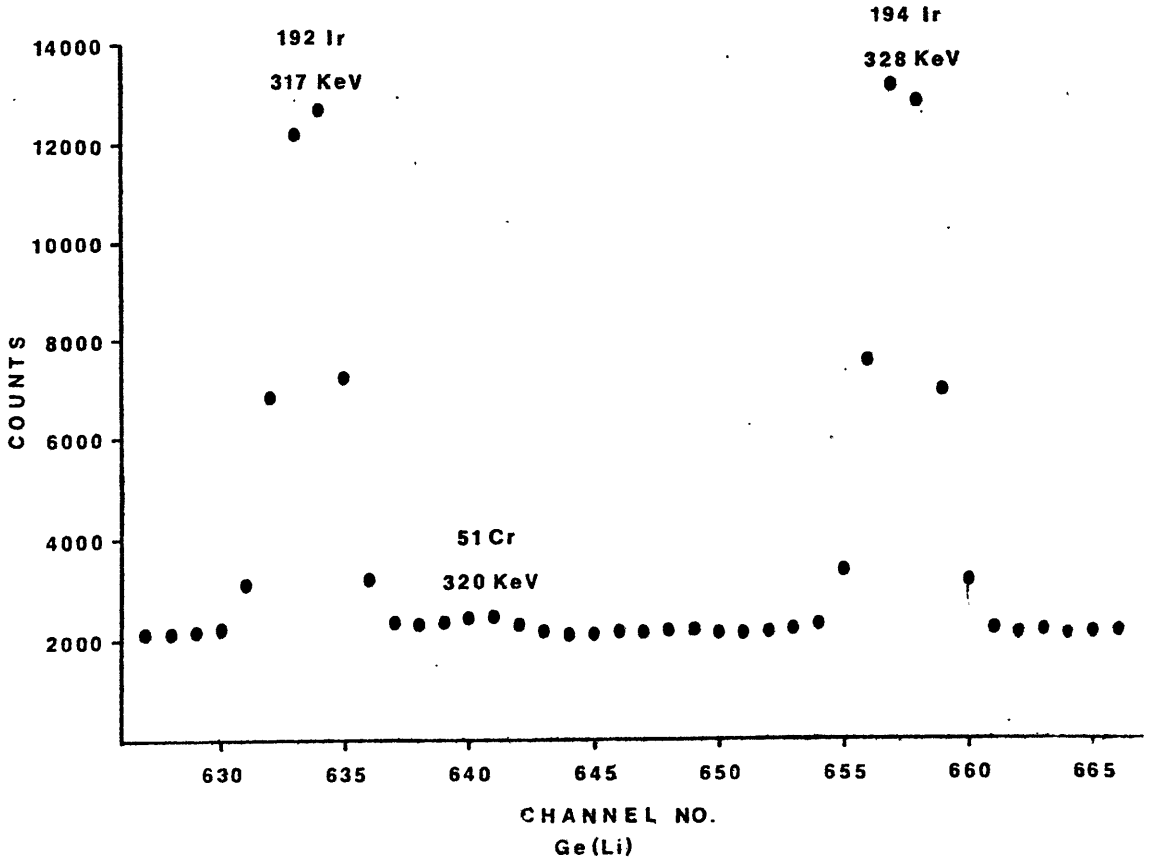
192 Ir
317 KeV
194 Ir
328 KeV
51 Cr
320 KeV
14000
12000
10000
8000
6000
4000
2000
COUNTS
630
635
640
645
650
655
660
665
CHANNEL NO.
Ge(Li)

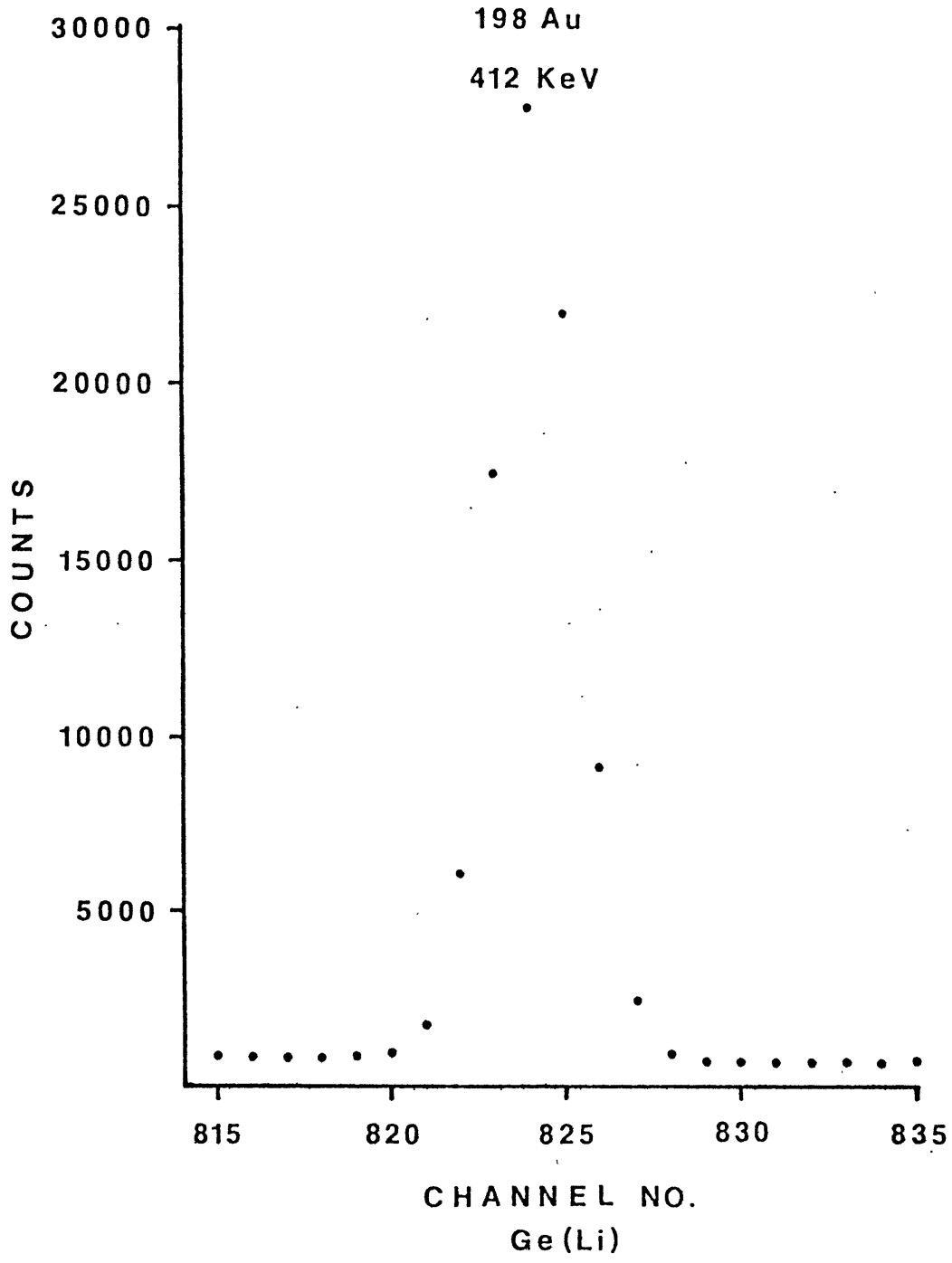
198 Au
412 KeV
30000
25000
20000
15000
10000
5000
COUNTS
815
820
825
830
835
CHANNEL NO.
Ge(Li)

CHAPTER III: NOBLE METAL GEOCHEMISTRY OF THE RONDA ULTRAMAFIC COMPLEX AND THE JOSEPHINE PERIDOTITE

Alpine ultramafics are probably the best mantle samples for determining the abundances of noble metals in the mantle, and for determining the behavior of the noble metals during partial melting. When compared to peridotitic nodules from basaltic rocks and kimberlites, alpine ultramafics tend to show more systematic interelement abundance correlations, and are more often amenable to simple interpretations as residues remaining after the extraction of basaltic melts from fertile* mantle (Frey, 1982). There are, however, few studies of noble metals in alpine ultramafics, primarily because the part-per-billion concentration levels are far below the detection limits of commonly available analytical techniques. None of the previous studies has attempted to examine in detail the geochemical relationships between the noble metals and other elements.

This chapter reviews the geochemistry and geology of two alpine ultramafic bodies, the Ronda Ultramafic Complex in Spain, and the Josephine Peridotite in Oregon,

---

* "Fertile" is used in this work to denote mantle sufficiently enriched in the magmaphile elements (e.g. Ca, Na, Al) so as to produce a basaltic liquid upon 20-30% partial melting; i.e., mantle such as "pyrolite" (Green and Ringwood, 1967).

and presents Au, Pd, Pt, and Ir analyses for ultramafic and mafic rocks from these bodies. Sections III-1 and III-3 are concerned with peridotites, the rocks which make up over 90% of the two complexes. Sections III-2 and III-4 deal with the less common, but geochemically significant rock types; the Ronda "mafic layers," and the Josephine chromitites. Correlations of noble metals with other elements are used to determine the geochemical behaviour of the noble metals, and the results are interpreted in terms of partial melting and fractional crystallization processes in the mantle.

III-1: THE RONDA ULTRAMAFIC COMPLEX

Introduction

The Ronda Ultramafic Complex is a large alpine-type peridotite body in southern Spain (Orueta, 1917; Dickey, 1970; Figure III-1). The present form of the body is interpreted as a nappe (Lundeen, 1976); the original emplacement of the body in the crust has been attributed to diapirism (Loomis, 1972). However, on the basis of Mg/Fe and Al diffusion rates in olivine and clinopyroxene, Obata (1980) estimates that the ascent of the body was too fast for diapirism, and interprets the emplacement as aided by "tectonic forces". Loomis estimated the contact emplacement temperature of the body as 800±100C, placing the Ronda in the "high temperature peridotite" category of Green (1967). More than 90% of the complex consists of peridotites, primarily harzburgites and lherzolites with

FIGURE III-1: Location map for samples from the Ronda Ultramafic Complex in Spain.

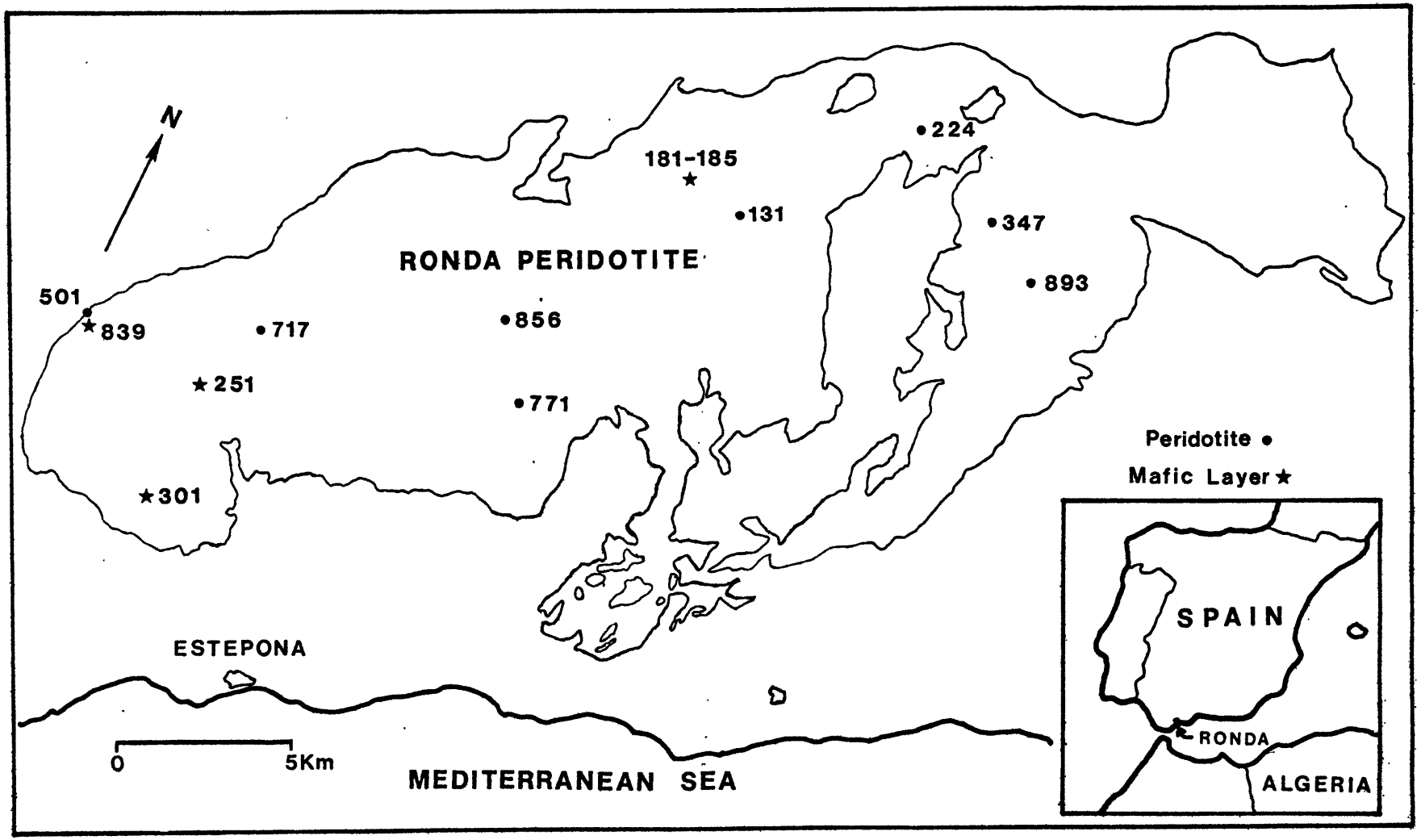
N
224
181-185
131
347
RONDA PERIDOTITE
893
501
839
717
856
251
771
301
Peridotite •
Mafic Layer ★
SPAIN
ESTEPONA
RONDA
ALGERIA
0
5Km
MEDITERRANEAN SEA

minor dunites; ca. 5% of the complex consists of "mafic layers" which are picritic to basaltic in composition. Dickey (1970) originally interpreted the mafic layers as primitive basalts derived by partial melting of the adjacent peridotites, but the mafic layers have been subsequently interpreted as complex accumulates* of partial melts (Suen, 1978; Obata, 1977, 1980). Four peridotite facies (Obata, 1980) may be mapped across the complex on the basis of the peridotite and mafic layer mineralogies, namely: the garnet lherzolite facies (highest pressure), seiland and ariegite subfacies of the spinel lherzolite facies, and the plagioclase lherzolite facies (lowest pressure). The average Ronda peridotite contains ca. 60% olivine by volume, 20% orthopyroxene, 5% clinopyroxene, 10-15% serpentine, and depending on facies, minor amounts of spinel or feldspar or up to 12% garnet (Obata, 1977). Sulfides, largely pyrrhotite, pentlandite, and chalcopyrite, make up less than 0.03% of the average peridotite.

Compared with rocks from harzburgitic alpine complexes which lack metamorphic aureoles (e.g., the Josephine Peridotite), the average Ronda peridotite contains more Ca, Al, Na, and other elements which are abundant in basaltic

---

* The term "accumulates" is used in this work to denote rocks which form as precipitates from silicate melts. Such rocks may be true cumulates, which underwent gravitational settling, or may be encrustations on the walls of magma conduits.

magmas (Table III-1). Indeed, it has been postulated that oceanic tholeiitic basalts are derived by partial melting of mantle rocks similar to the Ronda lherzolites (Frey and Suen, 1982; Ernst and Piccardo, 1979). The Ronda peridotites exhibit highly systematic interelement abundance correlations, and these trends may be interpreted as resulting from the removal of varied amounts of mafic melt from an initially homogeneous lherzolite source (Suen, 1978; Frey and Suen, 1982). Furthermore, the Ronda peridotites, on a chondrite-normalized basis, are depleted in light rare earths, as expected for residues from the removal of basaltic melts (Suen, 1978; Frey and Suen, 1982). The constancy of compatible element (e.g. Ni) contents in the Ronda peridotites makes an origin by fractional crystallization seem unlikely (Suen, 1978). Thus, it is likely that the geochemical variations seen in the Ronda peridotites result from the removal of varied amounts of basaltic melts from a fertile lherzolite source.

Noble metal analyses and interelement correlations

Analyses of Au, Pd, Pt, and Ir in eight Ronda peridotites are given in Table III-2, along with selected analyses for major and minor elements. The analyzed samples consist of four lherzolites (R717, R501, R224, R131) and four harzburgites (R347, R856, R771, R893); petrographic descriptions of these samples are given in Obata (1977), Suen (1978), and Frey and Suen (1982), and sample locations are given in figure III-1. Noble metal analyses were

TABLE III-1: Comparison of Peridotite Compositions (in wt.%)

	SiO_2	TiO_2	Al_2O_3	Cr_2O_3	FeO*	MgO	MnO	CaO	Na_2O	Volatiles
Primitive mantle estimate[a]	45.14	0.22	3.97	-	7.82	38.3	0.13	3.50	0.33	-
Ronda Peridotite R717[b]	44.86	0.17	3.93	0.37	8.26	37.73	0.14	3.56	0.31	-
Ronda peridotite average[b]	42.2	0.083	2.56	0.35	7.66	39.5	0.13	2.27	0.19	4.49
Josephine harzburgite average[c]	42.7	0.04	0.58	0.19	7.88	44.5	0.13	0.83	-	2.58
Josephine harzburgites[d]	-	-	-	0.42	-	-	-	0.69	0.021	-

* all Fe as FeO

a) Jagoutz et al. (1979).

b) Average of 15 harzburgites and lherzolites (Frey and Suen, 1982).

c) Average of 5 harzburgites (Himmelberg and Loney, 1973).

d) Average of 8 harzburgites and 1 dunite, this study.

TABLE III-2: Ronda Peridotites

Noble Metal[a] Analyses and Selected Major[b] and Minor[c] Element Analyses

Sample	Pd	Au	Ir	Pt	CaO	Na_2O	TiO_2	Sc	Cu	Ni	Mg/(Mg+Fe)	Volatiles
R717	6.1 (0.4)[d]	1.67 (0.01)	4.82 (0.04)	9.4 (1.3)	3.37	0.29	0.16	16	27	1920	0.891	5.32
R501	5.8 (0.4)	1.25 (0.01)	4.53 (0.03)	9.6 (1.2)	2.77	0.25	0.10	14	27	1950	0.897	8.03
R224	4.7 (0.3)	0.95 (0.02)	6.68 (0.06)	9 (3)	2.65	0.26	0.06	13	23	2150	0.898	2.12
R131	5.8 (0.4)	2.04 (0.02)	5.8 (0.1)	15 (3)	2.43	0.19	0.19	12	17	2150	0.893	3.35
R856	2.2 (0.2)	0.240 (0.003)	4.93 (0.05)	3.5 (0.6)	1.68	0.10	0.03	10	1	2330	0.909	2.39
R347	3.1 (0.3)	0.63 (0.01)	5.8 (0.1)	4.5 (1.5)	1.45	0.11	0.05	11	7	2370	0.906	1.96
R771	1.8 (0.1)	0.200 (0.004)	3.4 (0.1)	6.3 (1.0)	1.11	0.05	0.005	8	4	2350	0.916	8.75
R893	1.1 (0.3)	0.250 (0.005)	4.3 (0.1)	5.7 (1.2)	0.70	0.03	0.01	7	6	2380	0.913	8.95

All analvses except Mg/(Mg+Fe) are on undried samples.

a) Pd, Au, Ir, and Pt in ppb.
b) CaO, Na_2O, TiO_2 and volatiles (= H_2O^- + H_2O^+ CO_2) in wt.%
c) Sc, Cu and Ni in ppm.
d) Value in parentheses is 1σ counting statistics error, including errors in standard, backgrounds, and yield determinations.

obtained bv the radiochemical method outlined in the previous chapter; analvses of other elements were made by x-ray fluorescence (XRF) in the laboratory of Dr. B.W. Chappell at Australian National University (Frey and Suen 1982). However, rock powders analyzed in this study were not splits of the powders analyzed by Chappell, but were prepared fresh from slabs of the same rocks. Preparation of fresh powders was necessary for two reasons: first, the samples analyzed by Chappell were ground in a tungsten carbide ball mill, and the resulting tungsten contamination interfered with the radiochemical noble metal determination; and second, jewelry was worn by the person who prepared Chappell's samples, making contamination with Au, Pd, and Pt likely. Samples analyzed in the present study were scrubbed with silicon carbide to remove surface contamination, ground in a steel shatterbox, and never allowed to come in contact with jewelrv.

Correlations among the noble metals and other elements are illustrated in Figure III-2. Palladium and Au correlate positively with incompatible elements such as Ca, Na, Ti, and Sc, correlate negatively with Ni and the Mg/(Mg + Fe) molar ratio, and are depleted in the most refractory harzburgite, R893, by a factor of ca. 6 relative to the lherzolite R717. The data for Pt are less systematic, but the low-Ca rocks appear to be depleted by a factor of ca. 2 relative to the lherzolites. Iridium shows no systematic depletion or correlation with any element.

FIGURE III-2: Interelement plots for the Ronda peridotites. Where negative correlations are evident (e.g., Pd vs. Ni, Pd vs. Mg/(Mg + Fe)), the concentrations have been re-calculated on a volatile-free basis; for positive correlations, corrections for volatiles have very little effect on the correlation coefficient. Vertical lines are $\pm 1\sigma$ error bars from counting statistics; error bars for Au and Ir are very small on the scale of the plots.

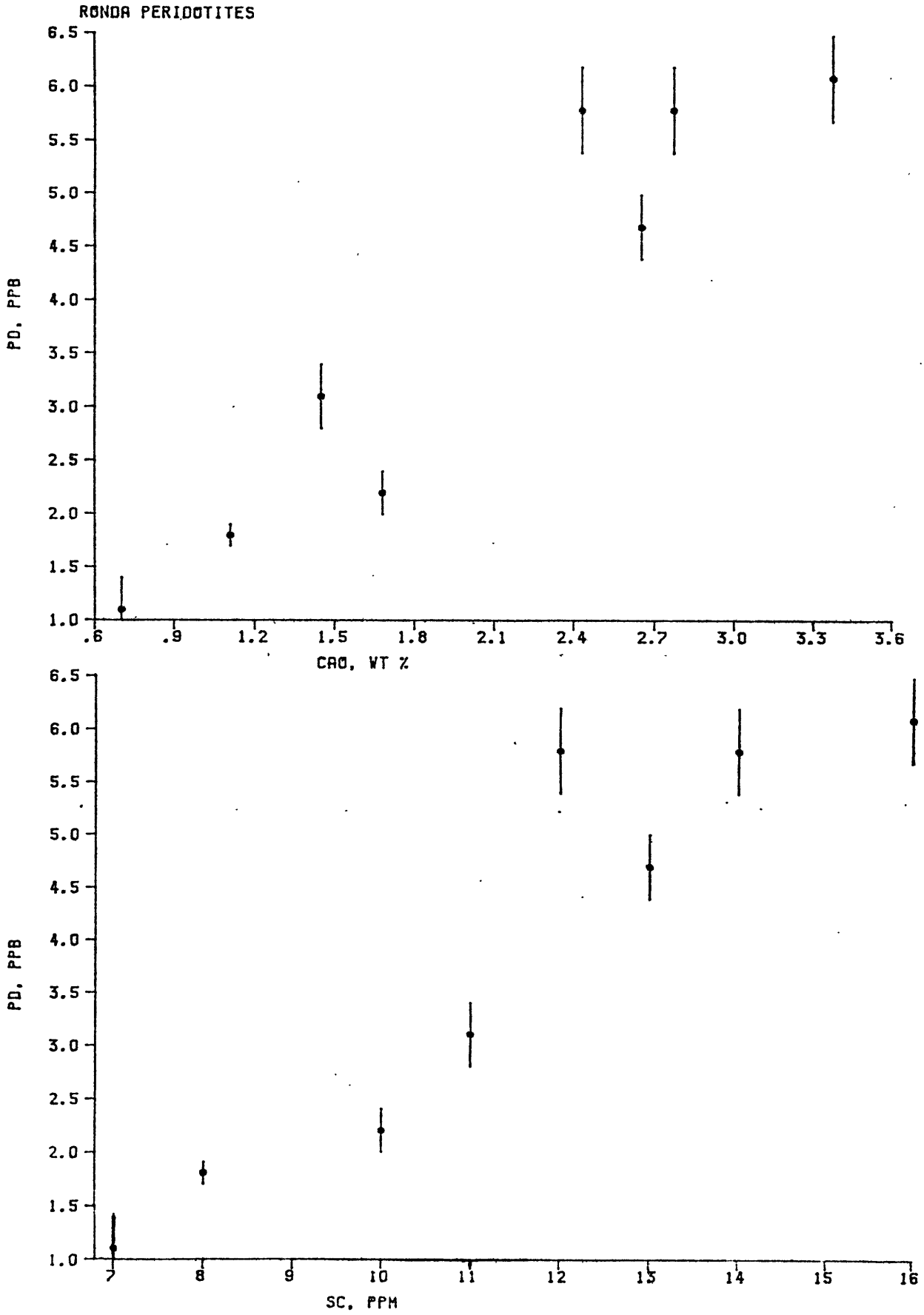
RONDA PERIDOTITES
PD, PPB
6.5
6.0
5.5
5.0
4.5
4.0
3.5
3.0
2.5
2.0
1.5
1.0
.6
.9
1.2
1.5
1.8
2.1
2.4
2.7
3.0
3.3
3.6
CAO, WT %
PD, PPB
SC, PPM
7
8
9
10
11
12
13
14
15
16

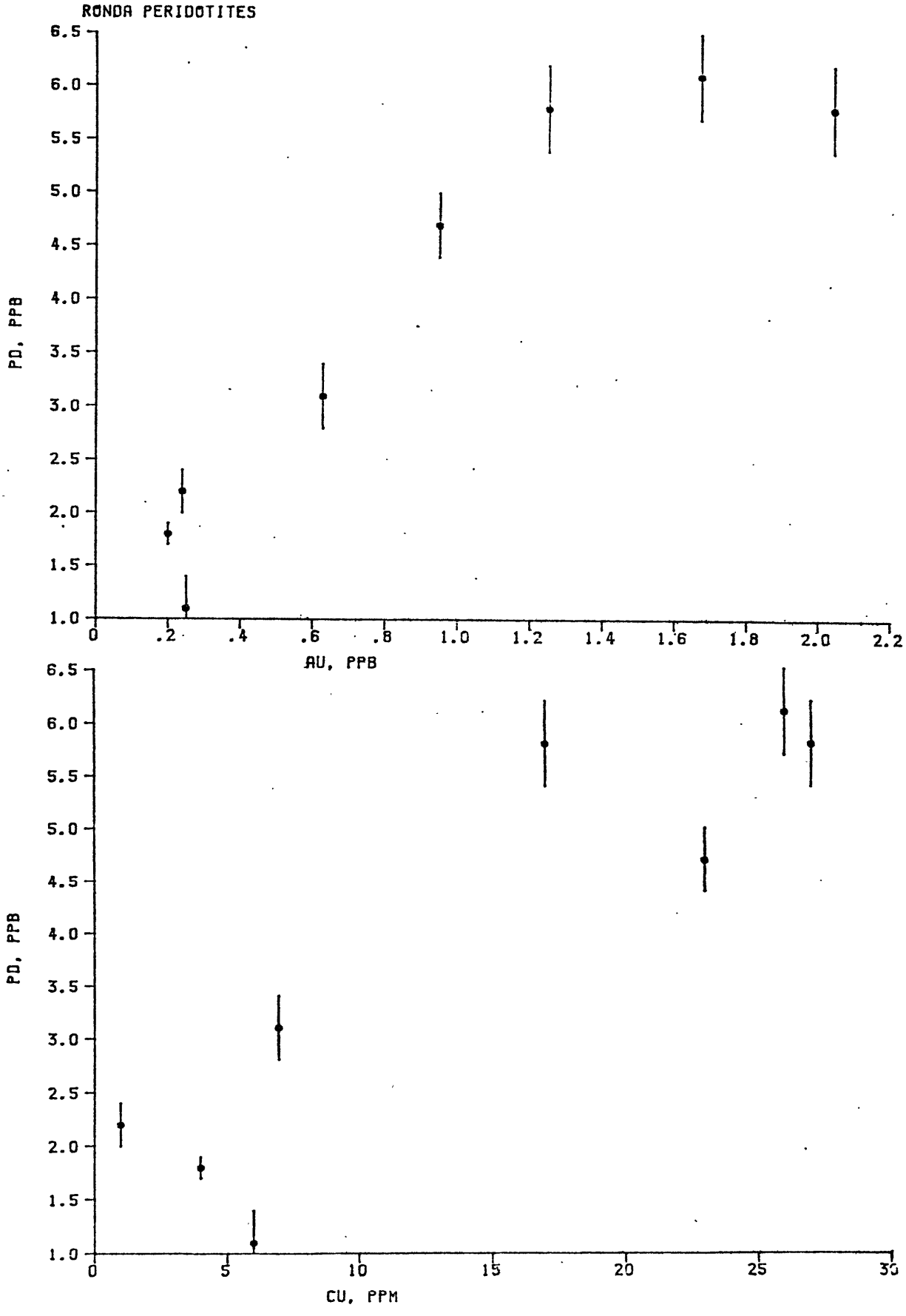
RONDA PERIDOTITES
PD, PPB
AU, PPB
PD, PPB
CU, PPM

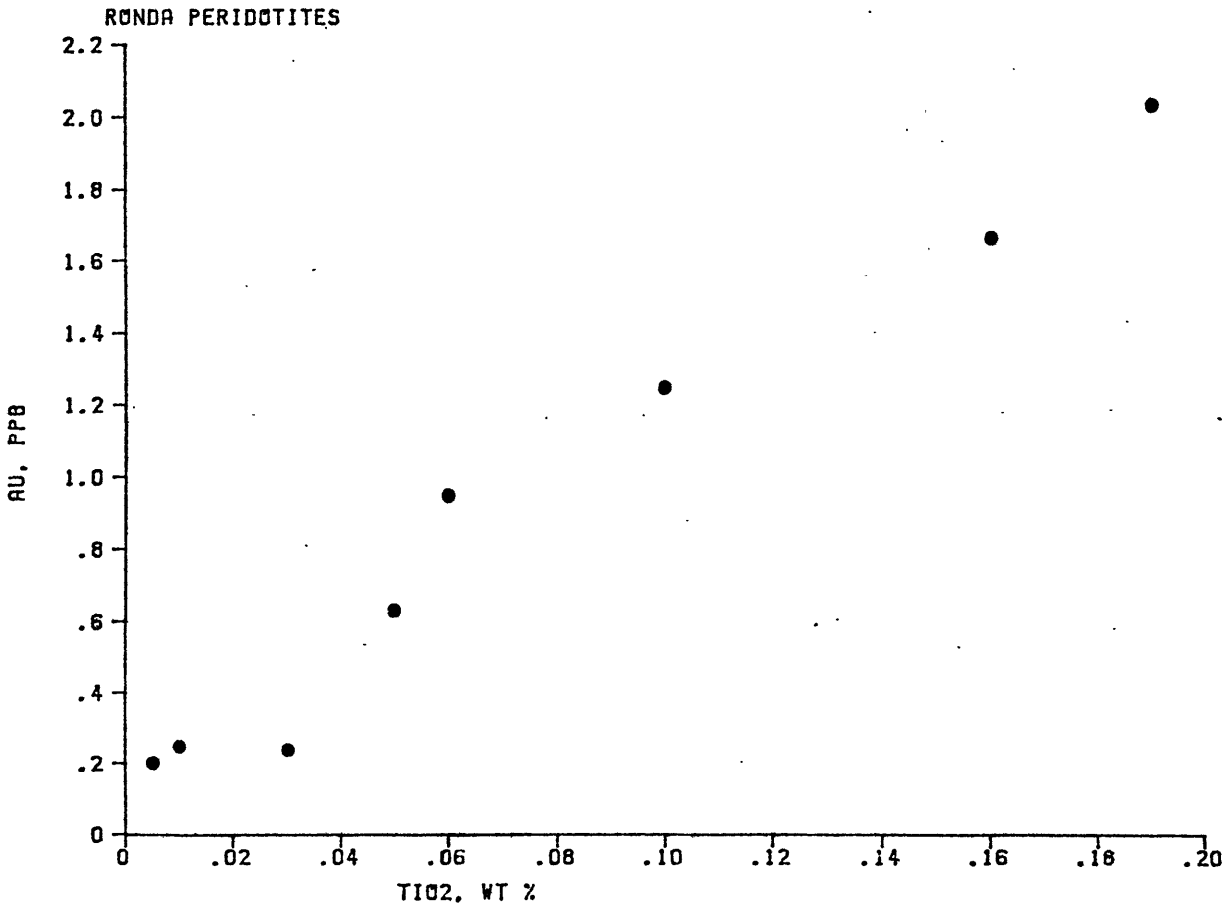
RONDA PERIDOTITES
AU, PPB
2.2
2.0
1.8
1.6
1.4
1.2
1.0
.8
.6
.4
.2
0
0
.02
.04
.06
.08
.10
.12
.14
.16
.18
.20
TIO2, WT %

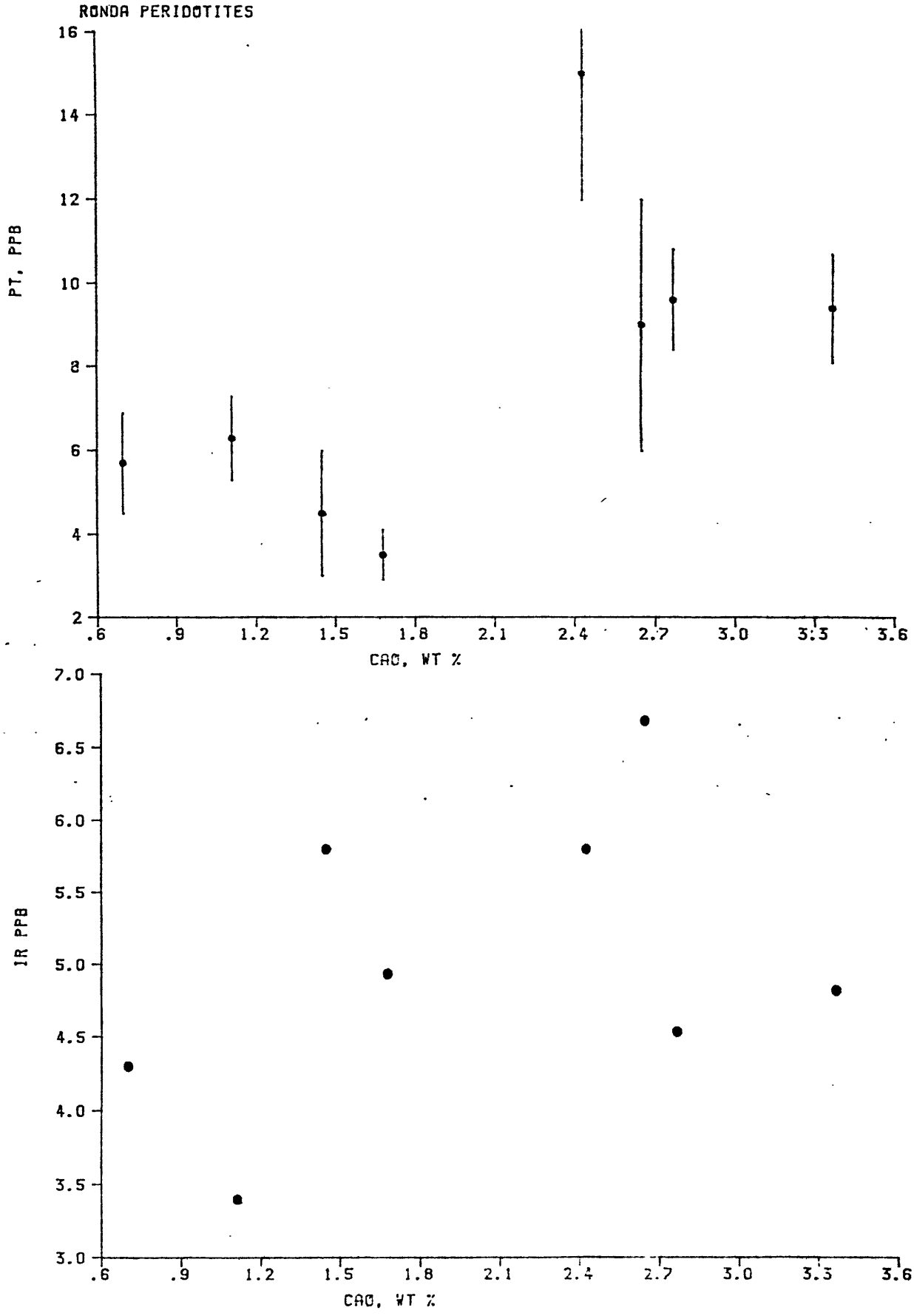
RONDA PERIDOTITES
PT, PPB
16
14
12
10
8
6
4
2
.6
.9
1.2
1.5
1.8
2.1
2.4
2.7
3.0
3.3
3.6
CAO, WT %
IR PPB
7.0
6.5
6.0
5.5
5.0
4.5
4.0
3.5
3.0
.6
.9
1.2
1.5
1.8
2.1
2.4
2.7
3.0
3.3
3.6
CAO, WT %

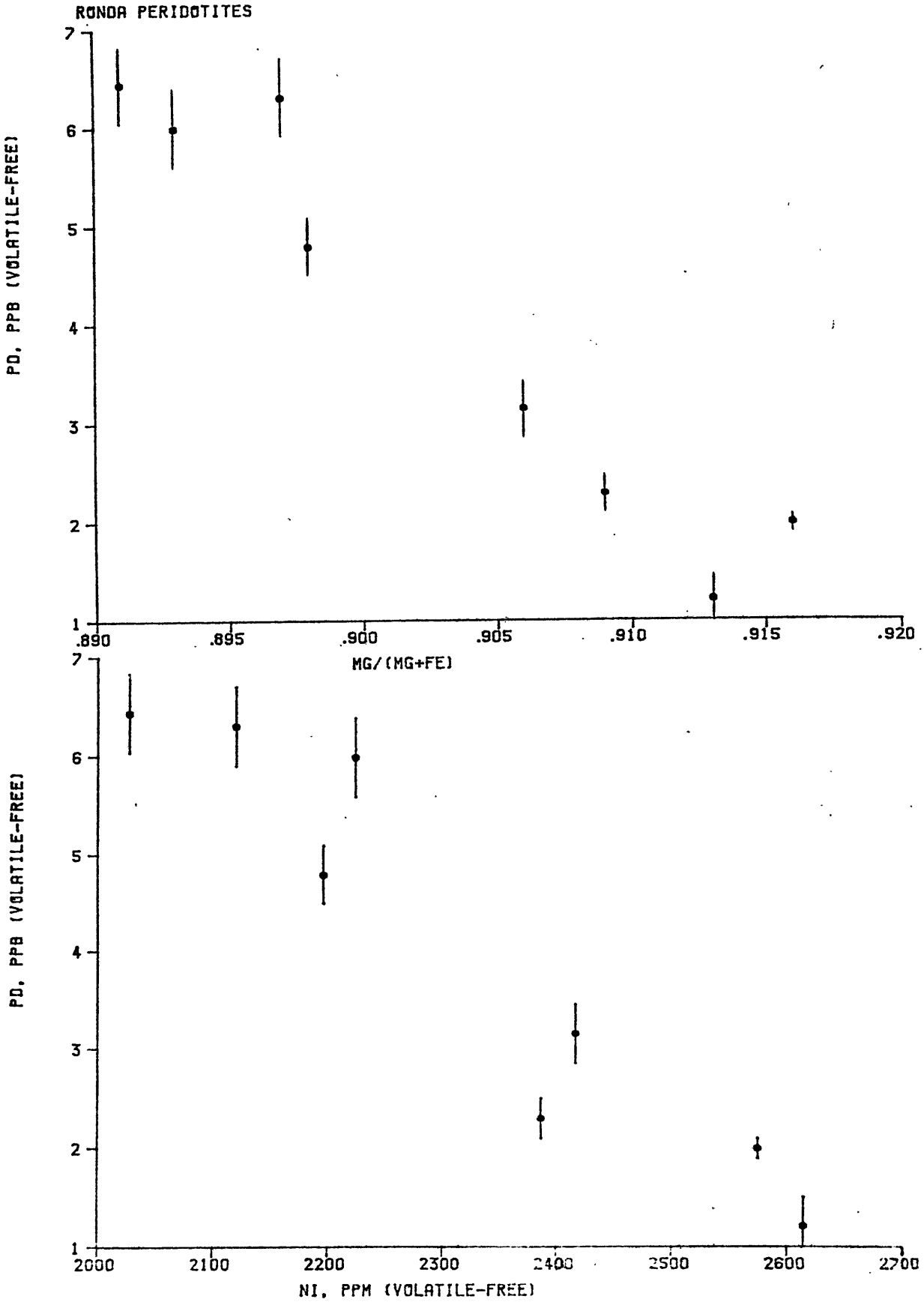
RONDA PERIDOTITES
PD, PPB (VOLATILE-FREE)
7
6
5
4
3
2
1
.890
.895
.900
.905
.910
.915
.920
MG/(MG+FE)
PD, PPB (VOLATILE-FREE)
7
6
5
4
3
2
1
2000
2100
2200
2300
2400
2500
2600
2700
NI, PPM (VOLATILE-FREE)

Sample R131 deviates from a number of the correlations; this sample is anomalous in many respects, possessing a convex-up chondrite normalized REE pattern and abnormally high Ti; R131 was sampled close to a mafic layer, and is perhaps contaminated with material from the layer (Frey and Suen, 1982).

The chondrite-normalized noble metal patterns of the Ronda lherzolites and harzburgites are given in figure III-3. The Ronda harburgites are all depleted in Pt, Pd, and Au relative to the lherzolites, and the extent of the depletion increases slightly in the order Pt-Pd-Au. However, the Ir abundances of the harzburgites and lherzolites are not significantly different. As the harzburgites are interpreted as residues after the partial melting of lherzolites, it appears that partial melting must produce a fractionation of the noble metals, such that Pt, Pd, and Au are enriched in the melt relative to Ir, in accordance with the predictions of section I-3.

Mantle noble metal abundances and the significance of chondritic noble metal ratios

The noble metal abundances of the Ronda lherzolites are ca. 10^{-2} x the abundances in C1-carbonaceous chondrites, and are within a factor of 2 of recent estimates of the noble metal abundances of the primitive mantle (table III-3). The Ronda lherzolites and Kilbourne Hole lherzolite nodules have similar noble metal abundances (table III-3), as well as similar major element and rare earth abundances and ratios

FIGURE III-3: Chondrite-normalized noble metal abundances for the Ronda lherzolites and harzburgites (stippled) and two Ronda mafic layers (R839 and R181). The stippled regions are the ranges for the peridotites, while the bold lines in the stipple regions are the averages.

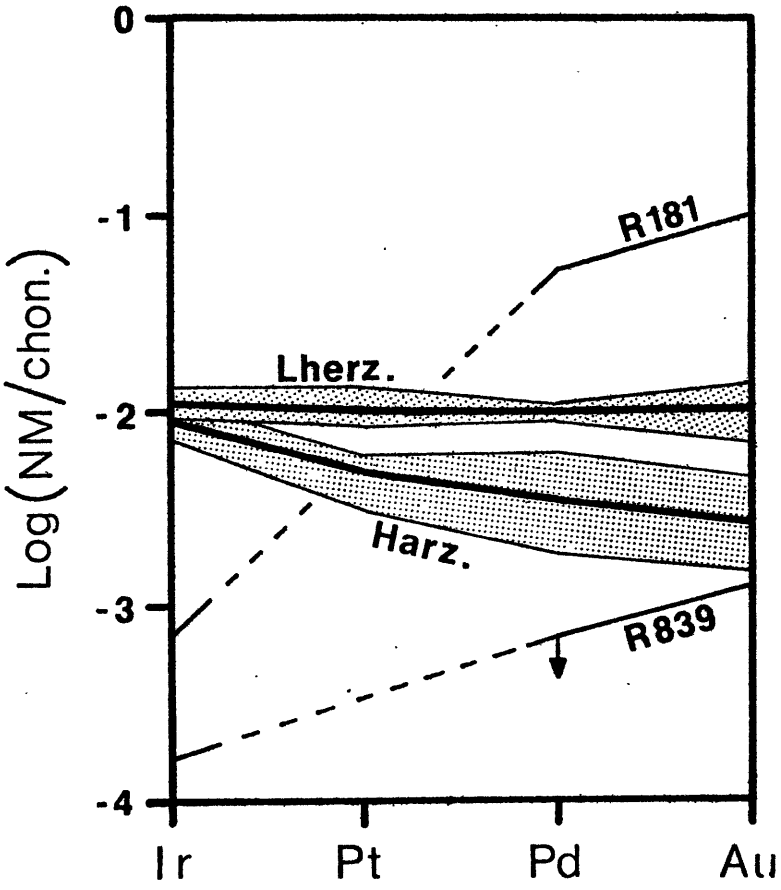
0
-1
-2
-3
-4
Log(NM/chon.)
R181
Lherz.
Harz.
R839
Ir
Pt
Pd
Au

TABLE III-3: Comparison of Noble Metal Abundances (ppb) in Lherzolites and Primitive Mantle Estimates

	Ir	Pt	Pd	Au	Pt/Ir[a]	Pd/Ir[a]	Au/Ir[a]
Average of Ronda lherzolites, volatile-free (this study)	5.7	11	5.9	1.6	1.93	1.04	0.28
Average of Kilbourne Hole lherzolite nodules[b]	3.7	-	5.7	0.99	-	1.54	0.27
"Pyrolite"[c]	3.0	-	8.2	3.0	-	2.73	1.00
"Pyrolite"[d]	3.0	-	4.3	0.9	-	1.43	0.30
C1-carbonaceous chondrites[e]	510	1110	570	140	2.17	1.11	0.27

a) Last digit of ratios may not be significant, but is given to prevent round-off errors.

b) Morgan et al. (1980).

c) Chou (1978).

d) Mitchell and Keays (1981).

e) Crocket et al. (1967).

(Morgan et al., 1980); the Kilbourne Hole noble metal analyses are the most consistent and reproducible nodule noble metal analyses, and are regarded by this author as the best nodule-based estimates of the mantle noble metal abundances. The noble metal ratios of the Ronda lherzolites are, within analytical error, the same as the ratios in C1-carbonaceous chondrites; in fact, the Ronda lherzolites have more nearly chondritic noble metal ratios than the primitive mantle estimates (table III-3). Hence, this study confirms previous suggestions (Chou, 1978; Arculus and Delano, 1981) that the noble metal ratios of the primitive mantle are nearly chondritic.

The significance of the absolute abundances and chondritic ratios of noble metals in the primitive mantle, in terms of the evolution of the core-mantle system, is not clear. Core-mantle equilibirum models predict mantle noble metal abundances of less than 10^{-3} x chondrites, and non-chondritic noble metal ratios (Chou, 1978; Arculus and Delano, 1981). These models are based on the speculations that the core is essentially Fe-Ni, the mantle is essentially silicate, and that the (silicate mantle)/(Fe-Ni core) partition coefficients should be small (10^{-4}-10^{-5}) and significantly different among the noble metals. It is notable that of all the noble metals, silicate/(Fe-Ni) partition coefficients are known only for Au (ca. $3x10^{-5}$, Kimura et al., 1974).

The most widely accepted explanation for the discrepancies between the predictions of the core-mantle equilibrium models, and the observed noble metal abundances and ratios of the mantle, is that the earth was subjected to a meteoritic bombardment after core separation. This meteoritic component is supposed to have been retained in the mantle, and to be the major source of the present mantle noble metal abundances (Arculus and Delano, 1981). However, Mitchell and Keays (1981) have pointed out that the use of (silicate)/(Fe-Ni) partition coefficients to describe core-mantle equilibrium is probably unrealistic, as most of the mantle noble metal content is not in silicates, and is apparently in sulfides. Mitchell and Keays suggest that the mantle noble metal abundances may reflect equilibrium between the core and mantle sulfides. However, it is doubtful that the mantle noble metal abundances could reflect equilibrium between mantle sulfides and an Fe-Ni core. The average mantle sulfide content, consisting largely of Fe-rich monosulfides, is ca. 0.03 wt.% (based on petrography and sulfur analyses of 17 lherzolite nodules by Morgan et al., 1980, and the average sulfide abundances of the Ronda peridotites, this study). Assuming that the mantle noble metal content is entirely in sulfides, and assuming C1-carbonaceous chondrite noble metal abundances for the bulk earth, and that the 10^{-2} x chondrites noble metal abundances of the mantle reflect equilibrium with the core, the (mantle sulfide)/core distribution coefficient is

calculated to be ca. 10. This calculated distribution coefficient is 30-150 times higher than the (Fe-sulfide)/(Fe metal) distribution coefficients determined by Noddack et al. (1940) for platinum group metals, and hence is unlikely to reflect equilibrium of sulfide with an Fe metal-rich core. The calculated distribution coefficient may, however, reflect equilibrium between mantle sulfide and an oxygen-rich core (such as the "protocore" postulated by Ringwood, 1977); this possibility cannot be tested until noble metal (sulfide)/(metal oxide) distribution coefficients have been determined experimentally.

Amount of melt removed and composition of partial melts of the Ronda peridotites

The amount of melt removed from the Ronda peridotites is important in estimating the noble metal contents of the partial melts derived from the peridotites, and in modeling the behavior of the noble metals during partial melting. Both the amount of melt removed and the composition of the melts can be calculated using mass balance relationships and experimentally determined olivine/melt partition coefficients for FeO and MgO.

It is assumed that each of the Ronda peridotites analyzed in this study is a residue from partial melting of a parent lherzolite with the composition of R717, the most fertile Ronda peridotite. This assumption is based on the similarltiy of the major element composition of R717 and estimates for the composition of the fertile mantle

(table III-1). The weight fractions (W) of an element or oxide in the parent (R717), residue, and melt are related by the mass balance equation (Shaw, 1970):

$$(III\text{-}1) \qquad W_{717} = W_{MELT}F + W_{RES}\,(1-F)$$

where F is the total weight fraction of the parent removed as melt (for the equilibrium or batch melting model W_{MELT} gives the composition of the single melt produced in equilibrium with the residue; however, for the fractional melting model, W_{MELT} is an <u>average</u> over all the extracted increments of melt). The mass balance equations for FeO* (defined as all Fe calculated as FeO) and MgO are, accordingly:

$$(III\text{-}2) \qquad FeO^*_{717} = FeO^*_{MELT}F + FeO^*_{RES}\,(1-F)$$

$$(III\text{-}3) \qquad MgO_{717} = MgO_{MELT}\,F + MgO_{RES}\,(1-F)$$

Equations III-2 and III-3 can be combined to give:

$$(III\text{-}4) \qquad F = 1 - \frac{FeO^*_{717} - \alpha MgO_{717}}{FeO^*_{RES} - \alpha MgO_{RES}}$$

where $\alpha \equiv FeO^*_{MELT}/MgO_{MELT}$

If the compositions of olivines in the peridotites are known, as from electron microprobe analyses, α can be

estimated using the experimentally determined olivine/melt "equilibirum constant" K_D (Roeder and Emslie, 1970):

(III-5) $\alpha \equiv FeO^*_{MELT}/MgO_{MELT} \approx FeO_{MELT}/MgO_{MELT} = (FeO/MgO)_{OLIVINE}/K_D$.

It should be noted that FeO_{MELT} includes only the Fe which actually occurs as Fe^{+2} in the melt, and hence differs from FeO* in proportion to the amount of Fe^{+3} in the melt. As will be shown, Fe^{+3}/Fe^{+2} for the Ronda melts was probably <0.1. For a melt $Fe^{+3}/Fe^{+2} <0.1$, the approximation in equation III-5 causes F to be overestimated by $<5\%$ (that is, an F of 0.250 would be calculated as <0.263), which is acceptable given the other uncertainties in the calculations.

The K_D in equation III-5 is a function of the melt composition and the pressure and temperature of melting. The variation of K_D with composition is apparently not large (Roeder and Emslie, 1970). Primitive basaltic partial melts are expected to be MgO-rich (Clarke, 1970; Stolper et al., 1981; Blanchard et al., 1976), so values of K_D for MgO-rich basalts (16.3-22.0 wt.% MgO; Grover et al., 1980) are used in this study; the assumption of an MgO-rich melt is consistent with the Ronda melt composition calculated below. The Ronda peridotites are interpreted to have melted at pressures of 25-40 Kbar and at 1,500-1,600C (Suen, 1978), which corresponds to a K_D range

of 0.264 to 0.398, including the uncertainty in the experimental determination of K_D given by Grover et al. (1980).

For batch melting, the olivine FeO/MgO in equation III-5 is the olivine composition in the residue at the end of melting. However, for fractional melting, the olivine composition in equilibrium with the melt changes throughout the melting interval from the value in the parent to the value in the final residue, and some average composition must be used to calculate α. However, the variation of olivine compositions in the Ronda peridotites is not great (Fo_{87} to $Fo_{91.5}$; Obata, 1977), and for this study it is adequate to calculate α using both the parent and residue olivine compositions, and hence to bracket the possible range of α for both batch and fractional melting models.

The Fs calculated from equations III-4 and III-5 for two parent-residue pairs (R717-R501; R717-R893) are given in table III-4, along with the melt compositions calculated from equation III-1 (major element analyses used to calculate the melt composition are given in Frey and Suen, 1982). The range of Fs and compositions reflects the range of K_D and olivine compositions used to calculate α. The MgO contents of the melts are high, justifying the use of K_D's for high-MgO basalts. Using the equations of Sack et al. (1980), Fe^{+3}/Fe^{+2} for the melt compositions is calculated to be ca. 0.1 at 1,500-1,600C, 1atm, and the

TABLE III-4: Calculated Amount of Melt Removed (F) and Major Element Compositions (wt.%) of Ronda Melts. Comparison with Possible Primary Magmas from the Mantle

	F	SiO_2	TiO_2	Al_2O_3	FeO*	MnO	MgO	CaO	Na_2O	TOTAL
Calculated Ronda melt (R717-R501)[a]	0.073	52.49	0.96	9.32	10.77	0.28	17.22	10.80	0.84	102.7
	(0.060-0.086)	(53.95-51.02)	(1.11-0.81)	(10.35-8.29)	(11.22-10.31)	(0.30-0.25)	(13.29-21.15)	(12.18-9.41)	(0.94-0.74)	(103.3-102.0)
Calculated Ronda melt (R717-R893)[b]	0.298	50.41	0.56	11.38	9.12	0.19	15.62	10.37	1.00	98.63
	(0.252-0.345)	(51.60-49.21)	0.64-0.48)	(12.98-9.77)	(9.30-8.93)	(0.20-0.18)	(11.08-20.15)	(11.84-8.90)	(0.85-1.14)	(98.78-98.47)
"Primitive" basalt glasses, DSDP legs 2 and 3[c]	-	50.20	0.77	17.0	8.06	0.13	9.96	13.00	1.97	-
"Primitive" basalts, DSDP leg 37 (type IV)[d]	-	47.18	0.72	15.55	9.17	0.14	9.57	11.50	2.35	-
Betts Cove lower lava (aphyric)[e]	-	50.73	0.15	11.91	10.08	-	14.15	10.91	1.89	-
Baffin Island tholeiite[f]	-	45.1	0.76	10.8	10.3	0.18	19.7	9.2	1.04	-

*All Fe as FeO

a) Mean and range (in parentheses) given. First value in parentheses calculated using K_D=3.79, olivine comp. of parent R717 (Fo 89.1); second value calculated using K_D=2.51, olivine comp. of residue R501 (Fo 90.1).

b) First value in parentheses calculated using K_D=0.264, olivine comp. of parent R717; second value calculated using K_D=0.398, olivine comp. estimated for residue P893 (Fo 91.3; using assumption the olivine Mg/(Mg+Fe) = whole rock Mg/(Mg+Fe)).

c) Frey et al. (1974); averages of 3 glasses.

d) Blanchard et al. (1976); averages of 15 type IV olivine phyric basalts.

e) Coish and Church (1979), recalculated on a volatile-free basis.

f) Clarke (1970). Average of 4 picrites without accumulative olivine.

oxygen fugacity of the quartz-fayalite-magnetite buffer (QFM). Higher pressures should lower the Fe^{+3}/Fe^{+2} (Mo et al., 1981), and lower oxygen fugacities (expected for mantle conditions, Arculus and Delano, 1981) should also lower Fe^{+3}/Fe^{+2}; hence the approximation in equation III-5 is justified.

The CaO contents of the two calculated melts in table III-4 are approximately the same, which suggests that the Ronda melt CaO content was relatively constant over a wide range of F; the constancy of melt CaO content is consistent with the linear correlations of CaO with other major element oxides in the Ronda peridotites (Frey and Suen, 1982). On the assumption of constant melt CaO content, F can be calculated for peridotites for which the olivine compositions are not known by the relationship:

$$F = \frac{CaO_{MELT} - CaO_{RES}}{CaO_{717} - CaO_{RES}} \qquad \text{(III-6)}$$

Estimates of F calculated by equation III-6, using the range of CaO compositions for the R717-R893 melt, are given in table III-5.

The calculated major element compositions of the Ronda melts are compared in table III-4 with several literature estimates of primitive mantle melt compositions. Considering the range of melt compositions proposed in the literature, the calculated Ronda compositions are considered to be reasonable, especially for CaO contents. The high

TABLE III-5: Amount of Melt Removed (F) from Ronda Peridotites, from Equation III-6

Sample	F
R717	0
R501	0.078±0.016
R224	0.115±0.022
R131	0.139±0.026
R856	0.219±0.037
R347	0.241±0.039
R771	0.262±0.042
R893	0.298±0.045

SiO_2 content of the Ronda R717-R501 melt is probably an artifact of the calculation process, and the SiO_2 content calculated for the R717-R893 melt is preferred.

Noble metal contents of the Ronda partial melts

The estimated average noble metal abundances of the Ronda partial melt are given in table III-6, along with the noble metal abundances of various basaltic rocks. The noble metal abundances of the Ronda melt have been calculated from the mass balance equation III-1, using the F estimates in table III-5; the abundances calculated from four parent-residue pairs have been averaged to obtain an estimate of the variation. Because of the scatter in the Ronda peridotite Ir analyses, the Ronda melt Ir abundances are poorly constrained.

TABLE III-6: Comparison of Noble Metal Abundances (ppb) in the Ronda Partial Melt and Mafic Rocks

	Pd	Au	Pt	Ir
Average Ronda melt (calculated)	19.0± 1.9	6.0± .9	24± 7	0-10
Ronda mafic layer R181 (this study)	28	14.9	-	0.37
Chilled gabbro margin, Skaergaard[a,b]	17.5	4.6	-	0.26
Calculated Bushveld[a]	-	-	-	0.20
Basal zone gabbro, Stillwater[a]	55	-	12	0.2-0.3
Olivine gabbro, DSDP leg 37[c]	49	34	-	0.49
W-1 diabase (USGS standard)[d]	9-18	4-6	≈18	≈0.3
Sea-floor basalts (mainly tholeiites)[e]	<0.1-6.3 avg<0.7	0.06-67 avg<3	-	<0.0008-0.11 avg<0.03
Continental basalts (mainly tholeiites)[f]	0.33-26 avg=5.5	0.5-11 avg=3.3	-	0.009-0.49 avg=0.1

a) Compilation by Crocket (1979).

b) Skaergaard Au from Vincent and Crocket (1960).

c) Crocket and Teruta (1977).

d) See Chapter II for summary of W-1 data.

e) Crocket and Teruta (1977) and Hertogen et al. (1980).

f) Paul et al. (1979).

The estimated Pd, Au, and Pt abundances of the Ronda melts are roughly comparable with the Pd, Au, and Pt abundances of gabbros and W-1 diabase, and with the upper range of abundances in continental basalts. The Ronda melt Pd and Au abundances are much higher than the average abundances in mid-ocean ridge basalts (MORBs); the difference is largest for Pd, and the Ronda melt Pd abundance is 3x the highest Pd abundance found in MORBs.

The difference between the Pd abundances of the calculated Ronda melt and MORBs is significant in view of the debate about whether MORBs are produced by melting of mantle similar to the Ronda peridotites (Frey and Suen, 1982). It is possible that the Ronda partial melts were parental to MORBs, but were depleted in Pd during ascent by precipitation of sulfide. Mysen and Popp (1980) suggest that precipitation of sulfide during ascent of mantle-derived melts is very likely, due to the strong pressure dependence of sulfur solubility in silicate melts. The sulfide/(basalt melt) partition coefficient for Pd is ca. 1,500 (Keays and Campbell, 1981), so that fractional precipitation of only 0.3 wt.% sulfide from the melt would cause a 100-fold decrease in the melt Pd content from the Ronda melt value to the lowest Pd values found in MORBs.

Models for the behavior of noble metals during partial melting of Ronda peridotites

Mitchell and Keays (1979, 1981) and Keays and Campbell (1981) suggest that base metal sulfide is the major host of noble metals in the mantle, and that the behavior of noble metals during up to 30% partial melting of the mantle is probably controlled by partitioning between residual base metal sulfide and silicate partial melts. This sulfide-silicate melt partitioning model, as well as an alternative model, are discussed below as possible interpretations of the variations in the noble metal abundances in the Ronda peridotites.

The essential requirement of the sulfide-silicate melt partitioning model is that sulfide exist as a residual phase throughout extensive partial melting. This requirement is probably unrealistic for partial melting of the Ronda peridotites, which have small sulfide contents relative to the solubility of sulfur in partial melts at high pressure and temperature. The solubility of sulfur in sulfide-saturated silicate melts is about 1 wt.% at 1,500-1,600C and 25-40kbar (Mysen and Popp, 1980)*, the inferred conditions of melting for the Ronda peridotites (Suen, 1978). The most sulfide-rich Ronda peridotites

---

* Mysen and Popp (1980) determined sulfur solubility on Fe-free systems; sulfur solubility is probably greater in Fe-bearing natural melts (Hoffman et al., 1974).

contain 0.03±0.01 wt.% sulfide*, which corresponds to roughly 0.01 wt.% sulfur; if this sulfur content is truly representative of the sulfur content of the peridotites prior to partial melting, then the entire sulfur content of the peridotites should have been consumed in the first 1% of partial melt, and sulfide should not have existed as a separate phase over most of the 30% melting interival inferred for the peridotites. It might be suggested that all the Ronda peridotites are residues from melting of a much more sulfur-rich source peridotite; however, fertile lherzolite nodules, thought to be representative of the primitive mantle, have sulfur contents similar to the Ronda peridotites (0.010±0.005 wt.% sulfur; based on 17 analyses by Morgan et al., 1980), and there is no evidence for a sulfur-rich fertile mantle source. Hence, the sulfur contents of the initial Ronda peridotites were probably very small, and it is therefore unlikely that sulfide existed as a separate phase during extensive partial melting of the Ronda peridotites.

As an alternative model for the behavior of the noble metals during partial melting of the Ronda peridotites, it is hypothesized that base metal sulfide was the host of the

---

* Determined by measuring areas of sulfides in polished sections of known area. X-ray fluorescence sulfur analyses given by Suen (1978; 0.02-0.03 wt.% sulfur) imply higher sulfide contents (0.05-0.08 wt.%), but are at the detection limit of the technique, and are probably not meaningful.

noble metals at temperatures below the silicate solidus, but with the formation of silicate melts and the disappearance of sulfide, Pd, Au, and possibly Pt were largely dissolved into the silicate melt; the variations in Pd, Au, and Pt contents of the peridotites are interpreted as resulting from retention of varied amounts of silicate melt in the solid residues of partial melting. With the cooling of the peridotites, and crystallization of the trapped melts, sulfide would precipitate from the melts and would probably once again become a major host for the noble metals. This model is consistent with the predicted preference of Pd, Au, and Pt for the melt phase (chapter I) and the experimentally determined high solubility of Pt in silicate melts (0.6 wt.% at 1,600C; Mysen and Popp, 1980), as well as the observation that solid silicates and oxides are not major hosts of the noble metals in mantle peridotites (Mitchell and Keays, 1981). The location of Ir after the disappearance of sulfide is less certain; it is possible that Ir formed refractory PGMs, such as Ir-Os alloys, or partitioned into spinel as suggested by Hertogen et al. (1980), which may account for the apparently compatible behavior of Ir during partial melting.

In the simplest form, the trapped melt model proposed above can be viewed as a mixing model; all the peridotites are interpreted as mixtures of a residue produced by a fixed degree of batch melting (from a single parent composition) with varied amounts of the batch melt. Two melting

parameters are defined; F', the actual weight fraction of the parent rock melted to form the residue, and F, the weight fraction of the melt removed from each peridotite; the difference (F'-F) is the amount of retained or "trapped" melt. It is F which is estimated by mass balance calculations such as those presented earlier in this section; F' is hypothetical, but would probably not exceed 0.40, at which point the residues would consist almost totally of refractory olivine. If this model were correct, all peridotites should fall on a single C_R/Cp versus F curve where C_R is the concentration of a given trace element in each peridotite, and Cp is the concentration in the parent peridotite (taken again as R717). From mass balance considerations (appendix III-A), the equation of the curve is:

$$\text{(III-7)} \qquad \frac{C_R}{C_P} = \frac{[F'-F + (F-FF')\ C_R'/Cp]}{F'-FF'}$$

where C_R' is the concentration in the solid residue produced at F' by batch melting.

The first logical complication on the trapped melt model is to allow F' to vary for different peridotites. In this case, the values of C_R/Cp for different peridotites may fall on any of the family of curves in figure III-4, so that a considerable scatter of data is possible; the only real restrictions are that all the peridotites must fall beneath the curve for the highest reasonable F' (<0.40), and

FIGURE III-4: Hypothetical C_R/Cp curves for the trapped melt model. F' denotes the degree of melting; F is the actual amount of melt removed, so that (F'-F) is the fraction of trapped melt. The lower boundary curve, C_R'/Cp, is the curve generated by the batch melting equation with no trapped melt (F'=F).

Case (A): Curves for a highly incompatible element (bulk D=0.005). Note how the C_R/Cp curves span a broad wedge-shaped region of possible values.

Case (B): Curves for a moderately incompatible element, with the bulk D decreasing from 0.5 at F'=0, to 0.4 at F'=0.1, to 0.3 at F'=0.2, to 0.2 at F'=0.3, to 0.15 at F'=0.4. Note the small region of possible C_R/Cp values (between the C_R'/Cp and F'=0.4 curves). These curves may simulate the behavior of Sc in residues with trapped melt, as the modal proportions change from 20% clinopyroxene, 25% orthopyroxene, and 55% olivine in the source rocks,to 100% olivine at F'=0.4 (assuming D's given by Sun et al., 1979; 1.5,0.4 and 0.15 for clinopyroxene, orthopyroxene, and olivine, respectively).

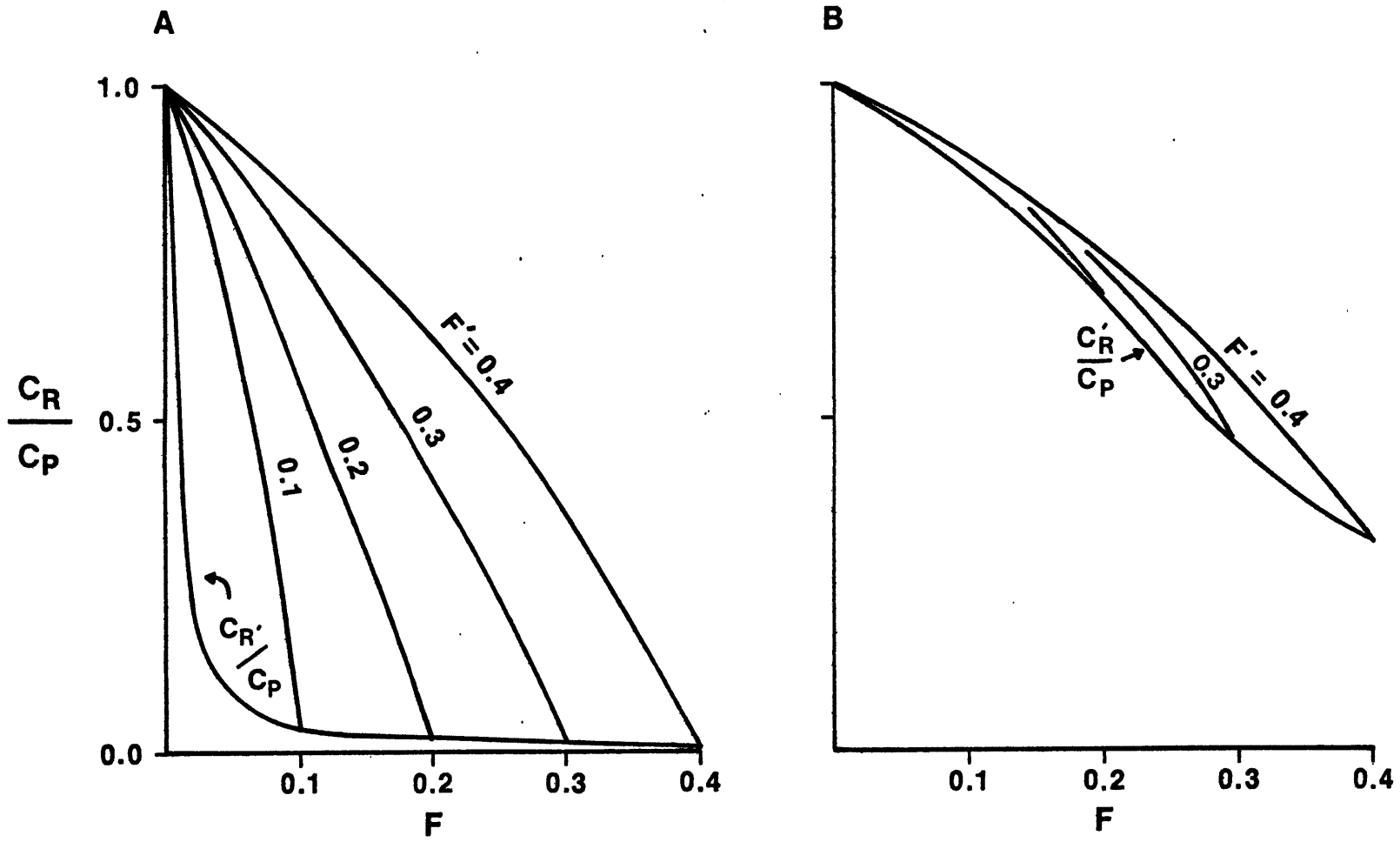
A
1.0
0.5
0.0
$\frac{C_R}{C_P}$
F'=0.4
0.3
0.2
0.1
$C_{R'}/C_P$
0.1
0.2
0.3
0.4
F
B
C'_R/C_P
0.3
F' = 0.4
0.1
0.2
0.3
0.4
F

above the batch melting curve for C_R'/C_P. The batch melting curve for C_R'/C_P is given by the batch melting equation (equilibrium melting equation of Shaw, 1970):

$$(III\text{-}8) \qquad C_R'/C_P = \left(\frac{F'}{D} + 1-F'\right)^{-1}$$

where D is the bulk peridotite/melt partition coefficient for the element being modelled; it is notable that D varies with F' as the proportions of the phases in the residue change. Depending on the slope of the C_R'/C_P curve and the range of F' represented by the peridotites, the C_R/C_P points may nearly fall on a straight line, or may fall in a broad wedge-shaped region (figure III-4).

Additional complications on the trapped melt models can be envisaged. For example, the movement of melt produced at a relatively small F' in one peridotite, into a peridotite residue produced at a larger F', would produce in the latter anomalously high concentrations of highly imcompatible elements (e.g., K and Rb). Alternatively, as the trapped melt solidified in the peridotites, highly incompatible elements would be concentrated in the remaining unsolidified melt; if the remaining unsolidified melt escaped from the peridotite, anomalously low concentrations of highly incompatible elements in the peridotite would result. It is not worthwhile to quantitatively model these complications, but they serve to illustrate how a considerable amount of apparent randomness in trace element data can be caused by processes involving trapped melt.

In figure III-5, C_R/Cp for Pd and Au in the Ronda peridotites are plotted, along with curves generated by equation III-7, on the assumption that C_R' is 0; i.e., that trapped melt was the only phase containing Pd and Au during partial melting. With the exception of R131, the "anomalous" peridotite, all points are within error of curves with F' = 0.2 to 0.4. It is possible that R131 represents a mixture of a residue derived at a relatively large F', with a melt derived elsewhere at a smaller F', and hence has anomalously high concentrations of Pd and Au. The overall fit for Pd could be improved by choosing a parent with slightly more Pd than R717; nevertheless, the simple trapped melt model is considered to be adequate. Similar plots could be produced for Pt and Ir, assuming different C_R'/Cp curves, but due to the scatter in the Pt and Ir data, the plots would probably not be meaningful.

On the basis of detailed melting models for La and Yb, Suen (1978) concluded that the Ronda peridotites contained less than 1% trapped melt during partial melting. As this conclusion negates the trapped melt model proposed above, it is important to consider Suen's (1978) reasoning in detail. Suen's conclusion that there was less than 1% trapped melt depends first on the assumption that the pre-partial melting La content of the Ronda peridotites was 2x chondrites (as opposed to 0.6x chondrites for R717), and second on F values calculated for the peridotites using variations in Yb contents (figures III-3-5 in Suen, 1978). The assumption of

FIGURE III-5: Plots of C_R/C_P vs. F for Pd and Au in the Ronda peridotites. C_P is taken as the concentration in R717. Also plotted are curves generated by equation III-7, assuming different degrees of melting (F'=0.2, 0.3, 0.4) and $C_R'/C_P=0$ (that is, assuming that all the Pd and Au were in trapped melt). The error bars for C_R/C_P are estimated from counting statistics only, and may be conservative.

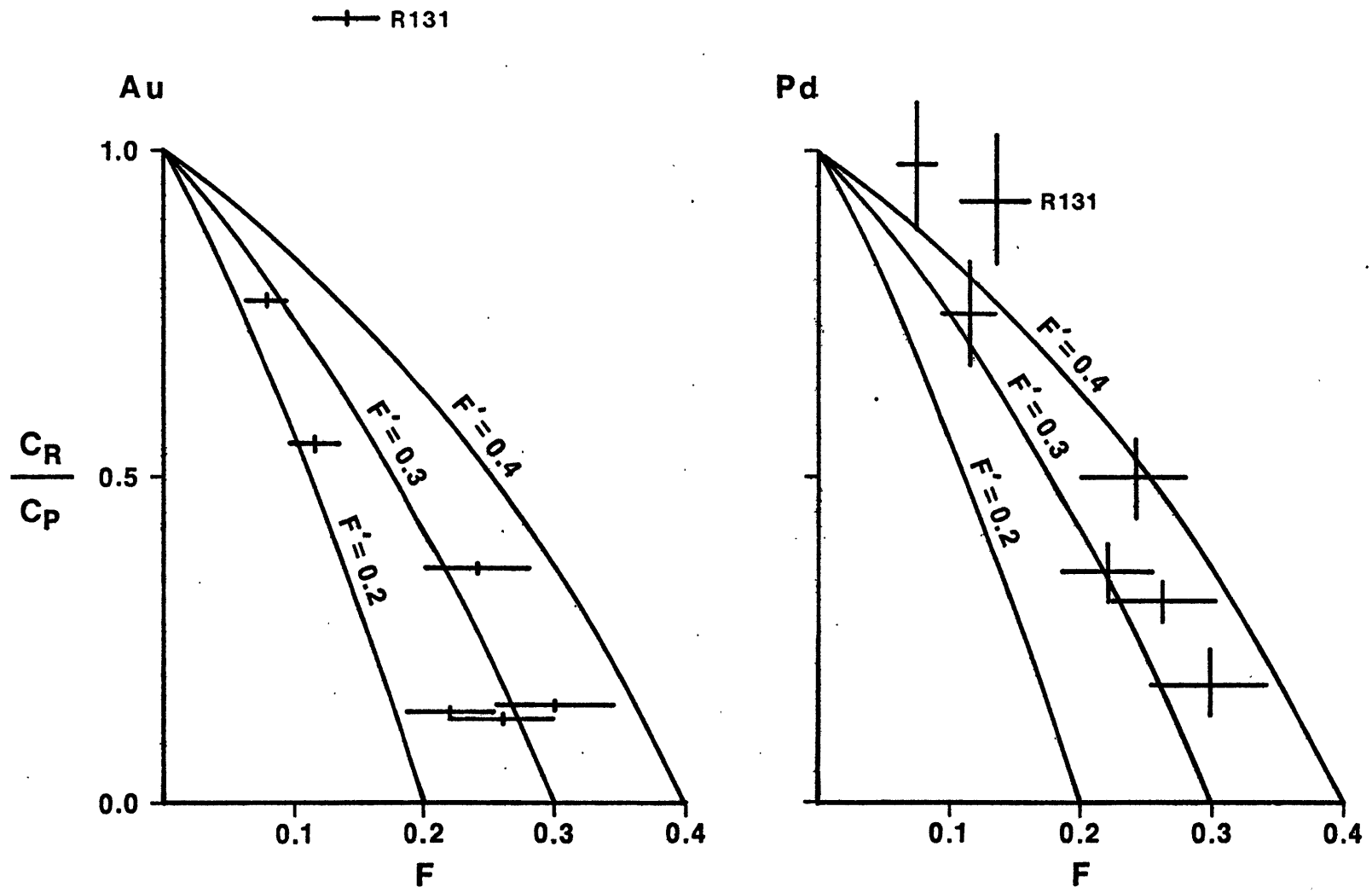
R131
Au
Pd
1.0
0.5
0.0
C_R / C_P
F'=0.4
F'=0.3
F'=0.2
0.1
0.2
0.3
0.4
F
R131

a 2x chondrites La content for the parent peridotite was based on a preliminary model which assumed no trapped melt; hence the conclusion that the peridotites contained little trapped melt is based on somewhat circular reasoning. The Yb-based estimates of F preferred by Suen (figure III-5 in Suen, 1978) are extremely dependent on the choice of Yb mineral/melt partition coefficients and the hypothetical source rock Yb content, and hence are unreliable; in fact, values of F calculated using mass balance and Suen's calculated Ronda melt major element composition are more than a factor of 2 higher than the Yb-based values of F preferred by Suen. Furthermore, the Yb-based estimates were made on the assumption of no trapped melt, again involving somewhat circular reasoning. Hence, Suen's conclusion that the Ronda peridotites contained little trapped melt was really a self-consistent assumption, and was not arrived at independently.

Depending on the composition chosen for the source of the Ronda peridotites, the trapped melt model may actually explain the variations of trace elements other than the noble metals better than batch and fractional melting models involving no trapped melt. As an example, the variation of TiO_2 in the Ronda peridotites (analyses from Frey and Suen, 1982) have been plotted versus the F estimates in figure III-6. Assuming R717 as the source, the composition ranges predicted by fractional and batch melting models assuming no trapped melt are given by the shaded area; the

FIGURE III-6: A plot of C_R/Cp vs. F for TiO_2 in the Ronda peridotites (additional data from Frey and Suen, 1982); Cp is taken as the concentration in R717, and the "anomalous" peridotite, R131, is not plotted. Also plotted is the C_R'/Cp curve, using partition coefficients from Sun et al. (1979; D's for clinopyroxene, orthopyroxene, and olivine are <0.2, 0.05, and 0.01, respectively; the D for garnet is assumed to be <0.2), and assuming the high pressure modes and melting proportions calculated by Suen (1978; initial mode 23% clinopyroxene, 9.5% orthopyroxene, 56% garnet; melting proportions 73% clinopyroxene, -51% orthopyroxene, 8% olivine, 70% garnet). The stippled region gives the values of C_R/Cp predicted for models involving no trapped melt; the curves labeled 0.1, 0.2, and 0.35 give the C_R/Cp predicted for the trapped melt models with F'=0.1, 0.2, and 0.35. The Ti partition coefficients used in the calculations are actually maxima, so that the upper boundary of the stippled area may be at lower C_R/Cp, and the trapped melt model curves for F'=0.1 and 0.2 may fall closer to the C_R/Cp axis, and extend to lower C_R/Cp.

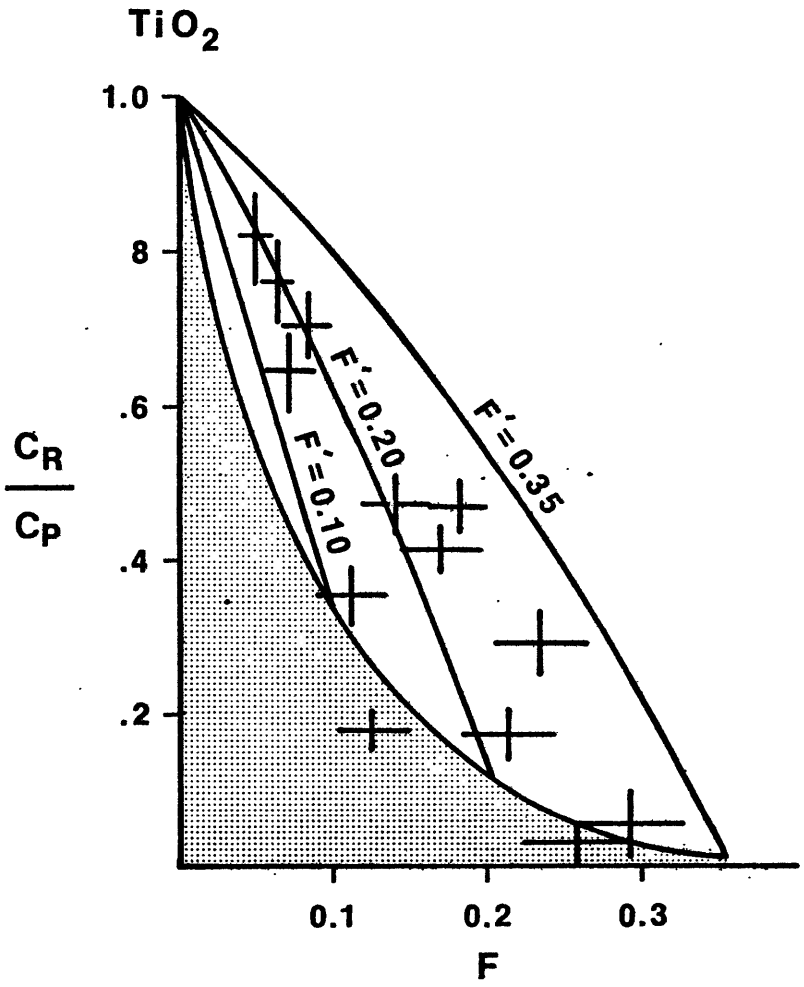
TiO2
1.0
.8
.6
.4
.2
CR/CP
F'=0.35
F'=0.20
F'=0.10
0.1
0.2
0.3
F

compositions predicted by the trapped melt model are given by the curves. While most of the points fall on trapped melt model curves for F' = 0.10 to 0.35, few of the points fall in the region predicted by the models involving no trapped melt.

A justifiable objection to the trapped melt model presented here is that it may not be physically possible to retain ca. 35% melt in residues of partial melting. Various arguments have been presented to show that the mantle could not hold more than 1% trapped melt (e.g., Waff and Holdren, 1977). However, most of these arguments are against the development of a static zone of trapped melt in the low velocity zone, and do not apply to the retention of large amounts of trapped melt in a mantle diapir, which is the preferred interpretation of the Ronda Ultramafic Complex. In addition, early arguments against retention of melt did not consider the decrease in buoyancy of the melt with increasing pressure, due to the high compressibility of the melt (Stolper et al., 1981). In fact, Stolper et al. argue that it may not be possible to segregate even large (>30%) amounts of basaltic melts from the mantle at pressures above 30-40 Kbar, close to the inferred pressure of melting of the Ronda peridotites.

III-2: THE RONDA MAFIC LAYERS

Introduction

The Ronda mafic layers are rocks with approximately basaltic major element composition occurring in the peridotites as millimeter-to meter-thick layers generally parallel to the structural grain of the complex (Dickey, 1970; Obata, 1977, 1980; Suen, 1978). These layers constitute 5-10% of the Ronda Ultramafic Complex by volume. Mineralogically, the layers fall into three groups, namely garnet pyroxenites, spinel pyroxenites and olivine gabbros, reflecting the large scale zonation of the complex into the pressure facies described in section III-1. Dickey (1970) distinguished between "magmatic" and "tectonic" mafic layers; the "magmatic" layers were interpreted as solidified primitive basaltic melts derived by partial melting of the adjacent peridotites, while the "tectonic" layers were interpreted as solid-state segregations of chromian pyroxene, formed during deformation of the peridotite. On the basis of petrological and trace element data, Suen (1978) and Obata (1977, 1980) concluded that most "magmatic" mafic layers do not represent solidified melts, but probably formed as complex accumulates from high pressure fractionation of such melts. In particular, La/Yb of the "magmatic" mafic layers is generally less than or equal to La/Yb for the Ronda peridotites, which is inconsistent with derivation of the layers as partial melts of the peridotites; the few "magmatic" mafic layers with

La/Yb greater than La/Yb of the peridotites have Mg/(Mg+Fe) too high for melts in equilibrium with the peridotite olivines. In addition, Obata (1977, 1980) found that one mafic layer did not have olivine on the liquidus above 9 Kbar, and hence this layer could not represent a liquid in equilibrium with the peridotites at the inferred pressures of partial melting (ca. 35 kbar; Suen, 1978). On the basis of interelement correlations, Suen (1978) interpreted most of the "magmatic" mafic layers as successive accumulates of melts undergoing fractional crystallization, such that the Cr-and Ni-rich, high Mg/(Mg+Fe) layers represent early, high temperature accumulates, while the Cr-and Ni-poor, low Mg/(Mg+Fe) lavers represent later, lower temperature accumulates. Both Obata (1977, 1980) and Suen (1978) suggested that the "tectonic" lavers did not have the same origin as the magmatic layers, and interpreted the tectonic layers as possible reaction zones between the peridotite and magmatic mafic layers.

Noble metal analyses and interelement correlations

Seven "magmatic" mafic layers and one "tectonic" mafic layer were analyzed for Au, Pd, and Ir in this study; Pt was not determined due to poor counting statistics and interference from 199 Au produced by Au activation. Noble metal analyses are given in table III-7, along with x-ray fluorescence analyses for Cr, Ni, Cu, and Mg/(Mg+Fe) from Suen (1978). Sample R839 is a garnet clinopyroxenite, R251 is a spinel plagioclase pyroxenite, samples R181-R185 are

TABLE III-7: Ronda Mafic Layers. Noble Metal[a] and Selected Trace Element[b] Analyses

Sample	Pd	Au	Ir	Cu	Ni	Cr	Mg/(Mg+Fe)
"Magmatic" layers:							
R181	28 (1)[c]	14.86 (0.04)	0.37 (0.06)	22	500	1490	0.840
R182	34 (1)	10.2 (0.1)	0.6 (0.3)	296	317	985	0.795
R183	6.7 (0.5)	3.79 (0.02)	-	35	195	820	0.756
R184	6.8 (0.6)	3.58 (0.02)	-	67	245	720	0.736
R185	7.0 (0.5)	1.98 (0.01)	-	99	170	890	0.771
R251	2.1 (0.2)	0.59 (0.02)	0.30 (0.05)	5	207	535	0.786
R839	<0.4	0.192 (0.005)	0.08 (0.02)	45	93	209	0.577
"Tectonic" layer:							
R301	<0.2	0.087 (0.008)	1.22 (0.06)	3	745	12900	0.933

All analyses except Mg/(Mg+Fe) on undried samples.

a) Pd, Au, Ir in ppb.
b) Cu, Ni, Cr, in ppm.
c) Value in parentheses is 1σ counting statistics error, including error.

olivine gabbros from a single thick mafic layer (numbered consecutively from "bottom" to "top"), and R301, the "tectonic" layer, is a websterite. Detailed petrographic descriptions of these layers may be found in Obata (1977) and Suen (1978), and sample locations are given in figure III-1.

Interelement correlation plots for the magmatic mafic layers are given in figure III-7. Unlike the Ronda peridotites, noble metal abundances in the "magmatic" mafic layers do not correlate with abundances of Ca, Na, Sc, Cu, and Ti, but as in the Ronda peridotites, Pd and Au abundances correlate positively in the "magmatic" mafic layers. However, Pd and Au have crude positive correlations with Ni and Cr in the "magmatic" mafic layers, whereas Pd and Au correlate negatively with Ni in the Ronda peridotites (figure III-2), and show no correlation with Cr. Hence, there are fundamental differences in the noble metal geochemistries of the Ronda "magmatic" mafic layers and the Ronda peridotites.

The abundances of noble metals in the Ronda "magmatic" mafic layers are within the range of noble metal abundances in gabbros and basalts (table III-6). Furthermore, the Pd/Ir and Au/Ir of the "magmatic" mafic layers are similar to Pd/Ir and Au/Ir in basalts and gabbros, and are much higher than the Pd/Ir and Au/Ir of the Ronda peridotites (figure III-3). In contrast, the Pd/Ir and Au/Ir of the "tectonic" mafic layer (R301) are very low for a mafic rock,

FIGURE III-7: Interelement plots for the Ronda "magmatic" mafic layers. Note the $\log_{10}$ scales.

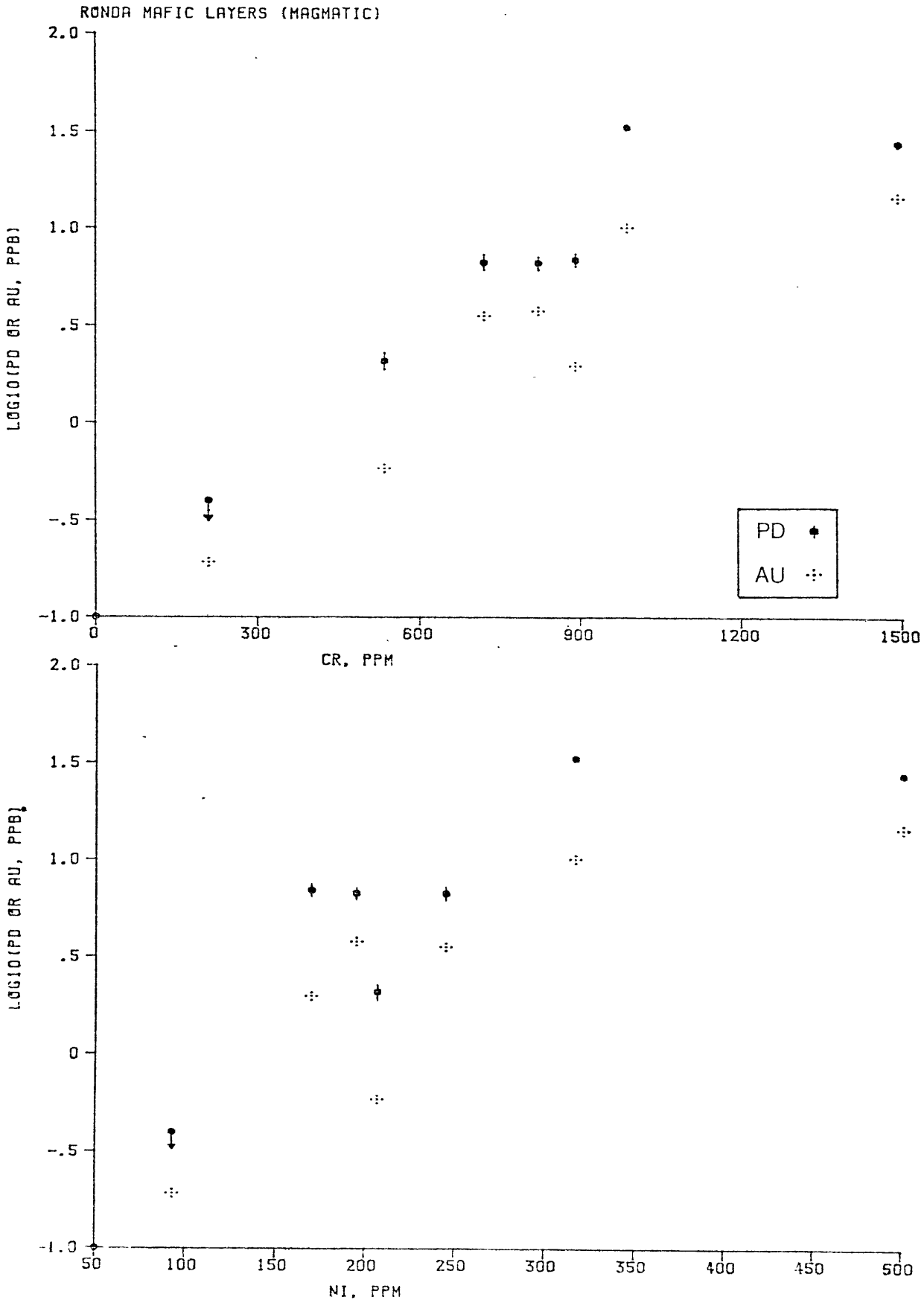
RONDA MAFIC LAYERS (MAGMATIC)
LOG10(PD OR AU, PPB)
2.0
1.5
1.0
.5
0
-.5
-1.0
0
300
600
900
1200
1500
CR, PPM
PD
AU
LOG10(PD OR AU, PPB)
2.0
1.5
1.0
.5
0
-.5
-1.0
50
100
150
200
250
300
350
400
450
500
NI, PPM

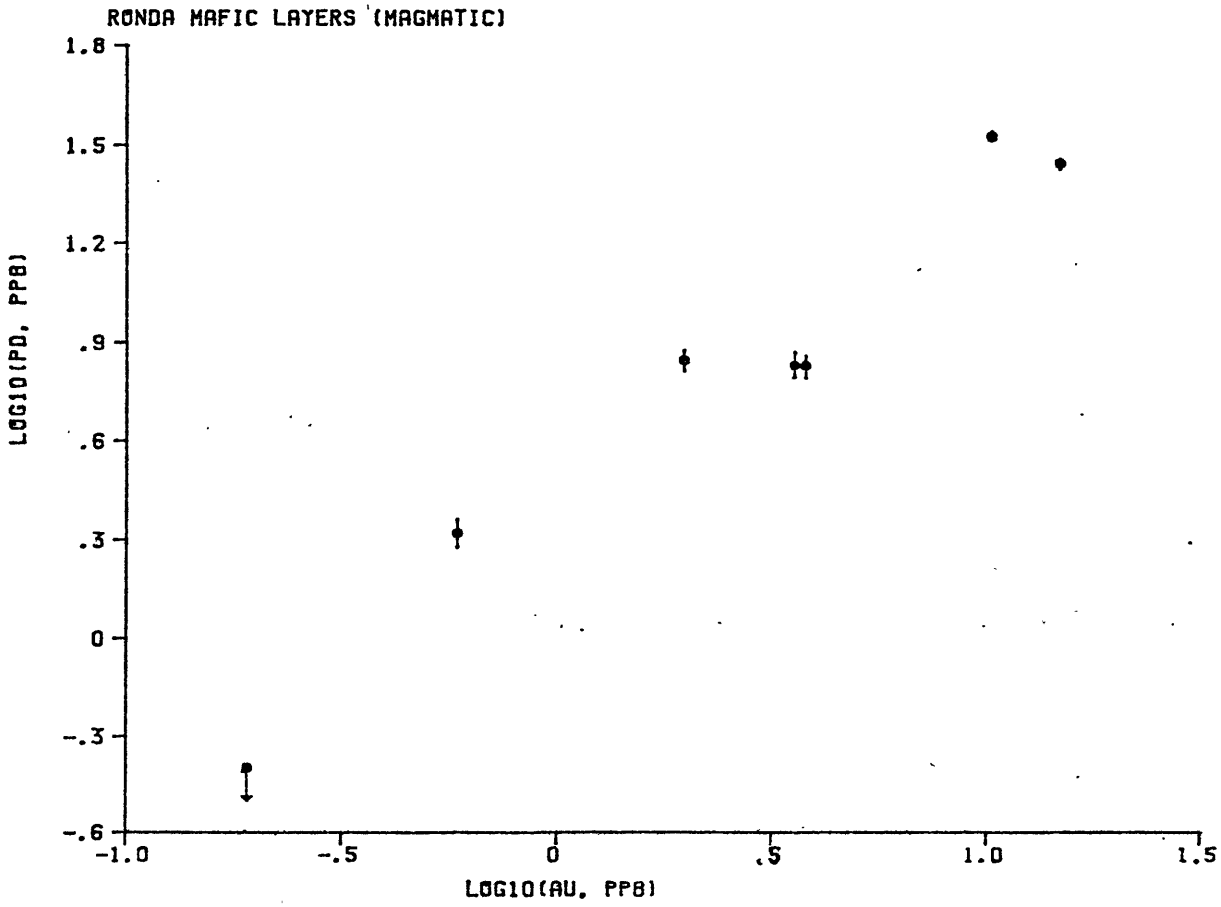
RONDA MAFIC LAYERS (MAGMATIC)
LOG10(PD, PPB)
1.8
1.5
1.2
.9
.6
.3
0
-.3
-.6
-1.0
-.5
0
.5
1.0
1.5
LOG10(AU, PPB)

and are in fact lower than the Pd/Ir and Au/Ir of the Ronda peridotites.

Because only one "tectonic" mafic layer was analyzed in this study, and because of the problematical origin of the "tectonic" layers, the following discussion is limited to the Ronda "magmatic" mafic layers, and the term "mafic layer" is hereafter synonymous with "magmatic mafic layer".

Origin of noble metal variations in the magmatic mafic layers

The positive correlations of Pd and Au abundances with Cr and Ni abundances in the mafic layers seems to reflect a basic change in the geochemical behavior of Pd and Au from the behavior found in the Ronda peridotites; namely, the change from incompatible to compatible behavior. Given the generally unsystematic behavior of other trace elements in the layers (Suen, 1978), the apparent compatible behavior of Pd and Au in the mafic layers may not be real, but simply the artifact of fortuitous sampling; however, there is also the reasonable possibility that the compatible behavior reflects the fractional precipitation of sulfides from the melts which formed the layers. The sulfide/silicate melt partition coefficient for Pd is >1,500 (Naldrett and Duke, 1980; Keays and Campbell, 1981) so that for some of the more sulfide-rich mafic layers, the bulk mafic layer/silicate melt partition coefficient for Pd would be >1, and compatible behavior would be expected (e.g., for

R182, which contains ca. 0.25 wt.% sulfide, the bulk mafic layer/silicate melt partition coefficient would be ca. 4). However, as with the Ronda peridotites, it is possible that the sulfides now found in the layers precipitated from trapped melts, and were not present in the original mafic layer assemblage.

The variation of Pd/Cu in the mafic layers suggests that sulfide precipitation did occur and hence was the cause of the compatible behavior of Pd, during formation of the layers. Both Pd and Cu are thought to enter silicate melts preferentially to silicate and oxide minerals, and hence precipitation of silicates and oxides alone does not tend to fractionate the two elements from one another (Keays and Campbell, 1981). However, both Pd and Cu partition strongly into sulfides relative to silicate melts; furthermore, the sulfide/silicate melt partition coefficients for the two elements are very different (>1,500 for Pd, ca. 245 for Cu; Naldrett and Duke, 1980; Keays and Campbell, 1981; Rajamani and Naldrett, 1978), so that small amounts of sulfide precipitation should cause a large decrease in Pd/Cu for successive accumulates of a melt undergoing fractional crystallization (Keays and Campbell, 1981). The mafic layer sequence R181, R182-185, and R839 has been interpreted by Suen (1978) as representative of successive accumulates of a partial melt, and shows a large decrease in Pd/Cu with decreasing Cr content (figure III-8), which strongly suggests fractionation of Pd and Cu by sulfide precipitation.

FIGURE III-8: Log_{10} (Pd/Cu) vs. Cr for Ronda mafic layers which are interpreted to represent successive accumulates of a partial melt.

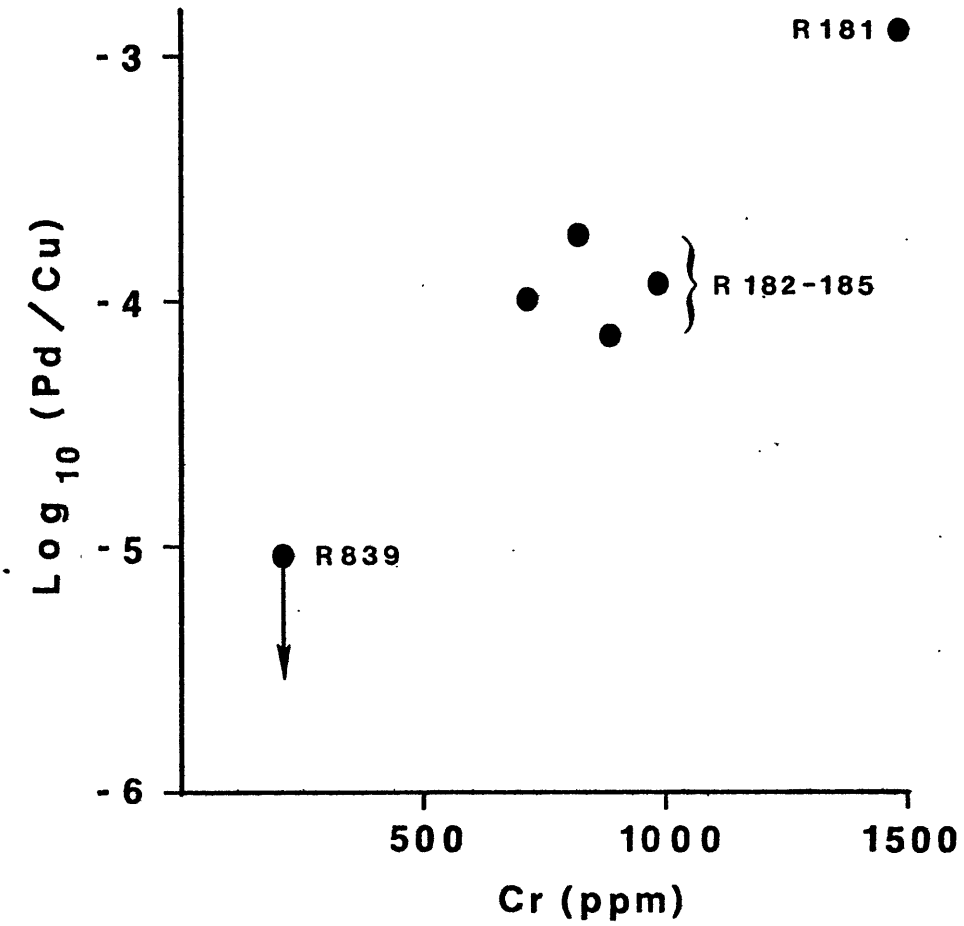
R181
R 182-185
R839
-3
-4
-5
-6
Log10 (Pd/Cu)
500
1000
1500
Cr (ppm)

Sulfide precipitation is therefore a viable possibility as the cause of the compatible behavior of Pd in the mafic layers. Sulfide/silicate melt partition coefficients are not available for Au, but on the basis of the geochemical similarity of Pd and Au, it is reasonable that sulfide precipitation may also have caused the compatible behavior of Au.

Several factors could have caused the precipitation of sulfide from the melts which formed the mafic layers. The solubility of sulfur in silicate melts, at sulfide saturation, decreases with decreasing pressure, temperature, and melt oxygen activity (MacLean, 1969; Haughton et al., 1974; Shima and Naldrett, 1975; Mysen and Popp, 1980). Hence, the cooling and decompression of a melt leaving its source region, as well as the precipitation of an oxidized component (such as $Fe^{+2}\ Fe^{+3}{}_2O_4$ in spinel) could all induce sulfide precipitation. In addition, the precipitation of silicates and oxides, which have very small sulfur contents, could also induce sulfide precipitation by reducing the melt volume, and hence increasing the concentration of sulfur in the melt. Obata (1977, 1980) and Suen (1978) proposed that the mafic layers formed when partial melts of the Ronda peridotites precipitated silicates and spinels as a consequence of decreasing temperature and pressure; this origin is qualitatively consistent with the factors which induce sulfide precipitation. The temperature, pressure, and oxygen

activity at which sulfides would precipitate from a melt would, of course, depend on the sulfur content of the initial partial melt, which in turn would depend on the sulfur content of the source peridotite and the F' at which the melts were produced. Batch melts produced from the Ronda peridotites at high degrees of F' would have sulfur contents of only 0.025-0.050 wt.%, well below the solubility of sulfur in silicate melts at sulfide saturation and at temperatures and pressures above 1200C and 1 atm. (Haughton et al., 1974; Mysen and Popp, 1980); hence it is unlikely that batch melts produced at high F' would saturate with sulfide under mantle conditions, unless the concentration of sulfur in the melts were greatly increased by a secondary process, such as precipitation of large volumes of sulfur-poor silicate and oxides. However, batch melts produced from the Ronda peridotites at small F' (i.e., F'=0.01-0.05) would have much higher sulfur contents, and hence a greater chance of becoming saturated with sulfide during cooling and decompression. At present, there is no independent means of assessing whether the mafic layers are accumulates from melts produced at low or high F'.

III-3: THE JOSEPHINE PERIDOTITE

Introduction

The Josephine Peridotite is a large, alpine-type peridotite located in the Klamath Mountains of southwest Oregon and northern California, and is one of numerous,

geologically similar peridotites in the Coast Ranges of California, Oregon and Washington (Diller, 1921; Wells et al., 1949; Medaris, 1972; Himmelberg and Loney, 1973; and Dick, 1976, 1977). Structurally, the peridotite is a sheet, emplaced in the Mesozoic by successive thrusting to the west over metavolcanic, plutonic, and metasedimentary rocks. The thrust contacts of the peridotite sheet are apparently low temperature contacts. The overthrust metavolcanics have not been metamorphosed to higher than amphibolite facies, and greenshist facies metamorphism is predominant. In the field area for this studv (southwest Oregon; figure III-9), the peridotite is primarilv a tectonite harzburgite with minor dunites, chromitites, and pyroxenites. South of the field area, in California, the tectonite harzburgites of the Josephine Peridotite are associated with cumulate ultramafics (dunites, pyroxenites and wehrlites), gabbroic sheeted dikes, and pillow lavas which together constitute a classic ophiolite sequence (Harper, 1980). The average reconstituted (serpentine-free) mode of the harzburgites in the studv area is ca. 80% olivine, 17% orthopyroxene, 2% clinopyroxene, and 1% spinel (Dick, 1975), with no garnet or feldspar. Most of the peridotites are 30-100% serpentinized, but some are remarkably fresh, with <2% serpentine. Sulfides (pyrrhotite, pentlandite, chalcopyrite, cubanite, and alterations to heazlewoodite, Ni-Fe alloy, magnetite, and Cu metal) comprise less than 0.05% of the typical peridotite.

FIGURE III-9: Location map for samples from the Josephine Peridotite in Oregon. The abbreviations TP, SR, DG, and LS refer to the Tennessee Pass, Salt Rock, Deep Gorge, and Lucky Strike chromitites, respectivelv.

JOSEPHINE PERIDOTITE

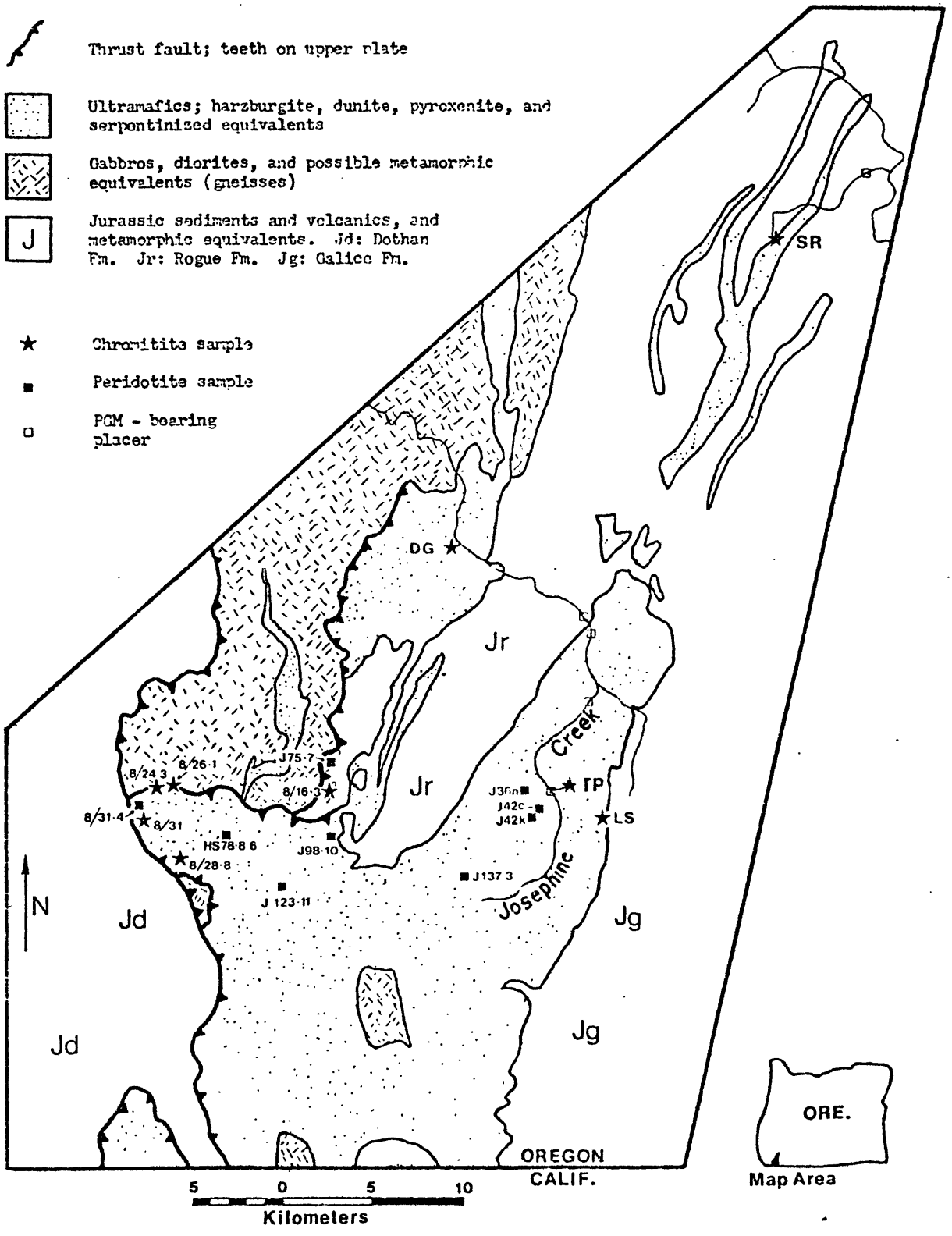

Compared with estimates of the composition of the primitive mantle, the Josephine peridotites are highly depleted in magmaphile elements such as Ca, Na and Al (Table III-1). Accordingly, alpine harzburgite bodies like the Josephine Peridotite have been interpreted as depleted residues from the removal of large amounts (20-35%) of partial melts from originally undepleted, lherzolite sources (Green and Ringwood, 1967), although some have interpreted alpine harzburgites as deformed cumulates from the fractional crystallization of mafic magmas (Thayer, 1969). Dick (1976) studied the petrology of the Josephine Peridotite, and concluded that the uniform mineralogy and large size of the tectonite harzburgites were more consistent with derivation as a residue of partial melting rather than as cumulates of fractional crystallization; Dick suggested that only minor rock types found within the harzburgite (some dunites and chromitites) might be accumulates of partial melts moving through the mantle.

As a working hypothesis, it is assumed that depleted alpine harzburgite bodies like the Josephine Peridotite probably represent residues from removal of large amounts of mafic partial melts from an originally fertile mantle, while lherzolite-harzburgite bodies like the Ronda are, on the average, residues from removal of smaller amounts of partial melts. However, geochemical trends established by the Josephine peridotites may not be simple extrapolations of the Ronda peridotite trends to higher degrees of melting.

In general, the Josephine peridotites are poorer in Na than the Ronda peridotites at a given Ca content. Furthermore, preliminary rare earth analyses of two Josephine peridotites (R. Hickey, pers. comm.) may indicate greater complexity in the rare earth geochemistry of the Josephine peridotites; while one Josephine peridotite (HS-78-8-6) has a light rare earth-depleted, chondrite-normalized rare earth pattern, much like the Ronda peridotite patterns, another Josephine peridotite (J42c) has an unusual, V-shape chondrite-normalized rare earth pattern, much like the pattern found for U.S.G.S. standard PCC-1 (Frey, 1982).

Noble metal analyses and interelement correlations

Eight harzburgites and one dunite from the Josephine Peridotite in southwest Oregon were analyzed for Au, Pd, Pt, Ir, Ca, Na, Sc, and Cr; the results are given in Table III-8. Noble metal analyses were made by the technique described in chapter II, and the same precautions were observed in sample preparation as were described in section III-1. Analyses for Na, Sc and Cr were by instrumental neutron activation; Ca was determined by a modification of the fluxed glass microprobe technique described by Gulson and Lovering (1967), using a working curve based on fluxed U.S.G.S. standards. The degree of serpentinization of the samples varies from less than 5% for HS-78-8-6, to ca. 50% for J36n. Sample locations are given in figure III-9.

TABLE III-8: Josephine Peridotites. Noble Metal Analyses[a] and Selected Major[b] and Minor[c] Element Analyses

	Pd	Au	Ir	Pt	CaO	Na_2O	Sc	Cr
HS-78-8-6	9.3 (0.4)[d]	1.70 (0.02)	5.6 (0.2)	13 (2)	2.18	0.027	13.5	2882
J98-10	9.1 (0.5)	2.21 (0.01)	8.2 (0.2)	-	-	0.060	12.2	2983
J42k	7.9 (0.5)	2.07 (0.01)	6.15 (0.08)	12 (2)	1.64	0.024	12.5	2436
J137-3	7.5 (0.4)	1.64 (0.01)	5.94 (0.08)	7 (1.2)	-	0.0096	10.4	2470
J42c	5.2 (0.2)	1.26 (0.01)	4.37 (0.08)	6 (2)	0.88	0.0093	10.4	2130
J123-11	2.5 (0.2)	0.47 (0.01)	8.3 (0.2)	-	0.28	0.013	5.7	3279
J36n	1.2 (0.2)	1.45 (0.02)	14.8 (0.3)	13 (3)	0.30	0.0096	4.1	5423
J75-7	0.5 (0.1)	0.241 (0.003)	4.70 (0.04)	4 (1)	0.67	0.032	7.1	2724
8/31-4 (dunite)	<0.5	0.12 (0.01)	0.08 (0.02)	<1.5	0.25	0.0066	4.5	1259
PCC-1 this study	4.2 SD=0.8[e]	0.86 SD=0.16	6.4 SD=1.2	8.0 SD=2.7	0.59	0.011	8.6	2872
PCC-1 literature values	(see Chapter II for discussion of PCC-1 noble metal analyses)				0.51[f]	0.006[g]	8.2[h]	2750[h]

All analyses on undried samples.

a) Pd, Au, Ir, and Pt in ppb.

b) CaO and Na_2O in %.

c) Sc and Cr in ppm.

d) Value in parentheses is a liberal 1σ counting statistics error, including error in standard, backgrounds, and yield determinations.

e) SD is the standard deviation for replicate analyses. 5 analyses for Pd, Pt and 6 analyses for Au and Ir. Degrees freedom = # analyses minus 1.

f) Flanagan (1976). Literature average.

g) ibid. Magnitude; poor agreement in literature.

h) Katz and Grossman (1976).

Correlations of the noble metals with other elements in the Josephine peridotites are given in figure III-10. As with the Ronda samples, there are significant positive correlations of Pd abundances with Sc and Ca abundances. Palladium and Au abundances correlate well, with the exception of sample J36n, which has a very high Au/Pd. Sample J36n is highly serpentinized, and was collected from a shear zone associated with diorite dikes. Gold veins are found associated with the contacts between mafic intrusives and serpentinites in the area, and it is possible that the high Au content of J36n is metasomatic in origin. Ir abundances do not correlate with Sc and Ca abundances, though there may be a correlation with Cr. If sample J36n is excluded as anomalous, Pt abundances correlate well with abundances of Ca and Sc.

Mantle noble metal abundances and the Josephine peridotites

There is difficulty in determining whether the Josephine peridotite or Ronda peridotite noble metal abundances are more typical of the primitive mantle. Compared with the Ronda peridotites, the Josephine peridotites are relatively enriched in Pd and Au. This enrichment is best seen by comparing the Pd contents of Ronda and Josephine peridotites with equal Ca or Sc (figure III-10). None of the Josephine peridotites are as Ca-rich as the Ronda peridotites, but extrapolation of the Josephine Pd-Ca trend to the CaO content of R717 yields a hypothetical Josephine "source rock" with ca. 10-15ppb Pd,

FIGURE III-10: Interelement plots for the Josephine peridotites. The dashed lines labeled "Ronda" on the Pd-CaO and Pd-Sc plots are the linear regression lines for the Ronda peridotites. The points labeled with stars are for PCC-1, a peridotite from the Cazadero Complex in California, which is geologicallv similar to the Josephine Peridotite.

JOSEPHINE PERIDOTITES AND PCC-1

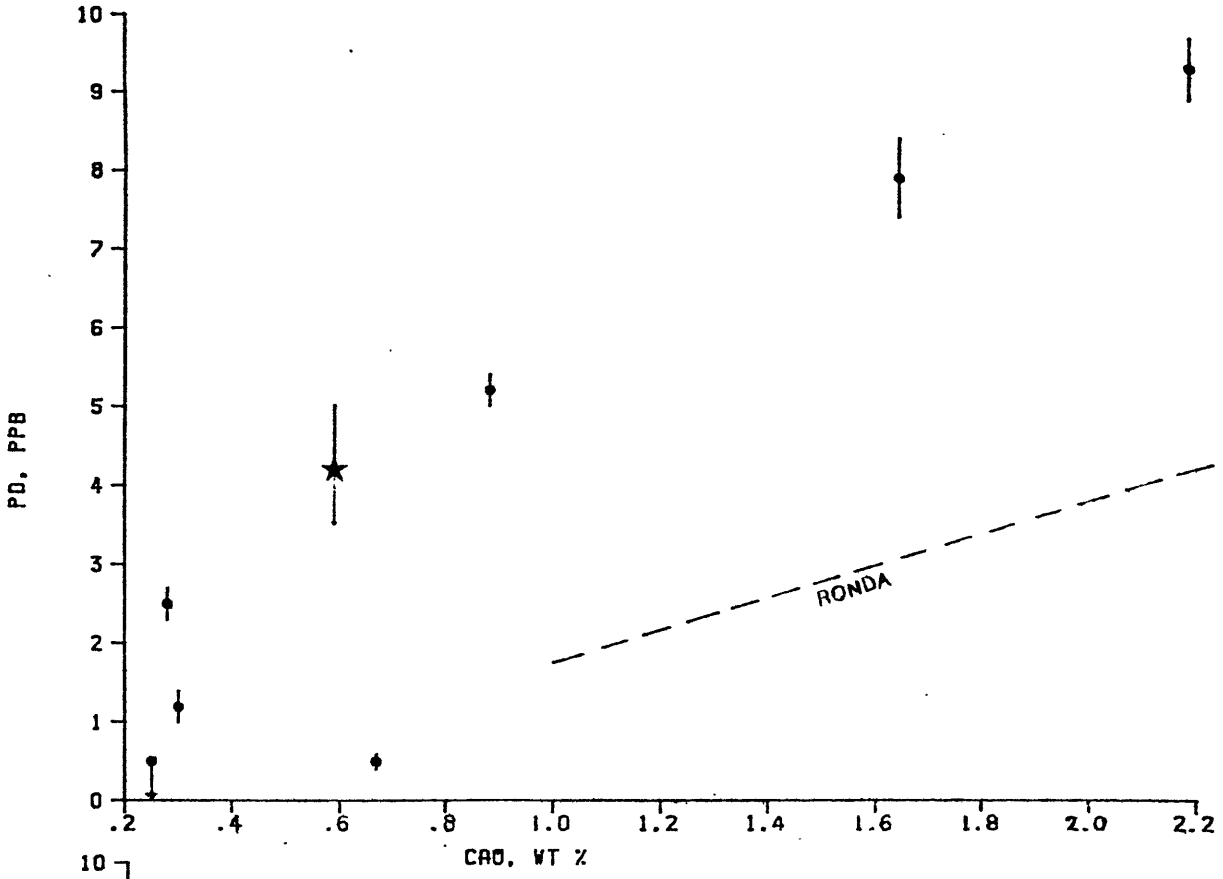

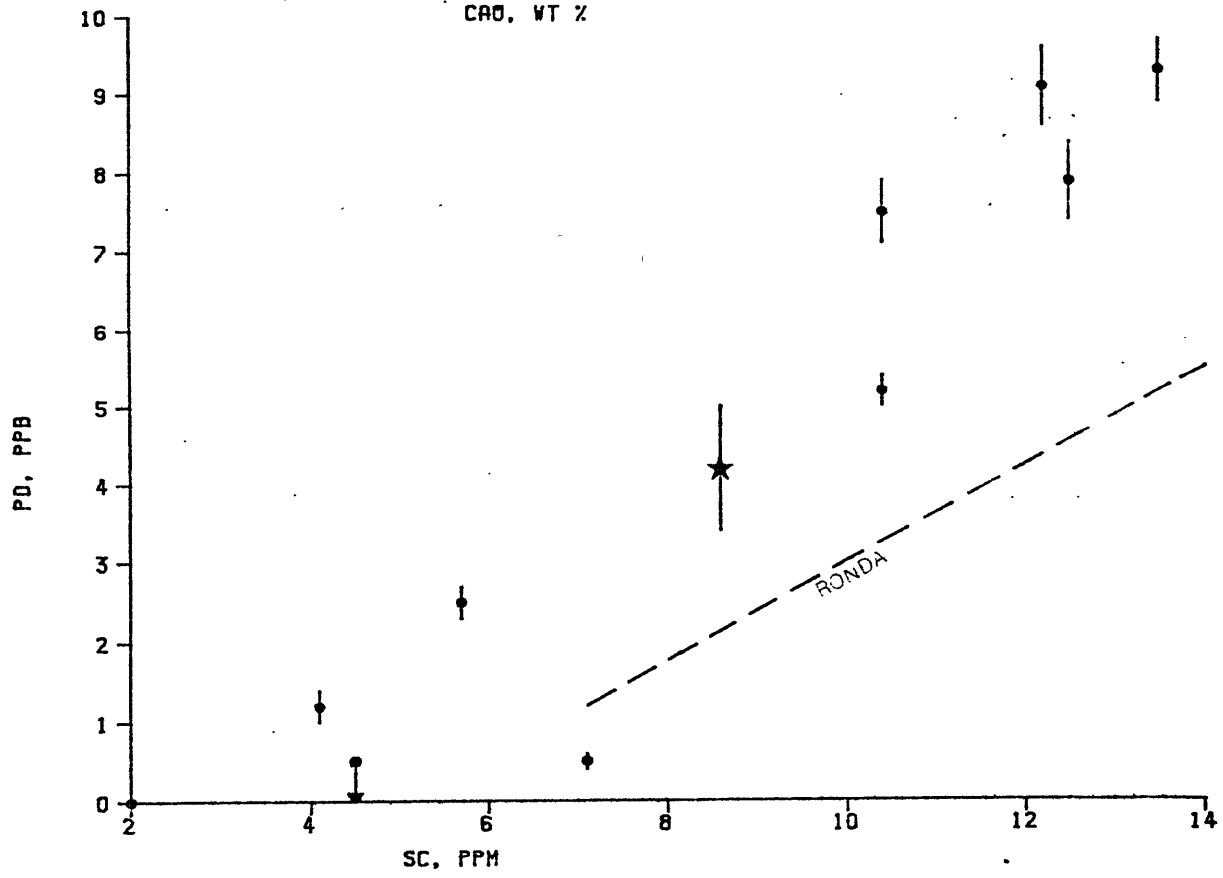

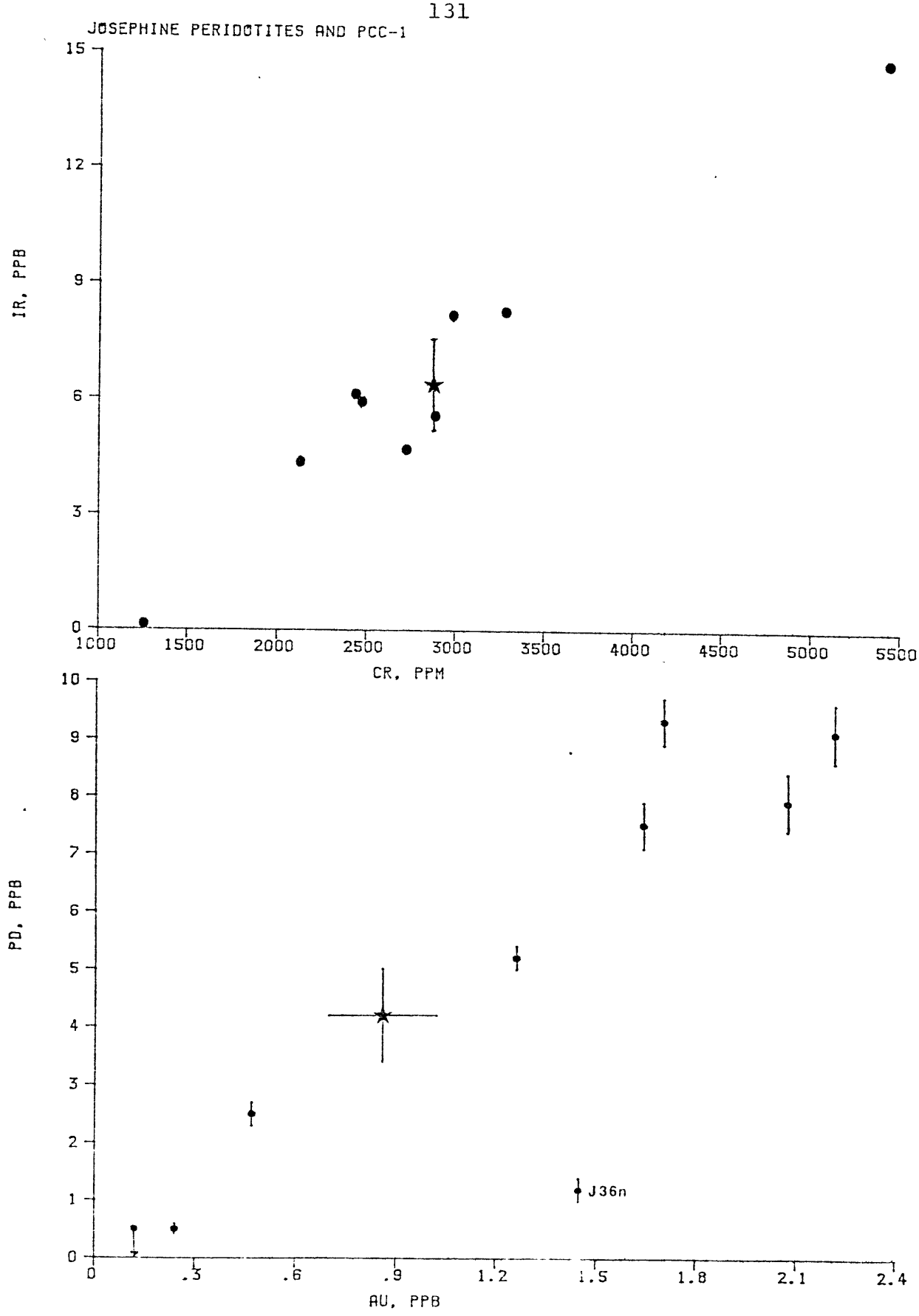
JOSEPHINE PERIDOTITES AND PCC-1
IR, PPB
CR, PPM
PD, PPB
AU, PPB
J36n

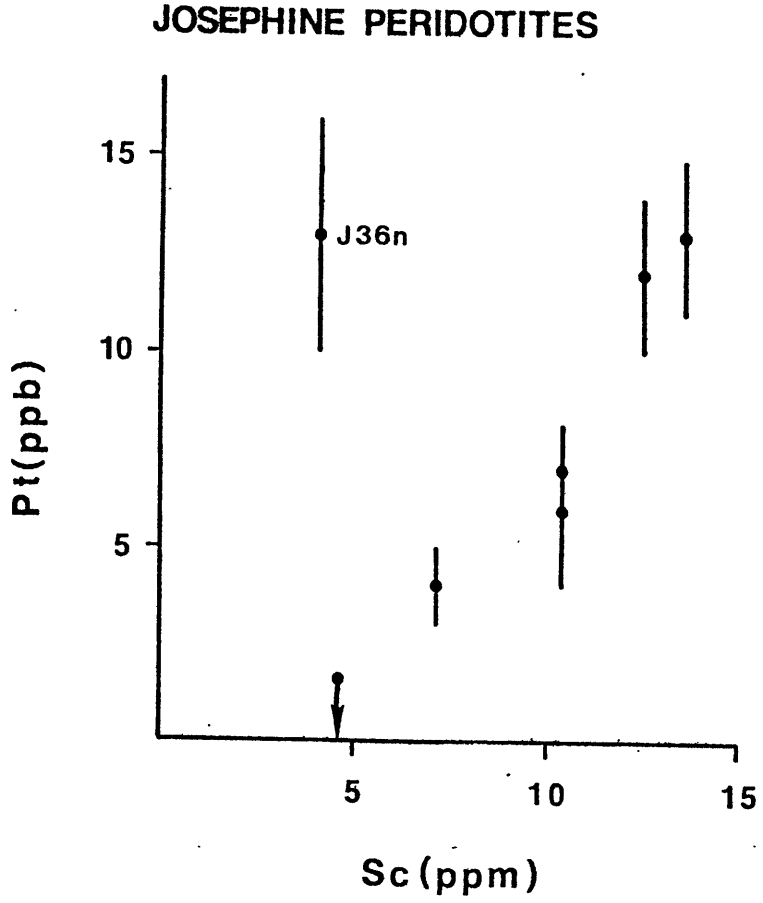
JOSEPHINE PERIDOTITES
15
10
5
Pt(ppb)
J36n
5
10
15
Sc(ppm)

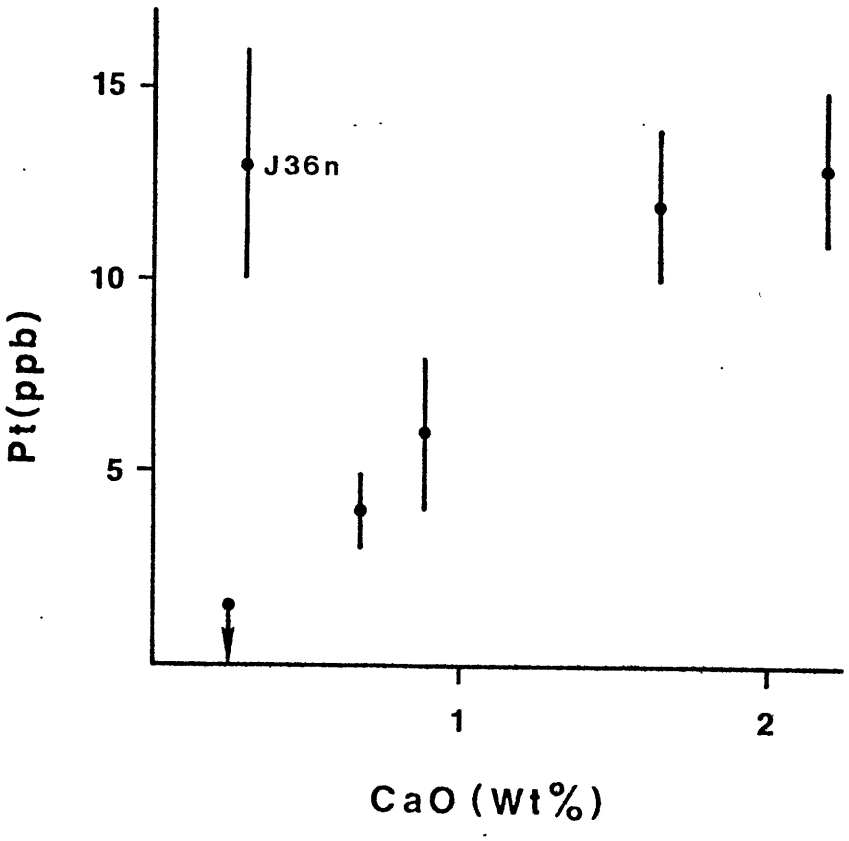
15
10
5
Pt(ppb)
J36n
1
2
CaO (Wt%)

twice as much Pd as R717, the most fertile Ronda lherzolite.

It is not clear if the relative enrichment of the Josephine peridotites in Pd and Au, at a given Ca content, reflects a significant heterogeneity of the mantle in Pd and Au abundances. Comparison of the Josephine harzburgite analyses with the very limited analyses of CaO-poor harzburgites from other alpine harzburgite complexes suggests that high Pd abundances, compared with the Ronda peridotites, may be typical of these bodies (table III-9). A sample from the Cazadero harzburgite body in California (PCC-1) falls on the Josephine Ca-Pd trend (figure III-9), also suggesting high Pd for alpine harzburgite complexes. Since rocks from alpine harzburgite complexes generally do not have major element compositions similar to the hypothetical primitive mantle, the Ronda lherzolite noble metal abundances are preferred as estimates of the primitive mantle noble metal abundances. Nevertheless, the <u>average</u> noble metal abundances of the Josephine harzburgites and Ronda lherzolites are quite similar (tables III-3 and III-9), and the most fertile (Ca-and Sc-rich) Josephine harzburgites have noble metal ratios which are within a factor of 1.5 of the chondritic noble metal ratios. Hence, the Josephine harzburgite analyses confirm both the approximate mantle noble metal abundances and chondritic noble metal ratios set by the Ronda lherzolites.

TABLE III-9: Comparison of Noble Metal Abundances (ppb) in Peridotites from Alpine Harzburgite Complexes

	Ir	Pt	Pd	Au
Average of 8 Josephine harzburgites, this study	7.3	9.2	5.4	1.4
Average of 6 Josephine harzburgites[a]	-	<15	7	-
Mt. Albert "ultramafic pluton"[b]	2.2	-	7.9	1.1
Average 2 Troodos harzburgites[c]	4.8	-	9.6	-

a) Page et al. (1975). Detection limits were 10ppb Pt, 4ppb Pd.

b) Crocket and Chyi (1972).

c) Becker and Agiorgitis (1978). Samples described as "enstatite and bronzite peridotites"; may be cumulates.

Location of noble metals in the Josephine peridotites

A selective leaching experiment was used to determine the relative importance of silicates, chrome spinel, and sulfides as hosts of noble metals in the Josephine peridotites. A neutron-irradiated ground sample of HS-78-8-6 (-160 mesh) was leached for 10 minutes in nitric-perchloric acid, and Pd, Au, Pt, and Ir were determined in the leachate by radiochemistry. Sample HS-78-8-6 was chosen for analysis because it is unusally fresh (<5% serpentine) and has a relatively high base metal sulfide content (ca. 0.03 wt.%) and relatively high noble metal abundances (table III-8). The nitric-perchloric leach is known to dissolve base metal sulfides much more easily than silicates and spinels (I.H. Campbell, pers. comm.), but as a check on the dissolution of silicates and spinel, Na, Sc, and Cr were determined in the leachate and undissolved residue by instrumental neutron activation. The leachate was found to contain 100±15% of the whole rock Pd, Au, and Pt contents, 50±10% of the whole rock Ir, but only 12±1% of the Na and Sc, and 2±1% of the Cr. Hence, virtually all of the whole rock Pd, Au, and Pt, and half the whole rock Ir are not in silicates and chromite. There are two probable hosts remaining for the noble metals; base metal sulfides, and PGMs or native gold. Although most PGMs and gold are generally considered to be insoluble in nitric-pechloric acids (Beamish and Van Loon, 1977), it is possible that, due to very small size, these minerals might have been dissolved

by the nitric-perchloric leach; the incomplete removal of Ir by the leach may indicate that some Ir is present in resistant Os-Ir alloys. Even if there are now PGMs and native gold in HS-78-8-6, these minerals were not necessarily present at high temperatures; if the base metal sulfides were present at high temperatures, any PGMs and gold would have probably been dissolved in these sulfides (see section I-3). Indeed, Mitchell and Keays (1981) have shown that Pt and Pd PGMs in mantle peridotites apparently exsolved from base metal sulfides at relatively low temperatures (below ca. 600C, breakdown temperature for the (Fe,Ni)S monosulfide solid solution.)

Behavior of noble metals during partial melting of the Josephine peridotites

It is expected that during partial melting, noble metals in the Josephine peridotites behaved similarly to the noble metals in the Ronda peridotites. It is postulated that base metal sulfide was the major host of the noble metals at temperatures below the silicate solidus, but with the formation of a few percent silicate partial melts, the base metal sulfide dissolved into the melt. Iridium may have formed refractory alloys after the disappearance of sulfide, but Pd, Au, and possibly Pt, dissolved into the silicate melts, and the covariation of Pd, Au, and Pt with Ca and Sc in the peridotites is attributed to the retention of varied amounts of partial melts rich in Pd, Au, Pt, Ca, and Sc. The base metal sulfides now found in the

peridotites are postulated to have precipitated from the trapped melts.

It is not possible at present to quantitatively model the partial melting of the Josephine peridotites, because of the uncertainty in the values of F represented by the peridotites. However, there is petrological evidence for the retention of noble metal-rich partial melts in the Josephine peridotites. Dick (1977) concluded that the Josephine orthopyroxenes were not saturated with clinopyroxene during partial melting, and hence interpreted the Josephine clinopyroxenes as precipitates from trapped melts. Qualitative microprobe analyses (this study) show that the base metal sulfides in the Josephine peridotites have a strong tendency to be adjacent to clinopyroxene grains or intergrown with unidentified Ca-, Al-, and Ti-rich silicates in the interstices of the olivines and orthopyroxenes. This association of base metal sulfides with clinopyroxene and other silicates rich in magmaphile elements suggests that the sulfides precipitated from trapped silicate melts. Hence, the phases which are now the major hosts of Ca and Sc in the peridotites (clinopyroxene and associated Ca-rich silicates), as well as the phases which are probably the major hosts of Pd, Au, and Pt (base metal sulfides), probably precipitated from trapped melts.

III-4: THE JOSEPHINE CHROMITITES

Introduction: noble metals in chromitites

The role of chrome spinels in concentrating noble metal and controlling noble metal geochemistry is not well understood. Economic platinum group element deposits in layered intrusions and zoned (Urals-type or Alaskan-type) ultramafic complexes have a persistent association with chromitite horizons, but the platinum group elements commonly occur as discrete PGMs, and not as solid solution in the chromite crystals (Crocket, 1979). Consequently, the reason for the association is not known.

Gijbels et al., (1974) postulated that Ir, Os and Ru in Bushveld chromitites were in solid solution in the spinel structure at magmatic temperatures, but exsolved to form discrete PGMs upon cooling; Hagen (1954) advocated a similar origin for Pt, Pd and Au mineralization in Bushveld chromitites. Agiorgitis and Wolf (1978) have found correlations of Ir and Cr in podiform chromitites, and interpret these correlations as resulting from Ir^{+3} substitution for Cr^{+3} in the spinel structure.

Chang et al. (1973) also interpreted correlations of Cr with Os, Ru, and Pt in chromitites as indicative of ionic substitution. Partitioning of Ir into mantle chrome spinels has been suggested as a major cause of the Ir depletion of theoleiitic basalts (Hertogen et al., 1980); however, Mitchell and Keays (1981) found that chrome spinels were not major hosts for Ir in peridotitic mantle nodules.

In this section, the geology and geochemistry of podiform chromitites from the Josephine Peridotite are reviewed, noble metal analyses for a number of Josephine chromitites are presented, and speculations are made on the role of chromitites in determining the noble metal geochemistry of the mantle and partial melts derived from the mantle.

The Josephine chromitites

The occurrence, chemistry and origin of podiform chromitites in the Josephine Peridotite have been discussed by Diller (1921), Ramp (1961), Thayer (1970), and Dick (1976, 1977). The Josephine chromitites typically occur as lenticular masses or "pods" less than one meter thick, and are almost exclusively associated with dunite patches in the harzburgite tectonite. The chromitites contain varied amounts of partially serpentinized olivine and rare pyroxenes, though in massive chromitites the silicates may be less than 1% of the rock. Chromite-silicate textures vary widely, from rocks in which olivine fills the interstices between rounded chromite grains, to rocks in which chromite fills the interstices between and surrounds rounded olivine grains. Some chromitites have "cumulate" textures reminiscent of those found in the chromitite horizons of layered complexes (Thayer, 1970). Several workers have suggested that podiform chromitites in alpine peridotites originate as cumulates of mafic magmas overlying the peridotite, and the

occurrence of chromitites within the peridotite is explained either in terms of the dense chromitites sinking into the hot, plastic tectonite basement (Dickey, 1975), or in terms of the syntectonic enfolding and mixing of the cumulates and tectonite harzburgite (Greenbaum, 1977; George, 1978). Dick (1976, 1977) and Cassard et al. (1981), however, advocate an origin of the chromitites within the tectonite peridotite mainly as accumulates of partial melts moving through the mantle. Dick (1976, 1977) interprets some of the Josephine chromitites as residues of the incongruent melting of chrome-rich pyroxenes; however, the majority of the larger chromitite bodies, such as those analyzed in this study, have textures consistent with an origin as accumulates.

Noble metal analyses and interelement correlations

Nine Josephine chromitites were analyzed for Au, Pd, Pt, and Ir by the radiochemical technique described in chapter II; the results are given in table III-10 along with microprobe determinations of the chromite $Cr/(Cr + Al + Fe^{+3})$ ratio (Fe^{+3} calculated assuming ideal spinel stoichiometry) and spectrographic analyses for Pt, Pd and Rh by Page et al. (1975).

The noble metal characteristics of the chromitites are quite distinctive. Log (Ir) correlates positively with the chromite $Cr/(Cr + Al + Fe^{+3})$ ratio (figure III-11), with Ir reaching ppm levels in the most Cr-rich samples. Some of the Ir-rich chromitites are also Pt-rich, but the number of

TABLE III-10: Analyses[a] of Josephine Chromitites

	Pd	Au	Ir	Pt	Spinel Cr/(Cr+Al+Fe^{+3})	≈ Spinel wt.frac.	Page et al. (1975)[b] Pd	Pt	Rh
Lucky Strike	4.9 (0.5)	0.07 (0.01)	337 (10)	120	0.724	0.95	7	81	58
Tennesee Pass	3 (1)	1.30 (0.05)	1053 (6)	660 (40)	0.792	1.00	<4	450	63
Deep Gorge	50 (1)	0.79 (0.01)	34.8 (0.3)	163 (5)	0.693	0.75	15	41	21
Salt Rock	<3	0.71 (0.04)	1159 (6)	1000 (30)	0.821	1.00	4	850	91
8/16-3 (Hawk's Rest)	1.3 (0.3)	0.23 (0.01)	143 (0.4)	<50	0.752	0.75			
8/24-3 (Gardner)	4.1 (0.4)	0.18 (0.01)	270 (0.5)	<50	0.724	1.00	16	16	22
8/26-1	5.9 (0.4)	0.36 (0.010	22.9 (0.4)	6 (2)	0.661	0.55			
8/28-8 (Chetco Lake)	1.1 (0.5)	0.260 (0.005)	86.5 (0.1)	<50	0.646	0.95			
8/31 (Nancy Hank)	4.2 (0.3)	1.38 (0.01)	12.9 (0.1)	<10	0.531	1.00			

All analyses on undried samples.

a) Pd, Au, Ir, Pt, and Rh in ppb.
b) Page et al. analyses are samples from same mines, but are not splits from sample analyzed in this study.

FIGURE III-11: Ir vs. $Cr/(Cr + Al + Fe^{+3})$ plot for Josephine chromitites. Note that the Ir axis is logarithmic, and that the Ir content has been divided by the spinel wt. fraction on the assumption that spinel is the major host for Ir in these rocks.

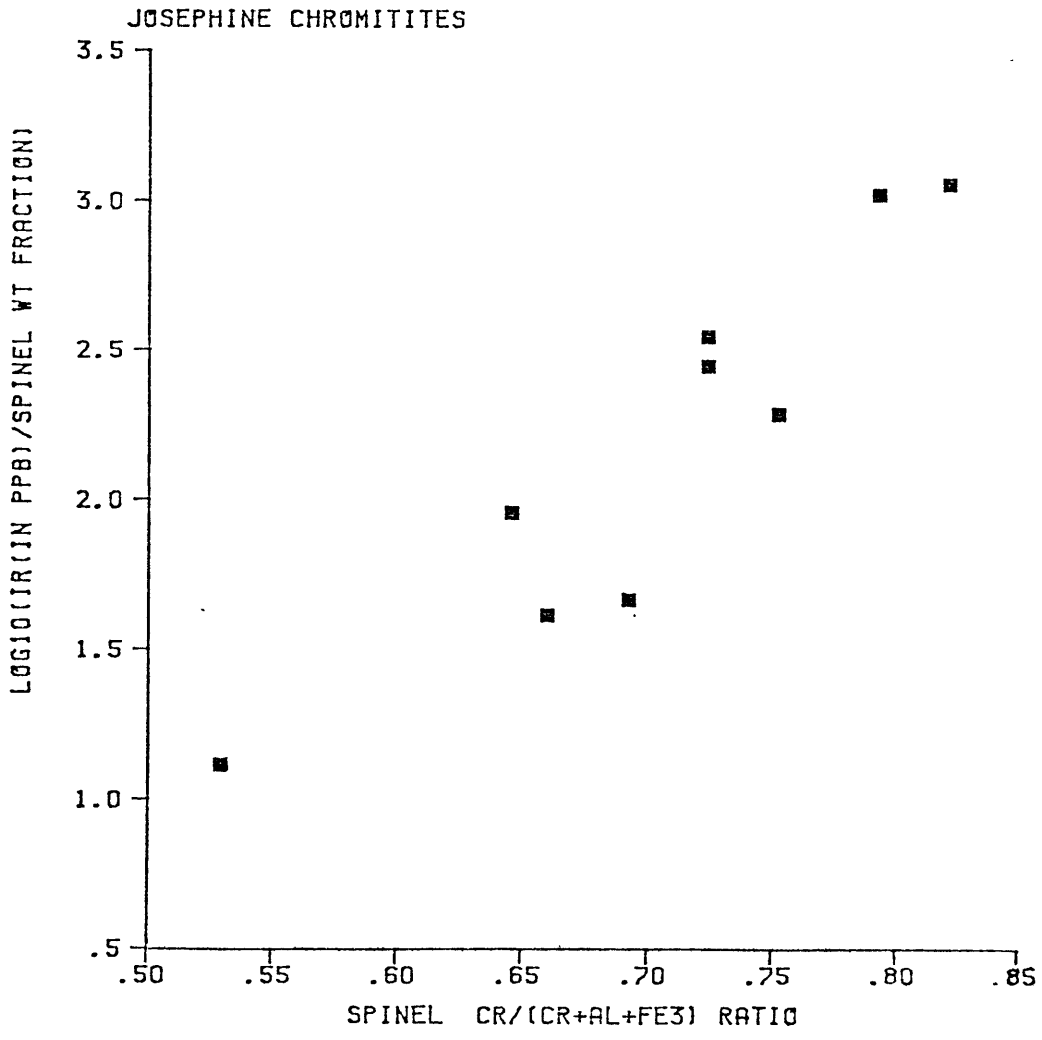
JOSEPHINE CHROMITITES
LOG10(IR(IN PPB)/SPINEL WT FRACTION)
3.5
3.0
2.5
2.0
1.5
1.0
.5
.50
.55
.60
.65
.70
.75
.80
.85
SPINEL CR/(CR+AL+FE3) RATIO

chromitite Pt analyses is insufficient to determine if Pt abundances correlate with the $Cr/(Cr + Al + Fe^{+3})$ ratio. Compared with Josephine peridotites and most basaltic rocks, the Josephine chromitites have much higher Ir/(Pd+Au) (figure III-12 and figure I-1), which suggests that chromitite precipitation may be important in fractionating noble metals during the evolution of partial melts.

Josephine chromitites: discussion

The interpretation of the Josephine chromitites as accumulates suggests that the Ir-$Cr/(Cr+Al+Fe^{+3})$ correlation may reflect the simultaneous depletion of Ir and Cr in a melt, due to fractional crystallization of chromite. Dickey (1975) has suggested that the variations in the Cr/Al of podiform chromitites are due to fractional crystallization of primitive magmas, such that as the temperature of crystallization decreases, the Cr/Al of the chromites decreases; hence the first chromites to precipitate are the most Cr-rich. From a study of Bushveld Complex chromitites, Gijbels et al. (1974) estimate the Ir chromite/(basaltic melt) partition coefficient to be ca. 1,600, so the first chromites to precipitate should also be the most Ir-rich. Assuming that the partition coefficient of Gijbels et al. (1974) is applicable, basaltic melts in equilibrium with the most Ir-rich Josephine chromitites would contain ca. 0.7ppb Ir, which is reasonably close to the highest Ir content found in basaltic melts (table III-6). If chromite were the only phase on the

FIGURE III-12: Chondrite-normalized diagram for ranges of noble metal abundances in the Josephine peridotites (stippled) and the Josephine chromitites (ruled). The averages for the peridotites and chromitites are given as thick lines.

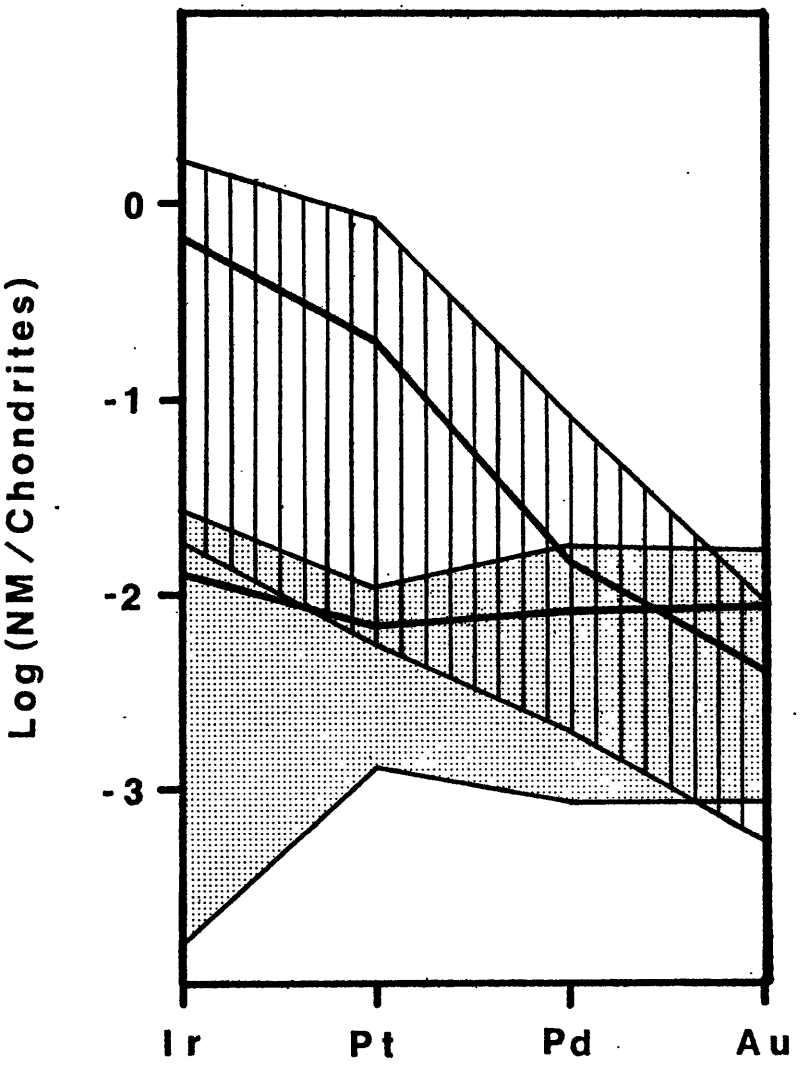
Log (NM / Chondrites)
0
-1
-2
-3
Ir
Pt
Pd
Au

liquidus, fractional precipitation of 0.3 wt.% chromite from the melt would reduce the Ir content of the melt by a factor of 100, at the same time bringing the Ir content of the precipitating chromites through the entire concentration range (ca. 1,200-12ppb) observed in the Josephine chromitites.* Hence, fractional crystallization of small amounts of chromite from the melt might not only account for the Ir-Cr/(Cr+Al+Fe^{+3}) correlation in the Josephine chromitites, but might also be an explanation for the wide range of Ir contents observed in basalts.

The major difficulty with the fractional crystallization hypothesis presented above is that it is not clear that the concentration of Ir in the chromite crystals is aptly described by a chromite/melt partition coefficient.

---

* Realistically, olivine as well as chromite would probably be on the liquidus simultaneously. However, the amount of chromite precipitation required to reduce the melt Ir concentration by a factor of 100 would probably still be ca. 0.3 wt.%, so long as the olivine did not significantly concentrate Ir (mantle olivines are generally very poor in Ir, <0.2ppb, so the latter assumption is good; Mitchell and Keays, 1980). The fractional crystallization equation is

$$\frac{C_m}{C_o} = (1-f)^{(D-1)}$$

where Cm is the concentration of the element in the melt, Co is the initial concentration in the melt, f is the fraction of the melt precipitated, and D is the bulk precipitate/melt partition coefficient. If, for example, the precipitate consisted of chromite and olivine in the ratio 2/98 (the ratio suggested by Irvine, (1969) for cotectic crystallization), D would be 0.02 x 1,600 = 32, and the f corresponding to Cm/Co = 0.01 would be 0.138; the weight fraction of chromite precipitated would be 0.02 x 0.138 = 0.0028, i.e. about 0.3 wt.%.

The Ir-rich Josephine chromitites (Salt Rock, Tennessee Pass, and Lucky Strike; table III-10) contain Ir-rich PGMs; the occurrence and origin of these PGMs is discussed in detail in chapter IV. It is difficult to estimate the contribution of the PGMs to the whole rock Ir content of the chromitites. However, on the basis of measurements of the area fraction of the PGMs in polished sections, electron microprobe analyses for Ir, and estimates of the PGM densities, the larger (>5μ diameter) PGMs alone can account for 30% of the whole rock Ir content of the Salt Rock chromitite; it is doubtful that all the PGMs in the polished sections have been found, so 30% is a minimum estimate, and PGMs may account for nearly all of the chromitite Ir content. One might appeal to the speculations of Hagen (1954), Gijbels et al. (1974), and Naldrett and Cabri (1976) that the PGMs represent Ir which was originally dissolved in the chromites at high temperatures, but which exsolved upon cooling; however, as will be shown in chapter IV, the Josephine chromitite PGM textures bear little resemblance to exsolution textures, and most of the PGMs appear to have been included as solids in the growing chromite crystals. Thus, in order to explain why the high $Cr/(Cr+Al+Fe^{+3})$ chromitites contain more Ir, one must explain why these chromitites should contain more PGMs. One possible explanation is that PGMs precipitating from melts nucleate chromite crystals, or preferentially attach to the chromite crystals due to some unknown surface property of

chromite (Hiemstra, 1979), so that Ir in PGMs is scavenged from the melt by the chromites in a manner which can be roughly described by an Ir chromite/melt partition coefficient.

Another objection to the fractional crystallization model is that the variations in $Cr/(Cr+Al+Fe^{+3})$ of the chromites may not represent fractional crystallization from a single type of melt, but rather precipitation from a variety of melts with different initial $Cr/(Cr+Al+Fe^{+3})$. The $Cr/(Cr+Al+Fe^{+3})$ of the melts might be, for example, a function of the degree of melting of the source peridotite, as melts produced in equilibrium with refractory, Al-poor peridotites at high degrees of melting would probably have high $Cr/(Cr+Al+Fe^{+3})$, while melts produced from fertile, Al-rich peridotites would probably have lower $Cr/(Cr+Al+Fe^{+3})$. This alternative is difficult to test, and offers no obvious explanation for the covariation of Ir and $Cr/(Cr+Al+Fe^{+3})$ in the chromitites.

Regardless of the specific mechanism for forming the Josephine chromitites, the high Ir contents and Ir/(Pd+Au) of the chromitites relative to all known basaltic rocks (table III-6) suggests that chromite precipitation in the mantle may be a significant means of fractionating Ir from Pd and Au, and in causing the wide range of Ir contents found in basalts. While most basalts contain small amounts of Cr, $\leq$ 200ppm (Carmichael, Turner, and Verhoogen; 1974), there is evidence that primitive basalts should contain

> 2000 ppm Cr (e.g., Clarke, 1970; Kurat et al., 1980), and the low Cr contents of most basalts may be indicative of extensive chromite precipitation at depth in the mantle.

III-5: SUMMARY

The most fertile Ronda and Josephine peridotites have noble metal abundances of ca. 10^{-2}x chondrites, and have noble metal ratios within a factor of 1.5 of the chondritic ratios. The noble metal ratios of the Ronda lherzolites are very nearly chondritic, and are believed to be typical of the primitive mantle, though the significance of the chondritic ratios is not clear. Palladium, Au, and possibly Pt apparently behaved as incompatible elements during partial melting of the Ronda and Josephine peridotites, and were enriched in the partial melts, while Ir behaved as a relatively compatible element, remaining in the residues. It is not clear which phases controlled the behavior of noble metals during parital melting of the peridotites; base metal sulfides probably contained the noble metals below the silicate solidus, but with the formation of silicate partial melts, the sulfide probably dissolved into the silicate melts. Palladium, Au, and Pt may also have dissolved into the melts, whereas Ir may have formed refractory PGMs, or may have been partly contained in spinel.

The Ronda mafic layers and Josephine chromitites give evidence for post-partial melting processes which may have altered the abundances of noble metals in the melts. Palladium and Au apparently behaved as compatible elements

in the mafic layers; the relatively high sulfide contents of the layers, and the variations of Pd/Cu, suggest that the compatible behavior was due to precipitation of sulfides. Precipitation of sulfide may be a general mechanism of reducing the Pd and Au abundances of melts, though it is not clear if sulfide precipitation should fractionate the noble metals. There is strong evidence for the fractionation of noble metals during precipitation of the Josephine chromitites, and chromite precipitation may be a significant post-partial melting process for reducing the Ir contents and Ir/(Pd+Au) of melts.

CHAPTER IV: THE OCCURRENCE AND ORIGIN OF PLATINUM GROUP MINERALS IN CHROMITITES OF THE JOSEPHINE PERIDOTITE

IV-1: INTRODUCTION

It was noted in chapter III that some of the Josephine chromitites contain PGMs. Descriptions of PGMs found *in situ* in mantle-derived ultramafic complexes are extremely rare, and hence the occurrence of PGMs in the Josephine chromitites is of general interest in determining the conditions for formation of PGMs in the mantle. This chapter is a description and paragenetic interpretation of PGMs and associated minerals found in the Salt Rock and Tennessee Pass chromitites of the Josephine Peridotite (see figure III-9 for locations). The interpretation is based on studies of mineral textures, electron microprobe and scanning electron microscope (SEM) analyses, and consideration of the chemical stabilities of the minerals. Platinum group minerals have previouslv been found in the streams and placers associated with the Josephine Peridotite (Mertie, 1969), but on the basis of an extensive survey of the literature, this study is believed to be the first description of PGMs found *in situ* in the rocks of the Josephine Peridotite. The possibility that the placer PGMs have been derived from PGM-bearing chromitites is examined in this chapter, as well as the alternative hypotheses (Bird and Bassett, 1980) that the placer PGMs represent "primitive" minerals remaining little changed since the

formation of the earth, or minerals formed near the earth's core, which have been weathered from refractory peridotites.

IV-2: ANALYTICAL METHODS

Sample preparation and optical microscopy

Chromitite samples were mounted in cold-setting epoxy resin, sectioned with a diamond saw, and successively polished with 1.0μ and 0.3μ alumina, 1.0 and 0.25μ diamond paste and 0.05μ alumina. The polished mounts were slowly scanned at 40x and 160x magnification on a reflected light microscope; key mineral grains were then examined and photographed at 1000x-2000x by use of an oil immersion lens.

Electron microprobe and scanning electron microscope analyses

Analyses of the PGMs and associated minerals were obtained on a Materials Analysis Corp. electron microprobe and International Scientific Instruments and CWIC scanning electron microscopes (SEMs). Microprobe analyses were made at accelerating potentials of 15, 20 and 25KV, take-off angles of 12° and 40°, and with an electron beam diameter of ca. 2μ. Microprobe x-ray spectra were taken with wavelength and energy dispersive (Si(Li)) spectrometers. The standards for sulfide and alloy analyses were pure metals for Cr, Fe, Ni, Cu, Zn, Pt, Ir, and Os; NiS and FeS_2 for S, Fe and Ni; and Ru-Fe alloy and an analyzed natural Os-Ir alloy for Ru,

Os and Ir. Standards for chromite analyses were oxides and silicates. The Kα lines were used for analyses of lower atomic number elements (Mg through Zn); L lines were used for analyses of Ru; and L and M lines were used for analyses of Os, Ir and Pt. X-ray intensities were corrected for atomic number, absorption, and fluorescence effects by the Tracor Northern version 10-D/37 ZAF program. For energy dispersive analyses, standard spectra were fit to sample spectra using the Tracor Northern SML-7J/30 multiple least squares regression program.

The samples were examined in the back-scattered and secondary electron modes on the SEMs. The accelerating potentials were from 15 to 30KV, beam incidence was ca. 20° off-normal, and spot sizes for x-ray analysis were less than 0.5μ x 0.5μ. Both the ISI and CWIC SEMs were equipped with Si(Li) x-ray spectrometers having resolutions of ca. 150eV FWHM at the FeKα peak. Qualitative and semi-quantitative x-ray analyses were made by using the larger, electron microprobe-analyzed PGMs in the samples as standards. SEM analyses provided estimates of the atomic proportions in minerals which were too small for microprobe analyses (≤5μ in diameter).

The sizes of the minerals examined in this study limited the quality of the microprobe and SEM anlyses. Some of the mineral inclusions were smaller than the theoretical minimum size for quantitative anlyses, as calculated by

Reed's (1975) formula;* consequently, excitation of the chromite matrix was observed in analyses of some inclusions. In cases where it was clear that the inclusion should contain no Mg, Al, or Cr, it was possible to use these elements to subtract the chromite spectrum from the inclusion spectrum, and to make rough corrections for the matrix excitation effect.

Although ZAF (atomic number (Z), absorption (A), and fluorescence (F)) corrections were applied to all microprobe analyses, they were probably of limited accuracy in the analyses of the smaller (<5μ diameter) inclusions made at the 12° take-off angle. The ZAF procedure requires that the entire x-ray path be within the analyzed inclusion (Fleetwood, 1968); however, at the 12° take-off angle, much of the x-ray path was probably in the surrounding chromite matrix.

---

* The diameter of the 99% x-ray source is approximately given by:

$$d_{99} = 0.23\ (E_o^{1.5} - E_a^{1.5})/\rho$$

(Reed, 1975)

where E_o and E_a are the energies in KeV of the impinging electrons and the absorption edge for the radiation of interest, respectively, and ρ is the density of the mineral in g/cm^3. For the analysis of S Kα x-rays in laurite at an accelerating potential of 15KV, d_{99} is ca. 2μ. This estimate is made on the assumption of an infinitesimal electron beam, and represents an absolute minimum size for quantitative analysis. The effects of finite beam diameter, take-off angle, and secondary excitation all increase the estimates of minimum size for quantitative analysis (Fitzgerald, 1973; Fleetwood, 1968).

In replicate microprobe analyses of the PGMs, the Ru/Os was reproducible to ±5%, and the Os/Ir to ±20%. As would be expected from the small size of the PGMs, the totals of the analyses were very sensitive to the position of the electron beam. Analyses reported in this chapter are those with the highest totals for each individual PGM.

IV-3: Descriptions

Tennessee Pass and Salt Rock chromitites

The Tennessee Pass and Salt Rock chromitites consist of ca. 95-100% chromite grains by volume, with minor silicates (largely serpentine). Analyses of the chromite grains are given in table IV-1. The individual chromite grains are from <1mm to ca. 5mm in diameter, and are packed together in "foam structures" similar to those described by Stanton (1972). The chromitites have been extensively fractured, and in some places, the chromite grains have been reduced to fine-grained cataclastites. Cracks in the individual chromite crystals, as well as the matrices of the cataclastites, are filled with magnetite, ferrit-chromite*, serpentine, and rarely, base metal alloys.

The chromite crystals contain numerous minute (<1μ to 50μ) inclusions of silicates, Ni-Fe sulfides, and platinum group minerals (PGMs). Most of these inclusions

---

* As defined by Bliss and MacLean (1975), ferrit-chromite is Fe_3O_4-rich chromite with a reflectivity higher than normal chromite.

TABLE IV-1: Electron Microprobe Analyses of Chromites as Weight Percent Oxides

Sample	MgO	Al_2O_3	TiO_2	Cr_2O_3	MnO	FeO[a]	Total
Tennessee Pass	13.03 ±0.11[b]	7.96 ±0.30	0.35 ±0.03	60.97 ±0.56	0.55 ±0.11	17.13 ±0.17	99.99
Salt Rock	14.09 ±0.11	7.51 ±0.41	0.20 ±0.03	63.83 ±0.54	0.62 ±0.06	14.21 ±0.18	100.46

a) All Fe as FeO.

b) Quoted error is the standard deviation of analyses of 4 randomly selected grains from a crushed 20 gram sample.

are completely isolated within individual, uncracked portions of chromite crystals; however, some of the inclusions are surrounded by radial cracks in the chromite, and these cracks often extend to meet larger cracks cutting across the chromite grains.

The PGM inclusions and the associated minor minerals of the Tennessee Pass and Salt Rock chromitites are the subject of this chapter.

Platinum group and associated minerals

The PGMs and associated minerals found in the chromitites are listed in table IV-2, and the minerals are illustrated in figures IV-1-3. Microprobe analyses of individual minerals are given in table IV-3. Forty PGM grains in 9 polished sections have been identified by microprobe and SEM analyses; an additional 40-60 PGMs have been tentatively identified optically. The PGM dimensions range from <1μ to 30μ in cross-section, with an average of about 5μ. The most frequently observed PGM was laurite, (Ru, Os, Ir)S_2, followed by Ru-Fe-rich, Os-Ir-rich, and Pt-rich alloys, and minor complex platinum group sulfides and an arsenide. Several of the chromitite PGMs have compositions unlike those of any previously described PGMs, and may constitute new mineral species; however, the limited occurrence and difficulties in obtaining analyses for these minerals preclude the suggestion of new mineral names.

TABLE IV-2: Platinum Group and Associated Minerals from the Tennessee Pass and Salt Rock Chromitites

Mineral	Approximate Composition[a]	Diameter	Optical properties[b]
Laurite	$Ru_{0.7}Os_{0.2}Ir_{0.1}S_2$ (EMP)	<3-25μ	Grey-blue, R<50%, isotropic
Ru-rich porous alloys ("type 2" alloys; see text)	Ru/Os/Ir=7/2/1, Fe, Ni variable (EMP)	3-25μ	White, R>60%; appear isotropic, may be cryptocrystalline
Os- and Ir-rich alloys	variable; Os or Ir > Ru (SEM, EMP)	≈ 5μ	White or yellow-white, R>60, isotropic and anisotropic
Pt-rich alloys	variable; contain Fe, Ir and Cu (SEM)	1-5μ	White to yellow-white, R>60, isotropic and anisotropic
Erlichmanite?	Os, Ru, Ir sulfide (SEM)	2μ	Whitish, R > laurite; isotropic
Ir, Cu, Ni sulfide	$Ir_{0.15}Cu_{0.1}Ni_{0.1}S_{0.65}$ (SEM)	3μ	Grey, R < laurite, isotropic
Cooperite?	PtS, minor Ni (SEM)	2μ	Yellow-white, R > laurite, anisotropic
Sperrylite?	Pt and As (SEM)	3μ	White, R > laurite, isotropic
Ni, Ir, Fe, Cu sulfide	$Ni_{0.4}Ir_{0.1}(Fe,Cu)_{0.1}S_{0.4}$ (SEM)	3μ	Brown-grey, R < laurite, anisotropic
Fe-Pt alloy ("type 2" alloy?)	$(Fe,Ni)_3Pt$ (EMP)	5μ	Grey-white, R≈60, isotropic
Millerite	(Ni,Fe)S, Ni>>Fe (EMP)	5μ	Yellow-white, R > 50, anisotropic
Pentlandite? Heazlewoodite?	Ni/Fe variable (SEM)	1-50μ	Creamy-white, R > 50, isotropic and anisotropic
Ni-Fe	$Ni_{0.6}Fe_{0.4}$ (SEM)	1-50μ	White, R > 60, isotropic
Cu-Zn	$Cu_{0.6}Zn_{0.4}$ (EMP, SEM)	1-20μ patches	Orange-gold, R > 60, isotropic
Native chromium	Cr(EMP,SEM); Cu,Zn in EMP analyses probably from excitation of Cu-Zn matrix	1-5μ	White, R > 60, isotropic
Bi, Sn-Sb intergrowth	Bi and $Sn_{0.7}Sb_{0.3}$	25μ	Creamy white, R > 60

a) EMP denotes composition derived by electron microprobe; SEM denotes composition derived from SEM x-ray spectra

b) Optical properties are for reflected light. R is the approx. reflectivity.

TABLE IV-3: Electron Microprobe Analyses of Platinum Group and Associated Minerals*

Mineral and Location	Ru	Os	Ir	Pt	Fe	Ni	S	Total
1) Laurite, Tennessee Pass	32.0	19.5	8.4	-	-	-	32.1	92.0
2) Laurite, Tennessee Pass	41.6	13.3	7.8	0.8	-	-	34.5	98.0
3) Laurite, Salt Rock	28.5	19.5	5.9	0.8	-	-	32.4	87.1
4) Laurite, Salt Rock	36.7	17.4	8.3	-	-	-	34.2	96.6
5) Type 2 alloy, Tennessee Pass	35.6	22.7	13.8	-	3.4	7.5	1.1	85.1
6) Type 2 alloy, Tennessee Pass	37.8	19.6	15.0	1.3	4.5	4.2	2.0	84.4
7) Type 2 alloy, Salt Rock	33.0	17.2	11.81	2.0	34.3	3.2	-	101.5
8) Type 2 alloy, Salt Rock	32.6	16.7	12.6	3.8	32.1	6.1	-	103.9
9) Type 2 alloy, Salt Rock	36.2	8.2	5.9	-	28.6	0.7	-	79.6
10.)Type 2 alloy, Salt Rock	40.5	18.6	8.1	-	32.0	3.3	-	102.5
11) Type 2 alloy ? Salt Rock	-	-	-	54.0	39.0	7.8	-	100.8
12) Type 2 alloy ? Salt Rock	10.1	41	14	3.3	34.0	-	-	102
13) Millerite adjacent to laurite, Salt Rock	-	-	-	-	0.7	61.8	35.3	96.8

Native Chromium, Copper-Zinc Alloy Intergrowth (Tennessee Pass)

	Cr	Cu	Zn	Total
14) "Bulk analysis"	32.1	42.8	25.6	100.5
15) Native chromium	84.5	8.5	5.0	98.0
16) Cu-Zn alloy	3.3	54.6	32.6	90.5

* A dash indicates that the element was not detected. Analyses are not significant to three places, but the last digit is retained to prevent round-off error in calculations.

Figure IV-1:

Type 1 PGMs. All are inclusions in chromite crystals. Photos a. - g. were taken with an oil immersion lens in reflected light; photo h is a back-scattered electron image. Dotted lines have been used to emphasize phase boundaries in some photographs.

a.) Laurite, (Ru, Os, Ir)S_2, with an attached silicate (Sil). The sharp outline of the laurite grain cuts across the boundary between the silicate and the chromite, which suggests that the laurite is idiomorphic.

b.) Laurite (L) and an Ir-Cu-Ni sulfide with an attached silicate (Sil).

c.) A zoned alloy grain and a laurite (L) with silicates (Sil).

d.) An Os-Ir alloy which cuts across the boundary between silicate (Sil) and chromite.

e.) Laurite (L) and PtS (probably cooperite), surrounded by a silicate (Sil) on one side.

f.) Laurite (L) with an anisotropic Ni-Ir-Fe-Cu sulfide and millerite.

g.) A relatively large laurite with an attached bleb of silicate.

h.) A detail of the grain in IV-1g, showing Pt arsenide (probably sperrvlite) and irregular patches of Pt-Fe alloy.

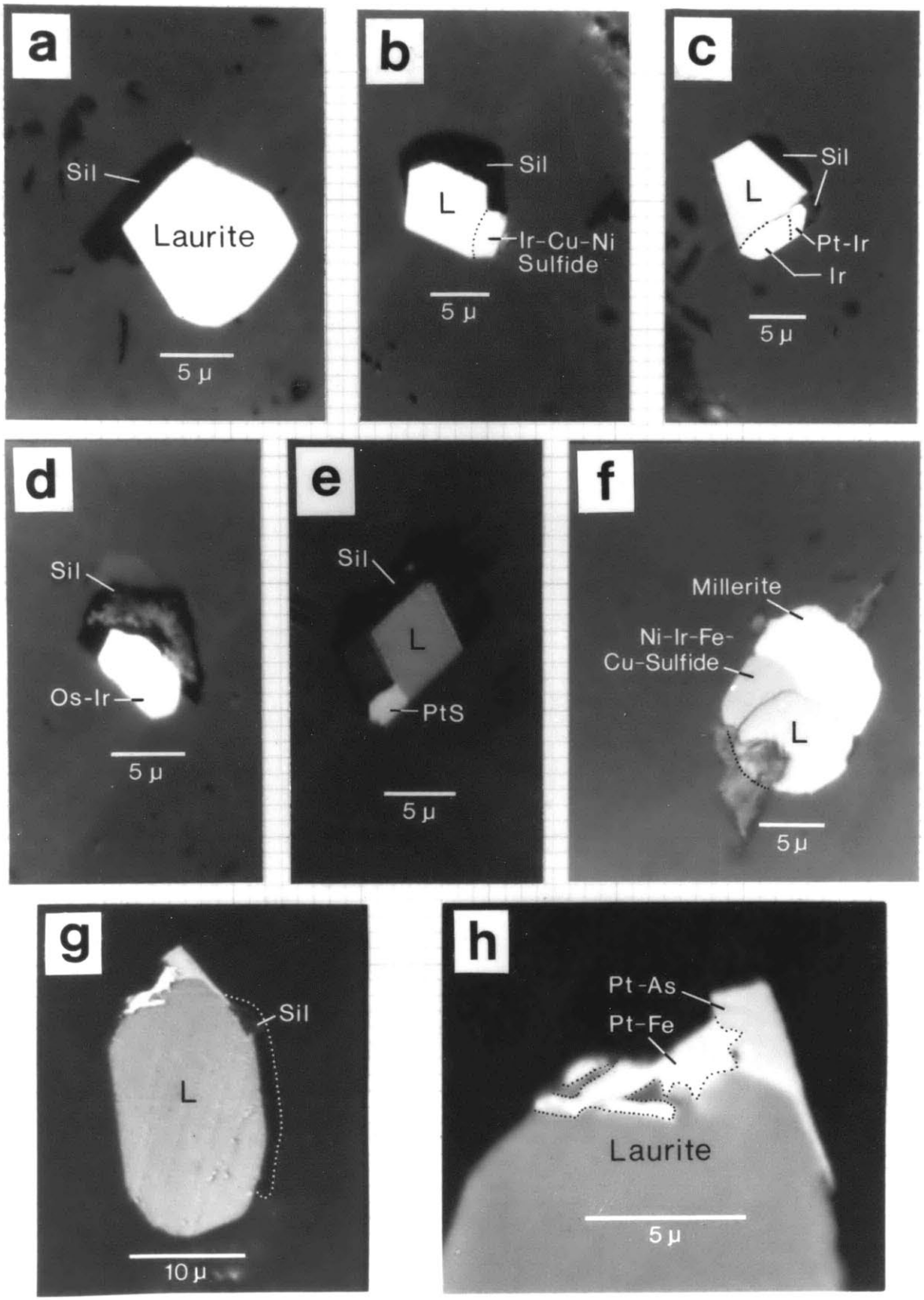
a
Sil
Laurite
5 µ
b
Sil
L
Ir-Cu-Ni
Sulfide
5 µ
c
Sil
L
Pt-Ir
Ir
5 µ
d
Sil
Os-Ir
5 µ
e
Sil
L
PtS
5 µ
f
Millerite
Ni-Ir-Fe-
Cu-Sulfide
L
5 µ
g
Sil
L
10 µ
h
Pt-As
Pt-Fe
Laurite
5 µ

Figure IV-2:

Type 2 PGMs. All are inclusions in chromite. Photos a. - c. were taken with an oil immersion lens in reflected light; photo d. is a back-scattered electron image.

a.) A porous type 2 alloy (T2) with radial cracks in the surrounding chromite. Portions of the cracks are filled with a light gray, Fe-rich material which is either magnetite or ferrit-chromite (M/F); the two minerals cannot be distinguished by x-ray spectra due to matrix excitation effects. A bleb of silicate (Sil) is on one side of the alloy.

b.) A detail of the grain in IV-2a., showing porosity and regions of magnetite or ferrit-chromite adjacent to the grain. The cracks and regions of M/F have been inked in for clarity.

c.) A Ru-rich type 2 alloy (T2), partly surrounded by an inhomogeneous alloy containing Os, Ir, Pt, Ni, and Fe. Both alloys contain small amounts of sulfur (<5%), inhomogeneously distributed. A crack radiating out from the alloys is partly healed with Fe-rich chromite.

d.) A relatively large, porous type 2 alloy.

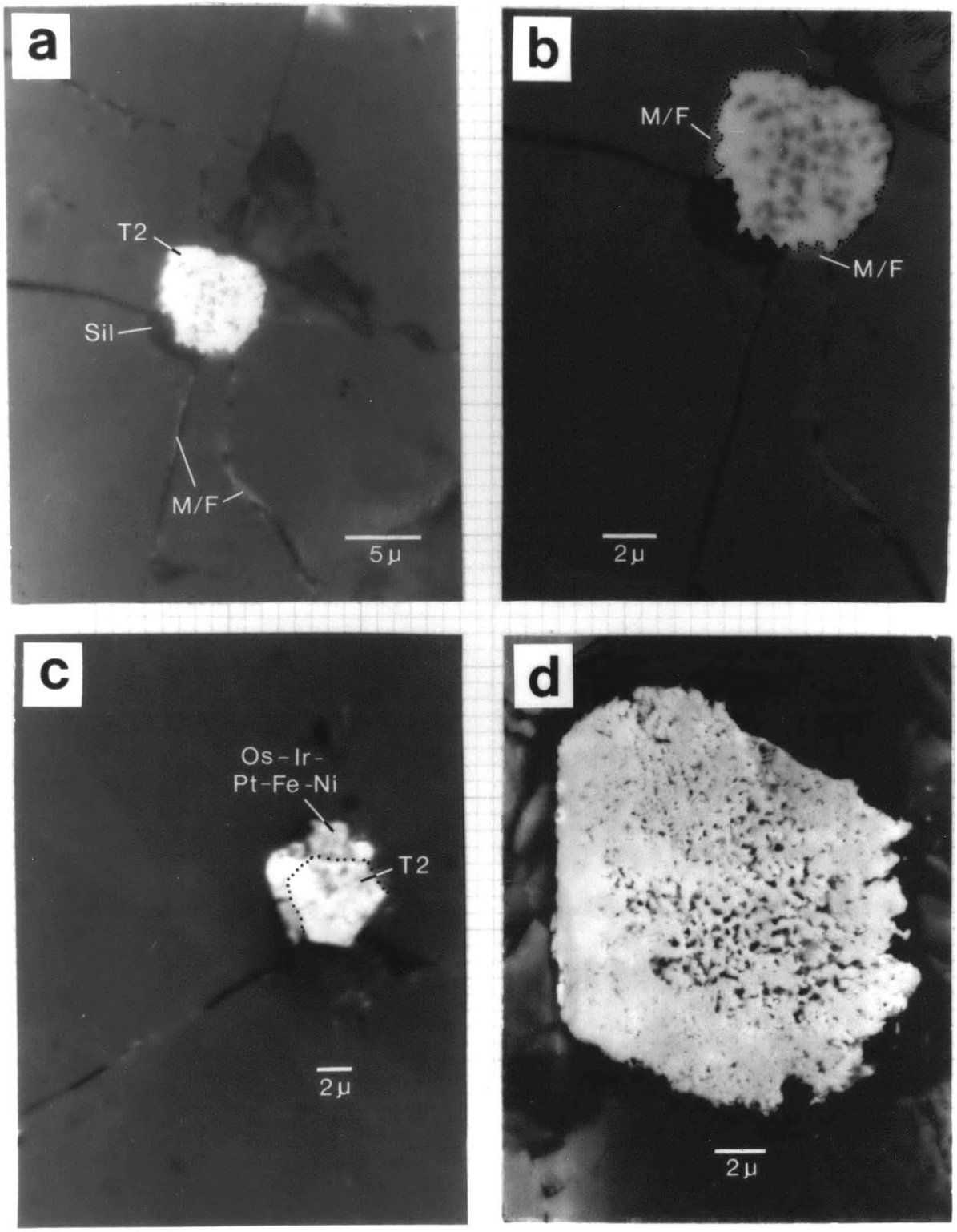
a
T2
Sil
M/F
5 µ
b
M/F
M/F
2 µ
c
Os - Ir -
Pt - Fe - Ni
T2
2 µ
d
2 µ

Figure IV-3:

Base metal alloys. All photos were taken in reflected light; photos b. and c. were taken with an oil immersion lens.

a.) An intergrowth of native chromium and a Cu-Zn alloy occurring in a relatively large crack. Note the thin vein of native chromium below the intergrowth.

b.) Detail of the intergrowth in IV-3a. The relief between the alloys has been emphasized by buffing the sample on a high-nap cloth.

c.) Ni-Fe alloys filling cracks in chromite in a cataclastite. The matrix minerals are Fe-rich chromite and serpentine.

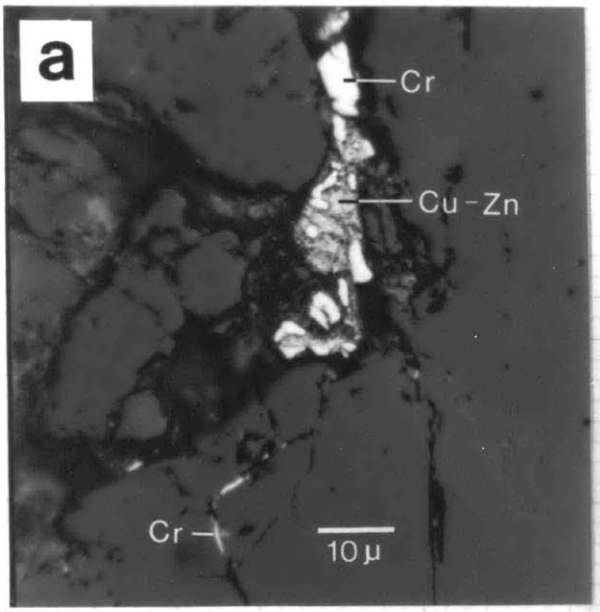
a
Cr
Cu - Zn
Cr
10 µ

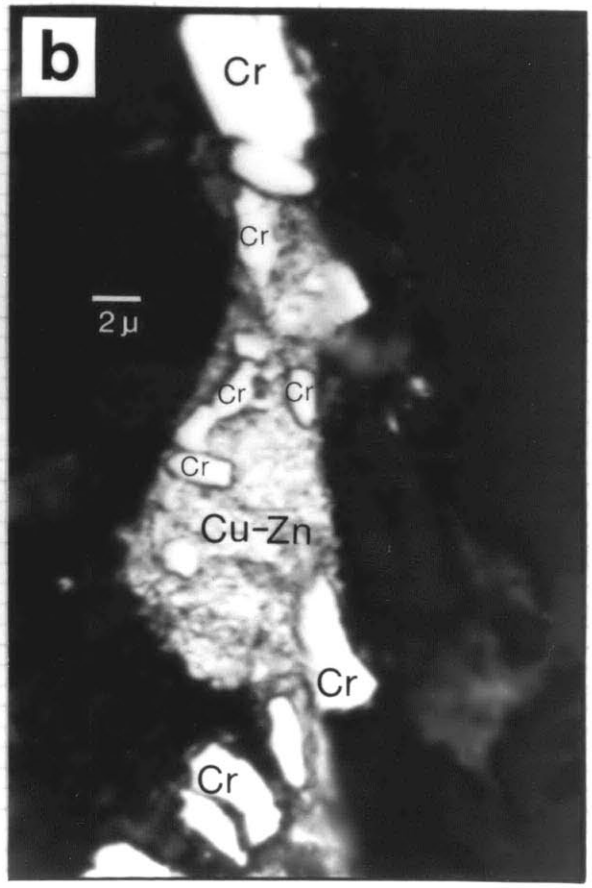
b
Cr
Cr
2 µ
Cr
Cr
Cr
Cu-Zn
Cr
Cr

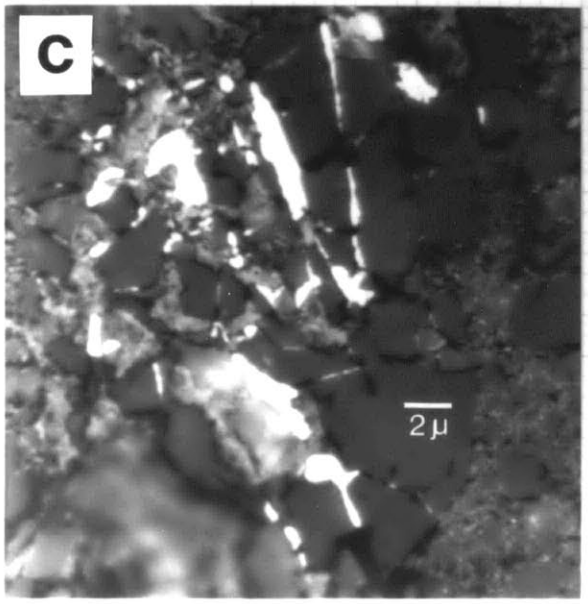
c
2 µ

About half the chromitite PGMs occur in composite grains with silicates, Ni-Fe sulfides, and other PGMs. The silicates in these composite grains have unusual compositions, with Mg/Al/Si roughly 1/1/4, substantial Ti contents (>1 wt.%), and traces of K; the Ni-Fe sulfides in the composite grains are typically millerite (analysis 13, table IV-3). In general, laurites and PGM alloys in composite grains have convex outlines against the surrounding minerals, and in many cases, the laurite grain boundaries cut across the boundaries between silicate and chromite (figure IV-1a). The textures in the composite grains are the most useful in interpreting the paragenesis of the PGMs, and figures IV-1 and IV-2 are strongly biased toward the composite PGM grains; it should be noted, however, that the chromitites also contain individual, isolated PGM grains similar in shape to the PGMs in the composite grains.

Texturally, most of the PGMs fall into two categories, hereafter referred to as "type 1" and "type 2." The type 1 PGMs are primarily sulfides and alloys with sharp, often polygonal grain boundaries; these minerals occur as inclusions in individual chromite grains, and are very rarely associated with cracks. The type 1 PGMs polish well and tend to have smooth, featureless surfaces. Type 1 PGMs are shown in figure IV-1. The type 2 PGMs are largely Ru-rich alloys with high porosity (up to 50% void spaces), high Fe+Ni contents (up to 75 atom %), and a persistent

association with late, often radial cracks in the host chromite crystals. Some type 2 PGMs tend to disintegrate during polishing. Type 2 PGMs are shown in figure IV-2. Compositionally and texturally, the PGMs from the two chromitites are quite similar, except that the type 2 PGMs from the Tennessee Pass chromitite are poorer in Fe than the type 2 PGMs from the Salt Rock chromitite (analyses 5-12, table IV-3).

The radial cracks which surround the type 2 PGMs are similar to those described by Sutton (1921), Rosenfeld and Chase (1961), and Simmons and Richter (1976), and probably resulted from the release of stresses developed during cooling and decompression of the host chromite. Most of the radial cracks are partly healed with magnetite, ferrit-chromite or serpentine, which indicates that the cracks are not artifacts of sample preparation.

The chromitite base metal alloys occur mainly as fillings in cracks and cataclastites. Thin (1-10μ) veins of Ni-Fe alloys are found in both of the chromitites, but are more common in the Salt Rock samples (figure IV-3c); alloys of similar composition have been found by the author in serpentinized portions of the Josephine harzburgites. Native chromium and Cu-Zn alloys are found in the Tennessee Pass chromitites (figure IV-3a., b. and analyses 14-16 in table IV-3); these alloys are fine-grained and intimately intergrown, and are difficult to resolve in microprobe analyses. The Cu and Zn in the microprobe

analyses of native chromium are probably due to excitation of the Cu-Zn matrix, as SEM x-ray spectra of the native chromium show little Cu and Zn. Similarly, Cr in analyses of the Cu-Zn alloys is probably due to matrix excitation. Microprobe analyses of the Cu-Zn alloys have low totals, probably because these alloys are soft and polish very poorly; no elements other than Cu, Zn, and Cr were detected in the energy-dispersive x-ray analyses, and the very high reflectivity of the mineral makes it unlikely that the low totals are due to oxygen. The Cu-Zn alloys have the composition of some man-made brasses, but it is extremely unlikely that these alloys represent laboratory contamination, as the samples never came in contact with brass, and as the alloys remained in the cracks after the samples had been re-ground and polished.

A single intergrowth of Bi and Sn-Sb alloy was found at the junction of two large cracks in a sample from Tennessee Pass. The intergrowth consists of alternating lamellae of the alloys.

In addition to the Ni-Fe sulfides which occur with PGMs in composite grains, Ni-Fe sulfides also occur as irregular, rounded inclusions in chromite grains, and as fillings in the interstices among chromite grains. These Ni-Fe sulfides are roughly 5-10 times more abundant than the PGMs by volume.

The textures of the type 1 and type 2 PGMs and the base metal alloys are schematically summarized in figure IV-4.

Figure IV-4:

A schematic summary of textures for the type 1 and type 2 PGMs (T1 and T2), base metal alloys (BMA), and the surrounding chromite matrix. Three chromite crystals (stippled) meet at a triple junction; cracks cut across two of the chromite crystals. The type 1 PGMs typically occur as isolated inclusions within uncracked portions of chromite grains. The type 2 PGMs are roughly similar to the type 1 PGMs in shape and size, but are typically porous and ragged, and are surrounded by radial cracks in the enclosing chromite; the radial cracks are often "healed" with magnetite or Fe-rich chromite. The base metal alloys typically occur as fillings in cracks cutting across the chromite crystals.

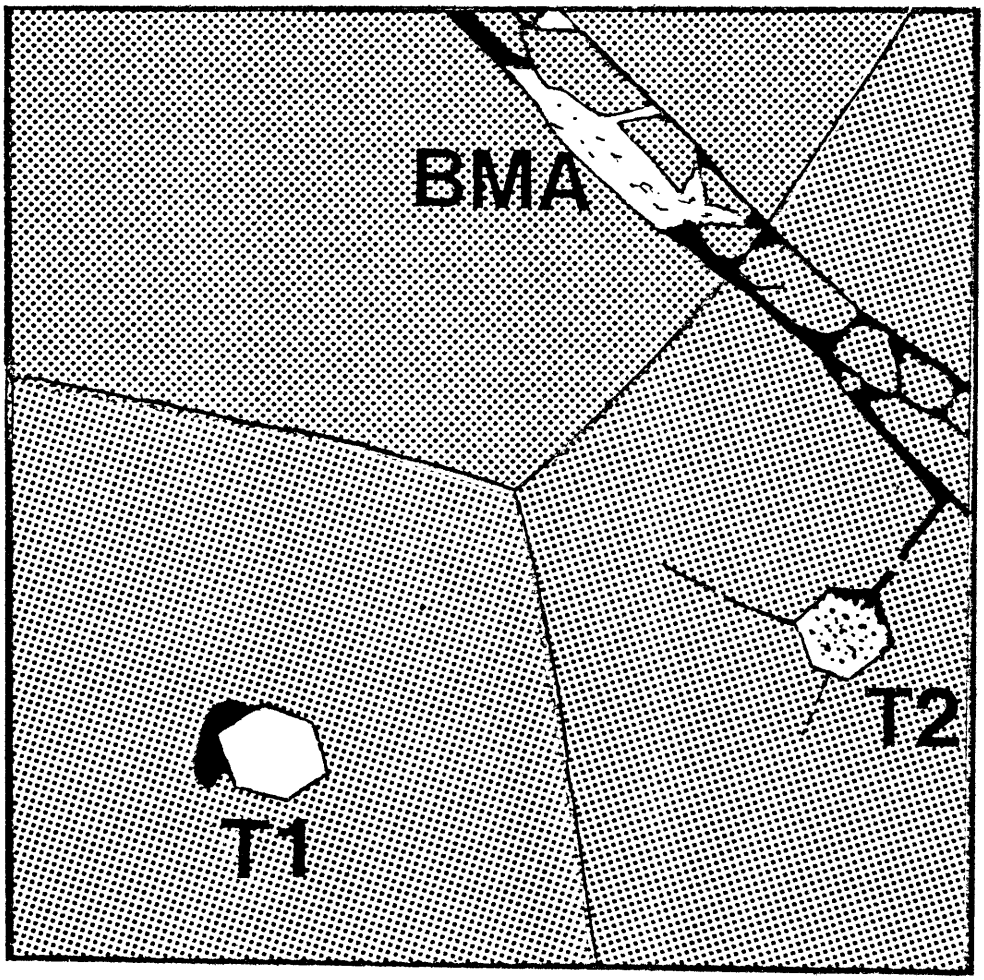
BMA
T2
T1

Comparison with in situ PGMs of other alpine ultramafics

There are few reports of PGMs found in place in alpine-type ultramafics. Constantinides et al. (1980) describe ca. 10μ diameter laurites and an erlichmanite, (Os, Ru, Ir)S_2, grain from chromitites of the Cyprus ophiolite. The sizes, shapes and textures of the Cyprus laurites are similar to those of the Josephine laurites. Base metal alloys (Cu-Zn and Ni-Fe) in the Cyprus chromitites are similar to those found in the Josephine chromitites. Chang et al. (1973) and Yu and Chou (1979) report PGMs in chromitites from possible ophiolites in China. The Chinese chromitites contain laurite, sperrylite, Ru-Fe alloys, and Os-Ir-rich alloys in common with the Josephine chromitites; however, the Chinese chromitites also contain a number of Os-Ir-Ru sulfarsenides not yet found in the Josephine chromitites. Shilo et al. (1978) report PGMs from Siberian ophiolites, including a number Os-Ir-Ru, Pt-Ir and Pt-Fe alloys, sperrylite, laurite and numerous arsenides, but it is not clear from the descriptions if these minerals were actually found in place. Genser et al. (1938), Cabri and Harris (1975), and Ford (1981) refer to reports of Os-Ir alloys found in Tasmanian peridotites.

IV-4: DISCUSSION: ORIGIN OF THE CHROMITITE PGM ASSEMBLAGE

Chromite formation temperatures

Application of the revised olivine-spinel geothermometer (Roeder et al., 1979; Fabries, 1979) to the

Salt Rock and Tennessee Pass chromitites yields temperatures of 900C-1400C, compatible with a magmatic origin. These temperatures are derived using the chromite compositions given in table IV-1 and the range of olivine compositions (Fo_{89} - $Fo_{92.5}$) observed for dunites associated with chromitites in the Josephine Peridotite (Dick, 1976, 1977). The compositions of olivines from within the chromitites were not used in the temperature estimates, as there is strong evidence (Irvine, 1967; Roeder et al., 1979) that temperatures calculated using chromitite olivines are in error due to subsolidus re-equilibration.

Origin of type 1 PGMs

The occurrence of the type 1 PGMs as isolated inclusions within individual chromite grains suggests several possible origins:

1) The type 1 PGMs exsolved from the cooling chromite crystals, as suggested by Hagen (1954) and Gijbels et al. (1974) for PGMs in Bushveld chromitites.

2) The type 1 PGMs crystallized from trapped melts, as suggested by Constantinides (1980) for PGMs in Cyprus chromitites.

3) The type 1 PGMs represent solids engulfed in growing chromite crystals.

There is no evidence to support the first hypothesis. The type 1 PGM textures do not resemble exsolution textures reported by Ramdohr (1980) and Rostoker and Dvorak (1965), and the wide compositional variation of the PGM inclusions

is not an expected consequence of exsolution; hence the exsolution hypothesis is considered unlikely. The second hypothesis is plausible for a few of the PGMs, particularly the PGM sulfide inclusions with rounded outlines (e.g., figure IV-1f). However, many of the type 1 PGMs have sharp, often polygonal outlines which cut across the boundaries between chromite and silicate (figures IV-1a,b,d), which suggest hypothesis 3, that these PGMs are idiomorphic, and existed as solids before becoming enclosed in the chromite grains.

The sulfuration curves (log $a(S_2)$ vs. 1/T) for Ru and Pt are plotted in figure IV-5. It is evident that the formation of laurite ((Ru, Os, Ir)S_2) and cooperite (PtS) requires sulfur activities considerably in excess of those required to sulfurate Ni-Fe, and Cu-Zn alloys; it follows that these platinum group sulfides could not coexist in chemical equilibrium with Ni-Fe and Cu-Zn alloys. The existence of both laurite and the base metal alloys in the chromitites suggests that the unbreached chromite grains were effective in chemically isolating the laurites from the conditions which formed the base metal alloys.

Origin of Ni-rich sulfides

The Ni-sulfide inclusions in the chromite grains may have originated as trapped sulfide liquids; such an origin is suggested by the rounded shapes and low melting temperatures of the sulfides. Some of the sulfide inclusions are Fe-poor millerite; millerite melts at

Figure IV-5:

Log_{10} $a(S_2)$ vs. $10^3/T(K)$ for alloy-sulfide equilibria. The dashed line is the sulfuration curve for a Zn activity of 0.1, the estimated minimum Zn activity in the chromitite Cu-Zn alloys. "Pent." is pentlandite, $(Ni,Fe)_9S_8$. Relatively high sulfur activities were required to form the type 1 laurite ($(Ru,Os,Ir)S_2$) and cooperite (PtS). In contrast, the crack-filling Ni-Fe and Cu-Zn base metal alloys formed at much lower sulfur activities, and could not exist in chemical equilibrium with the type 1 platinum group sulfides. Thermodynamic data are from Balling (1965), Larson and Elliott (1967), and Craig and Scott (1974).

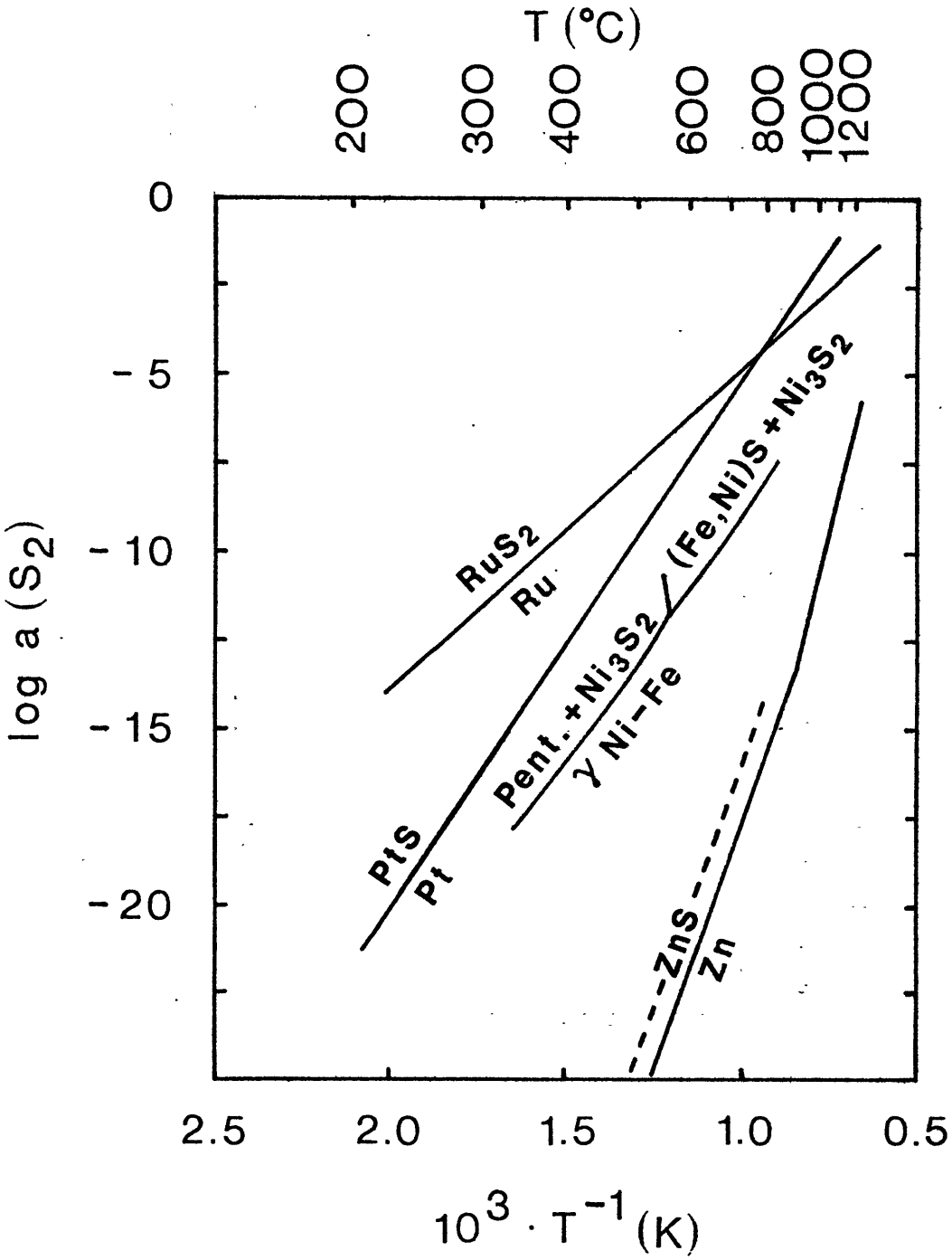
T (°C)
200
300
400
600
800
1000
1200
0
- 5
- 10
- 15
- 20
log a (S2)
RuS2
Ru
PtS
Pt
Pent. +Ni3S2
(Fe,Ni)S +Ni3S2
γ Ni-Fe
ZnS
Zn
2.5
2.0
1.5
1.0
0.5
10^3 · T^-1 (K)

ca. 1000C at 1 atm., at the low end of the estimated temperature range for formation of the chromitites (900-1400C). The T-P slope of the millerite melting curve is apparently not known, but the slope of the pyrrhotite melting curve (6C/Kbar according to Sharp, 1969; 2C/Kbar from data in Brett and Bell, 1969) probably provides a reasonable estimation; hence at pressures up to 60-70 Kbar, the melting temperature of millerite may be within the range of chromitite formation temperatures. However, the Ni/Fe ratios of the sulfide inclusions are very high (up to 100); such high ratios are not expected for mantle-derived sulfide melts in equilibrium with olivine. Rajamani and Naldrett (1978) predict Ni/Fe ratios more in the range of 0.1-0.2 for mantle-derived sulfide melts, and the experiments of Fleet et al. (1977) predict Ni/Fe ratios no greater than 2 for sulfides in equilibrium with olivines of typical mantle composition (ca. Fo_{90}, 0.2-0.5 wt.% NiO). Thus, the origin of the Ni-rich sulfide inclusions is not clear; an origin as trapped melts is reasonable purely on grounds of melting temperatures, but the compositions of the sulfides are not those expected for melts in equilibrium with olivine.

Origin of base metal alloys

Whereas the type 1 PGMs probably formed before or during the growth of the chromite crystals, the base metal alloys probably formed at a later time, during or after brittle fracture of the chromite crystals. As previously noted, the Ni-Fe and Cu-Zn alloys must have formed at S_2

activities much lower than those required for formation of the type 1 laurites (figure IV-5). Formation of native chromium requires extremely low O_2 activities, approaching those needed to form native silicon (figure IV-6).

The cause of the low O_2 and S_2 activities required to form the base metal alloys is not clear. Chamberlain et al. (1965), Dick (1974), and Eckstrand (1975) have suggested that high H_2 activities are produced during serpentinization by reactions similar to:

(IV-1) $3Fe_2SiO_4 + 2H_2O = 2Fe_3O_4 + SiO_2 + H_2$

(in olivine) (magnetite)

Oxygen and sulfur activities are lowered by reactions such as:

(IV-2) $H_2 + 1/2\ O_2 = H_2O$

(IV-3) $H_2 + 1/2\ S_2 = H_2S$

Because silica activity can be several orders of magnitude below quartz saturation during serpentinization (Hemley et al., 1977), reaction IV-1 can produce H_2 activities much higher than those associated with the familiar quartz-fayalite-magnetite buffer. It is therefore possible that serpentinization of the dunites surrounding the Josephine chromitites may have induced formation of the base metal alloys. However, reaction IV-1 can produce conditions no more reducing than the Fe-Fe_3O_4 buffer; while this reaction may be adequate for explaining the existence

Figure IV-6:

Log_{10} $a(O_2)$ vs. $10^3/T(K)$ for metal-oxide equilibria. QFM is the quartz-fayalite-magnetite buffer. The dashed line is the Fe-Fe_3O_4 curve for an Fe activity of 0.1, which is estimated to be a lower limit for Fe activity in the chromitite Ni-Fe alloys. The formation of native chrome requires extremely reducing conditions, approaching those for native silicon. Thermodynamic data from Kubaschewski and Evans, 1958 and Pehlke et al., 1975.

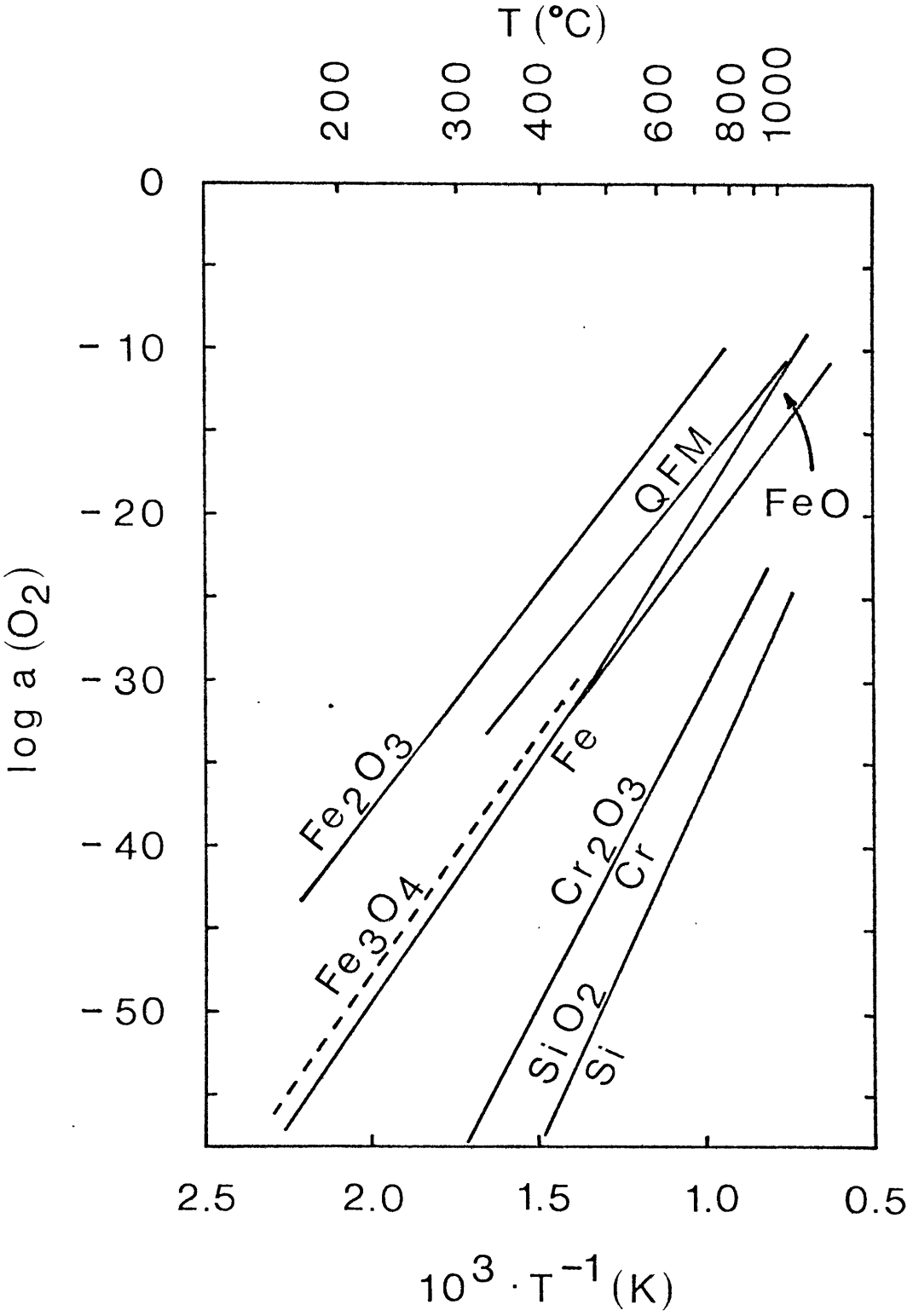
T (°C)
200
300
400
600
800
1000
0
- 10
- 20
- 30
- 40
- 50
log a (O2)
QFM
FeO
Fe2O3
Fe
Fe3O4
Cr2O3
Cr
SiO2
Si
2.5
2.0
1.5
1.0
0.5
10^3 · T^-1 (K)

of Ni-Fe alloys, it cannot, by itself, explain the existence of native chromium. It may be possible that more reducing fluids could be produced during serpentinization by separation of H_2 gas from O_2 and H_2O through selective diffusion (Sato, 1978).

Origin of type 2 PGMs

The type 2 PGMs are dominantly porous Ru-Os-Ir alloys with high and variable Fe+Ni contents. The porosity and ragged appearance of these alloys, as well as the strong association with cracks, suggest that the type 2 PGMs may have been derived by alteration of pre-existing PGMs. In addition, some type 2 PGMs are bordered by ferrit-chromite and magnetite, which were probably formed by alteration of chromite (Bliss and MacLean, 1975). Two hypotheses for origin of the type 2 PGMs by alteration are considered here:

1) The type 2 PGMs formed by reduction of laurites or similar sulfides* and arsenides after cracks formed in the host chromite and exposed the laurites to reducing conditions (e.g., low S_2, high H_2).

2) The type 2 PGMs are Fe-rich alloys which developed porous textures due to oxidation, dissolution and removal of material during weathering. This hypothesis follows Bird and Bassett's (1980) interpretation of porous textures in alloys from Port Orford, Oregon placers.

---

* The few Pt-Fe-Ni alloys which fit the type 2 description might have been derived by reduction of sperrylite or cooperite.

The first hypothesis is supported by a number of observations. First, the existence of crack-filling base metal alloys (particularly Ni-Fe and Cu-Zn) is evidence for the existence of low S_2, reducing conditions during or after the formation of cracks in the chromite crystals. Second, the Ru/Os/Ir ratios of most of the type 2 alloys are similar to the ratios of the type 1 laurites, but are unusual for Os-Ir-Ru alloys in general (figure IV-7). Third, the type 2 alloys and laurites are similar in size, and sometimes in shape. Fourth, the porous textures of the type 2 alloys are similar to textures in alloys produced by H_2- reduction of oxides (Goetzel, 1949); and fifth, some type 2 PGMs contain sulfur-rich patches similar to laurite in composition.

Formation of type 2 alloys from laurite requires the addition of metallic Fe and Ni; however, the existence of Ni-Fe alloys in the cracks indicates that high activities of metallic Fe and Ni were available. The addition of Fe and Ni would have the effect of reducing the type 2 porosity, but the porosities predicted for alloys formed by addition of Fe and Ni to reduced laurites are in agreement with the observed porosities (appendix B).

The second hypothesis is implausible, because there is no evidence in the chromitites for oxidative weathering conditions severe enough to partially dissolve the type 2 alloys. Some of the chromitite base metal alloys are very susceptible to oxidative corrosion (particularly Cu-Zn; Uhlig, 1948), yet show no signs of attack. In contrast, the

Figure IV-7:

Comparison of laurite and Os-Ir-Ru-rich alloy compositions. Open squares are laurites from Josephine chromitites, solid squares are type 2 alloys from Josephine chromitites; the single square with a question mark denotes an alloy with several type 2 characteristics, but with low porosity. The stippled region is the area of over 400 analyses of Os-Ir-Ru alloys reported in Harris and Cabri (1973), Cabri and Harris (1975), Feather (1976), Bird and Bassett (1980), and Ford (1981). The star is a single alloy from Japan (Urashima, 1974). The "U" denotes a single alloy composition from the Urals (Snetsinger, 1974) which is nearly the same as three of the type 2 alloys.

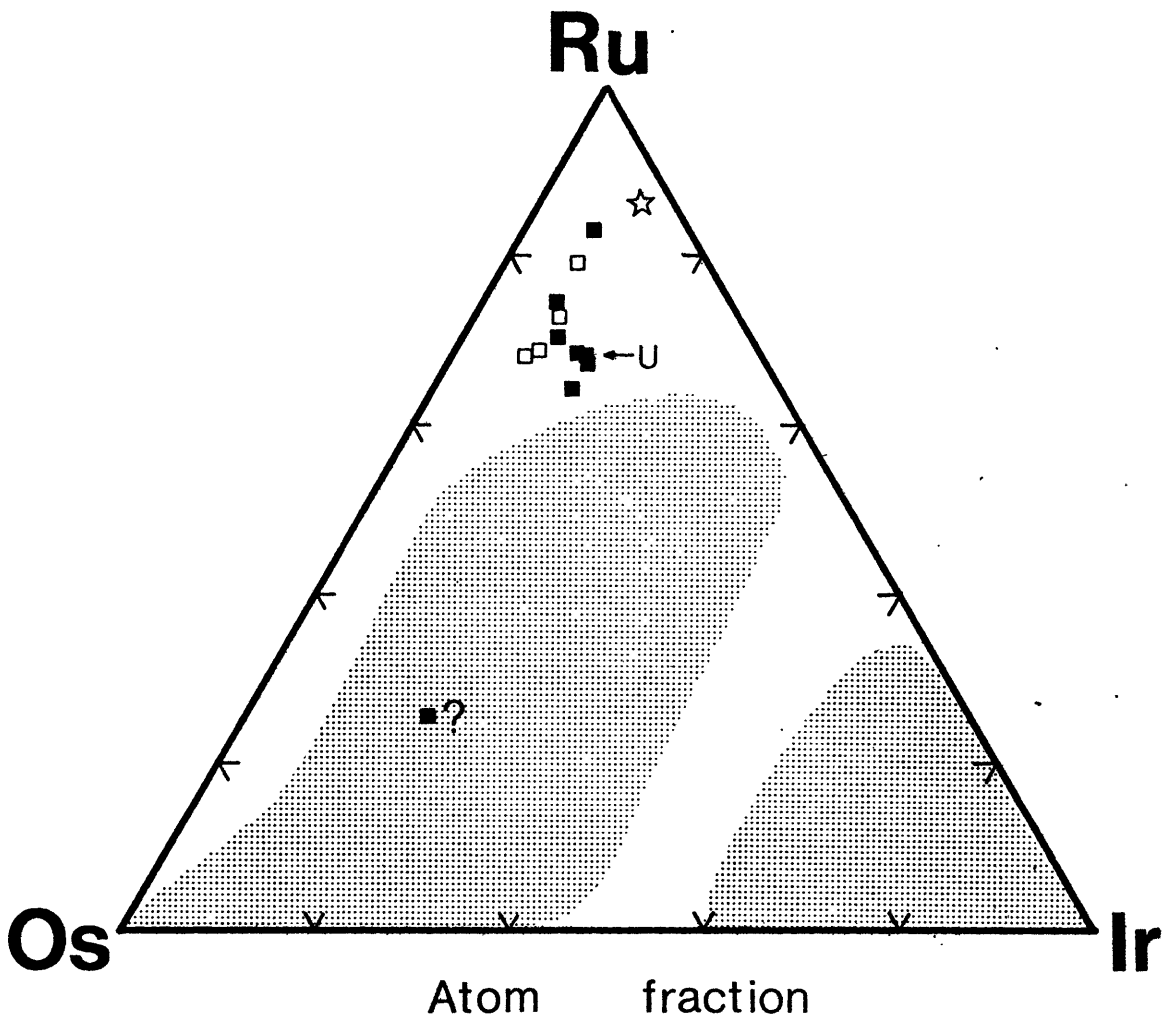
Ru
U
?
Os
Ir
Atom fraction

type 2 alloys should be quite resistant to oxidative attack, despite their high Fe contents; Miyagi and Wayman (1966) find Fe-Ir alloys with 50-80 wt.% Fe are "extremely corrosion resistant," and Griffith and Raub (1980) report that Os is an excellent passivator for Fe under oxidizing conditions. Hence, it is doubtful that oxidizing solutions could have pervasively formed holes in the type 2 alloys without totally removing the base metal alloys. In addition, the cracks around many of the type 2 PGMs have been sealed, probably since serpentinization, with magnetite, ferrit-chromite and serpentine. Hence, some type 2 PGMs have never been exposed to weathering.

Overview: origin of the chromitite-PGM assemblage

Podiform chromitites, such as the PGM-bearing Josephine chromitites, are generally thought to form in the upper mantle by precipitation from mafic melts (Dickey, 1975; Dick, 1977; Cassard et al., 1981). Textural observations suggest that some type 1 PGMs formed before or during the formation of the chromite crystals, but do not preclude the possibility that the type 1 PGMs existed in the mantle prior to the formation of the chromitites. However, the strong association of PGMs and chromitites, in the Josephine Peridotite and world-wide (Crocket, 1979), suggests that the type 1 PGMs and the chromite crystals are cogenetic, and tha both formed by precipitation from melts. The sharp, euhedra shapes of many of the type 1 PGMs are consistent with unrestricted growth in a melt (Vermaak and Hendriks, 1976).

It is possible that the type 1 PGMs nucleated the growth of the silicates found attached to the PGMs, as well as the chromite crystals. Liquid Ni-Fe sulfides may have precipitated with the type 1 PGMs; since these liquid sulfides would necessarily have been saturated with PGMs, they may have precipitated PGMs upon cooling, perhaps forming composite Ni-sulfide-PGM grains as shown in figure IV-1f.

After lithification, the chromitites apparently underwent brittle failure, cracking and forming cataclastites. After brittle failure, the chromitites were exposed to highly reducing conditions, and base metal alloys formed in cracks in the chromite crystals. There is evidence that some of the type 1 laurites were exposed to reducing conditions through cracks, and were subsequently reduced to form the type 2 PGMs.

IV-5: DISCUSSION: POSSIBLE RELATIONSHIP OF CHROMITITE AND PLACER PGMS

Platinum group minerals are found in the gold placers associated with the Josephine Peridotite, and in the placers of the associated Coast Range peridotites in northern California. Genthe (1853), Silliman (1873), Kemp (1902), Pardee (1934) the Oregon Department of Geology and Mineral Industries (1942), Mertie (1969), and Bird and Bassett (1980) report Os-Ir-Ru, Pt-Fe and Pt-Ir alloys, while Woehler (1869) And Snetsinger (1971) report laurite ((Ru, Os, Ir)S_2) and erlichmanite ((Os, Ir, Ru)S_2) from the

Oregon and California placers. In addition, the author has panned Os-Ir alloys from the Chetco River in Oregon. The placer PGMs range in size from "truly microscopic" (<5μ x 50μ; Mertie, 1969) to nuggets several millimeters across.

The source of the placer PGMs is not known, although it is generally agreed that the ultramafic rocks are the probable source (Twenhofel, 1943). Prior to this report, however, local occurrences of bedrock "platinum" were known only from quartz veins (Kellogg, 1922). Pardee (1934) notes that "platinum" and chromite are strongly associated in the placers, but "platinum" shows no systematic association with any other placer heavy mineral; Pardee thus attributes the placer platinum to chromite-bearing ultramafics. The placer gold is generally attributed to the gold-quartz veins and gold-sulfide-arsenide deposits found associated with metavolcanics, metasediments, intermediate intrusives, and greenstone-serpentinite contacts (Winchell, 1914; Pardee, 1934; Twenhofel, 1943; Brooks and Ramp, 1968).

Chromitites may be sources of the placer PGMs found associated with the Josephine Peridotite. Both the chromitites and placers contain Os-Ir-Ru, Pt-Fe and Pt-Ir alloys and laurite. In addition, there is a plausible geographic relationship between the placers and chromitites; for example, the Tennessee Pass PGM-bearing chromitites are several kilometers up-drainage from the Josephine Creek PGM placers (figure III-1). However, there are two important

differences between the chromitite PGMs reported in this study and placer PGM assemblages: first, the ratio of PGM alloys to PGM sulfides is much higher in the placer assemblage; and second, while both chromitites and placers contain very small PGM grains (<30μ), the placers contain much larger PGM grains than have been found in the chromitites.

The difference between the chromitite and placer PGM assemblages may indicate that the placers are derived from sources other than the chromitites. However, it is equally plausible that the differences arise purely from beneficiation, stream transport, and observational biases. Placer PGMs are usually beneficiated from the much more abundant "black sands" (largely chromite and magnetite) by panning, sluicing, or other density-based operations. These operations are efficient for the recovery of dense minerals, such as gold and Os-Ir-Ru alloys, but according to Taggart's (1945) "concentration criterion," they should be inefficient for the recovery of relatively low density minerals such as laurite and other PGM sulfides.* It is

---

* The "concentration criterion" (CC) for density-based separation of heavy minerals from light minerals is:

$$(\rho_h - \rho_f)/(\rho_l - \rho_f)$$

where ρ_h, ρ_l, and ρ_f are the densities of the heavy mineral, light mineral, and fluid medium, respectively. For sluice operations, separation is efficient if CC exceeds 3.5. For separation of laurite (ρ_h = 7.0 g/cm^3) from chromite (ρ_l = 4.5 g/cm^3) in water, CC = 1.7.

also well established that sluice operations are biased toward recovery of large minerals, with severe losses of minerals less than 300μ in diameter (Peele and Church, 1945; Masson, 1953). On the other hand, microscopic examination of the polished chromitites is probably biased against observation of large PGMs (Cabri and Harris, 1975); for example, if the chromitites contained equal weight fractions of 100μ diameter PGMs and 5μ diameter PGMs, the 100μ diameter PGMs would occur in polished sections with 1/400th the frequency of the 5μ diameter PGMs. Laurite may also be removed from the placer assemblage by comminution during stream transport; the mineral is apparently very brittle (Palache et al., 1944). Until these effects can be evaluated, the chromitites should be considered as possible sources of at least some of the placer PGMs.

IV-6: DISCUSSION: "PRIMITIVE MINERAL" AND HIGH PRESSURE, HIGH TEMPERATURE ORIGINS FOR TERRESTRIAL PLATINUM GROUP ALLOYS

Bird and Bassett (1980)* have proposed origins for the Josephine placer PGMs, as well as terrestrial PGMs in general, which are very different from the origins suggested in this study. BB suggest that terrestrial PGM alloys, and especially Os-Ir-Ru alloys, do not form in the upper mantle, but are either "primitive minerals" remaining unaltered

---

* Hereafter referred to as "BB".

since accretion of the earth, or are minerals which formed in the region of the earth's core. Furthermore, BB propose that PGM sulfides form by alteration of PGM alloys, and not the reverse. As the proposals of BB are contrary to the results of this study, BB's reasoning is critically reviewed below.

Chondritic origin

BB suggest that terrestrial Os-Ir-Ru alloys are analogous to platinum group alloys found in chondritic meteorites, and may actually be "primitive minerals originally incorporated in the earth during earth accretion [that] have survived essentially intact throughout the history of the earth." If this suggestion is correct, terrestrial Os-Ir-Ru alloys, which have extremely low Re contents (Allegre and Luck, 1980; Noddack and Noddack, 1931), should have $^{187}Os/^{186}Os$ ratios like the initial ratios of chondritic meteorites. However, terrestrial alloys analyzed to date have distinctly non-chondritic $^{187}Os/^{186}Os$ ratios (Allegre and Luck, 1980). Furthermore, the $^{187}Os/^{186}Os$ ratios of terrestrial alloys and the emplacement ages of the associated ultramafics define a mantle growth curve, which suggests that the alloys formed by mantle processes at times close to the emplacement of the ultramafic bodies.

BB emphasize the compositional similarities of terrestrial and chondritic Os-Ir-Ru-rich alloys. However, the compositional similarities of terrestrial and chondritic alloys are debatable. Most chondritic Os-Ir-Ru-rich alloys have much higher contents of Ni, Mo, W, Re, and Nb than are found in terrestrial Os-Ir-Ru-rich alloys; this point is illustrated in figure IV-8, a plot of Ni vs. Mo for terrestrial and chondritic alloys with Os+Ir+Ru > 20 wt.%. Of ca. 100 chondritic Os-Ir-Ru-rich alloy analyses, 2 or 3 fall in the region of terrestrial Os-Ir-Ru-rich alloys. If terrestrial Os-Ir-Ru-rich alloys are derived from chondritic Os-Ir-Ru alloys with little or no alteration, it is puzzling why the terrestrial alloys have such low Ni and Mo contents.

Sources of Os-Ir-Ru alloys: ophiolites and residual rocks vs. zoned ultramafics and cumulates

BB emphasize the association of Os-Ir-Ru alloys with ophiolitic ultramafic rocks, the "refractory residues of the material from which partial melts had been produced," and conclude that the Os-Ir-Ru alloys are probably refractory residues of partial melting of peridotites, and hence have been derived from the primitive mantle. BB state that Os-Ir-Ru alloys from British Columbia and the Urals "are almost certainly derived from ultramafics of obducted ophiolites... In fact, almost every known occurrence of these alloys can be argued to have been derived by erosion of peridotites of ophiolites."

Figure IV-8:

Mo vs. Ni plot for chondritic and terrestrial alloys with Os+Ir+Ru > 20 wt.%. For the chondritic alloys, the black stars are analyses from Wark and Lovering (1976), the dots are from Blander et al. (1979), the diamonds from Fuchs and Blander (1980), and the open stars from El Goresy et al. (1979). Many of the chondritic analyses are superposed; e.g., there are two analyses on the origin. For the terrestrial alloys, the diagonally ruled region represents the limits for the Josephine chromitite PGMs (this study), and the horizontally ruled region represents the limits for other terrestrial alloys (Noddack and Noddack, 1931; Genser et al., 1938; Cabri and Harris, 1975; Feather, 1976; Bird and Bassett, 1980; and unpublished analyses of Josephine placer alloys, this author). For the Josephine chromitite Os-Ir-Ru-rich alloys, the upper limit for Mo is the detection limit for energy-dispersive microprobe analyses; no Mo was ever detected. Molybdenum has been determined in very few terrestrial Os-Ir-Ru-rich alloys; the upper limit for Mo in the literature analyses of terrestrial Os-Ir-Ru alloys is inferred from: 1) the ppm levels of Mo found by Noddack and Noddack (1931) in terrestrial Os-Ir-Ru, 2) Bird and Bassett's (1980) failure to find Mo in "detailed" microprobe wavelength scans of Os-Ir-Ru alloys, and 3) the generally high summations (100±1%) found for microprobe analyses of Os-Ir-Ru alloys in which Mo was not determined (e.g., Cabri and Harris, 1975; Feather, 1976).

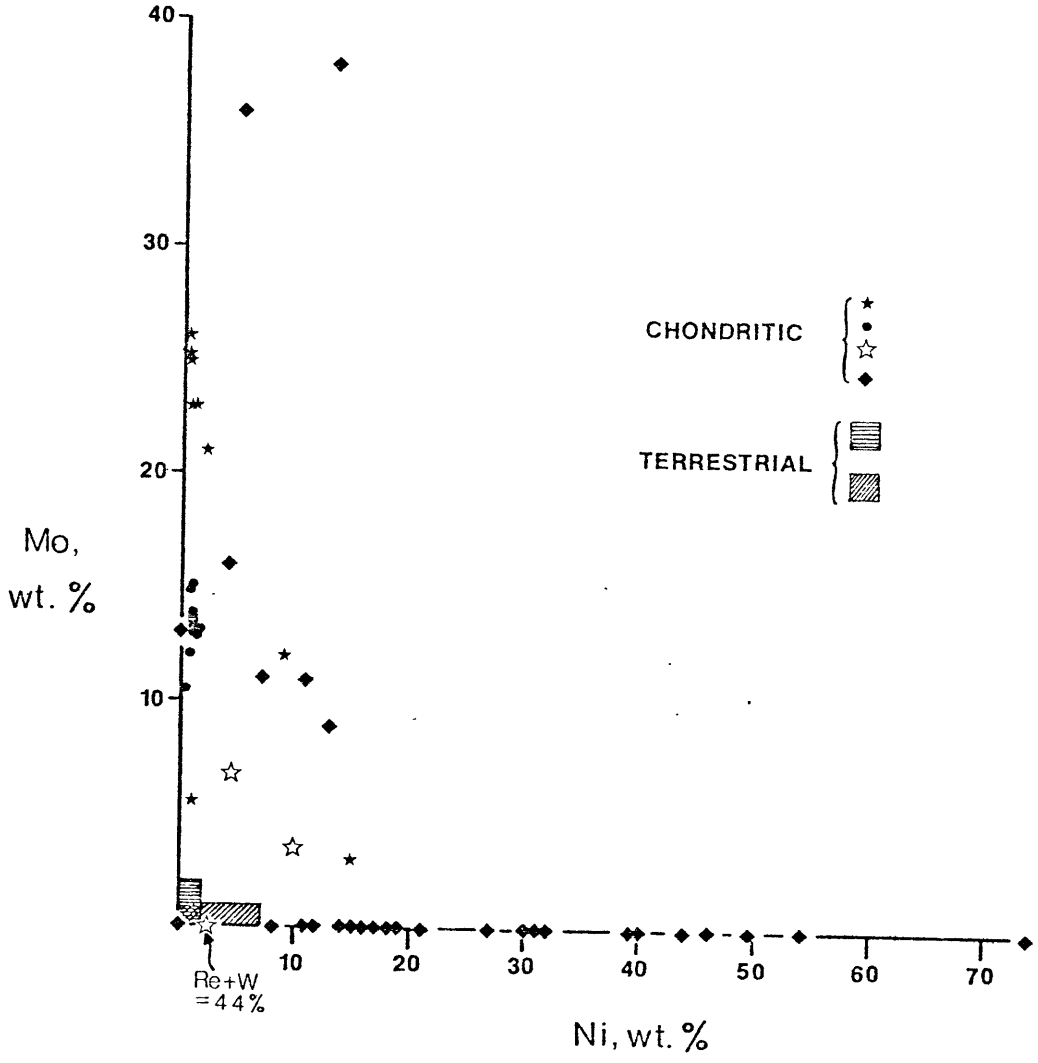
40
30
20
10
Mo,
wt. %
CHONDRITIC
TERRESTRIAL
Re+W
=44%
10
20
30
40
50
60
70
Ni, wt. %

The emphasis BB place on ophiolites and residual peridotites as sources of Os-Ir-Ru alloys is extremely misleading. Many of the Urals Os-Ir-Ru-bearing placers are associated with concentrically zoned (Urals-or Alaskan-type) ultramafic complexes (Cabri and Harris, 1975; Naldrett and Cabri, 1976). Os-Ir-Ru alloys are also found in bedrock in the zoned complexes, typically in chromitites (Razin, 1976). These zoned complexes are widely interpreted as cumulates of magmas (Taylor and Noble, 1969; Murray, 1972; Naldrett, 1973; Irvine, 1974; Carmichael et al., 1974), and not as obducted ophiolites or residues of partial melting. The Tulameen, British Columbia Os-Ir-Ru-bearing placers are also associated with a zoned ultramafic complex (Cabri and Harris, 1975). Even in ophiolitic terrains, it is far from clear that the Os-Ir-Ru alloys in the placers have been derived from residual mantle peridotite. Most reports of bedrock Os-Ir-Ru alloys from ophiolites (Chang et al., 1973; Yu and Chou, 1979; and this study) deal with occurrences in chromitites; ophiolitic chromitites are generally regarded as precipitates of magmas, not as direct residues of partial melting of peridotite (Dickey, 1975; Dick, 1976, 1977; Greenbaum, 1977; George, 1978; Cassard et al., 1981).

Refractory residues of melting versus primitive minerals

BB suggest that Os-Ir-Ru alloys may exist in mantle rocks as refractory residues of partial melting. BB further imply that refractory residues of partial melting are inert minerals which have not been involved in the melting event,

and hence represent "primitive minerals" which existed in the primitive mantle. This is a somewhat distorted view of the partial melting process. "Refractory residues" may be generated during partial melting, and need not have existed in the primitive mantle; for example, incongruent melting of chromian diopside in the upper mantle probably generates chromite (Dickey, 1975), which has a melting temperature in the range of 2,100-2,350C (Muan, 1975). Refractory Os-Ir-Ru alloys might similarly be produced during melting or desulfuration of Os-Ir-Ru-bearing sulfides in the mantle, as suggested in chapter I.

High temperature, high pressure origin

BB base the argument for a high pressure, high temperature origin of Os-Ir-Ru alloys on compositions and textures observed in alloy intergrowths from Port Orford, Oregon. Some of the Port Orford samples consist of randomly oriented, euhedral Os-Ir-Ru lamellae set in a fine-grained Os-Ir-Ru matrix; the matrix and lamellae have different compositions. BB's argument for high pressure, high temperature formation for these samples consists of several points: 1) Interpretation of the textures as the result of peritectic crystallization of lamellae and matrix from an Os-Ir-Ru metal melt. 2) Observation that Os-Ir-Ru alloys melt only at very high temperatures, and inference that the alloys must have formed at high temperatures.
3) Observation that lamellae and matrix compositions are not compatible both with peritectic crystallization and the

1 atm. Os-Ir-Ru phase diagram. 4) Derivation of molar volumes. 5) Conclusion that high pressure should alter the Os-Ir-Ru phase diagram so as to make the observed alloy compositions compatible with peritectic crystallization. This conclusion is based on a comparison of matrix and lamellae molar volumes, as derived in (4).

Points (1), (4), and (5) are considered below.

1) BB note the strong textural evidence for crystallization of the lamellae from a melt. However, there is no direct textural evidence to suggest that the melt which precipitated the lamellae and matrix was molten Os-Ir-Ru metal. It is equally plausible that the lamellae and matrix represent successive precipitates from a lower-melting liquid, for example a sulfide melt. BB object to such an interpretation, stating, "Apparently, the terrestrial alloys are not produced from sulfide melts...(Feather, 1976; Cabri and LaFlamme, 1976; Skinner et al., 1976);" however, this statement does not follow from the cited references or any cogent argument given by BB.

4) This author suspects that BB have misinterpreted the x-ray data used to derive molar volume data for sample Os2. BB state that diffraction patterns for Os2 were obtained by placing the polished microprobe mount at 45° in a Debye-Scherrer camera; the sample could not be rotated. BB state that diffraction lines from the sample "were sufficiently well-defined to permit accurate measurements,"

and that the lamellae "produced fairly sharp, intense diffraction lines." However, given the nature of the sample and the diffraction geometry, it is unlikely that the lamellae could have produced more than a few spots on the film, and would certainly not have produced "well-defined" lines. The number of the lamellae per mm^2 of Os2 surface can be estimated from figure 4 in BB; there are about 200 lamellae/mm^2. Hence, a reasonably well-collimated x-ray beam (0.5mm diameter) would intercept ca. 50 large lamellae on the Os2 surface; the beam would be 99% attenuated within 10μ of the sample surface, and would intercept few additional lamellae (the absorption coefficients of Os-Ir-Ru alloys are very high at commonly used x-ray wavelengths; from data in Liebhafsky et al., 1972). Of these 50 lamellae, only a small fraction would be in a position to diffract without rotation of the sample; probably much less than 10%, unless the crystals were extremely disordered. However, disorder is not indicated, as the lines are said to be "sharp." Of the few x-ray beams diffracted by the lamellae, only about 10-20% could be subtended by the x-ray film. Hence, the lamellae might produce a few spots on the film, but would hardly produce "well-defined" lines; any well-defined lines should be attributed to phases other than the lamellae--perhaps to the fine-grained matrix phases.

5) BB imply that it is possible to predict the shift of a miscibility gap with pressure by comparing the molar volumes of a pair of phases coexisting at the gap (at some P,T), and

applying the rule, "The effect of pressure is to shift the miscibility gap in the direction of the phase with the larger molar volume." This reasoning is not correct. The effect of pressure is to favor a change which lowers the total volume of the system. Because the molar volume of each phase is a function of composition, shifting the miscibility gap toward the phase of large molar volume does not necessarily lead to a decrease in the system volume; this point is illustrated for a hypothetical binary system in figure IV-9. In this system, the average molar volume of a bulk composition X in the miscibilitv gap is given by $\overline{V}_{avg}$ on the tie line PQ. The phase with the larger molar volume at the gap is β; shifting the gap toward β shifts the tie line to P'Q', and results in a new average molar volume of $\overline{V}'_{avg}$, which is larger than $\overline{V}_{avg}$; such a shift is obviously not favored by pressure.

Alteration of PGM sulfides to PGM alloys

BB imply that there are no evidence in the literature for the formation of PGM alloys by alteration of PGM sulfides. This is incorrect; Ramdohr (1980) and Cousins and Kinloch (1976) give evidence for the alteration of PGM sulfides to PGM allovs. This study also gives evidence that PGM allovs may form by reduction of PGM sulfides. Cousins and Kinloch (1976) have pointed out the likelihood of reduction of PGM sulfides to alloys during serpentinization.

Figure IV-9:

Molar volume-composition curves for a hypothetical system A-B, with two phases (α,β) and a miscibility gap, at a given pressure and temperature. $\overline{V}\alpha$ and $\overline{V}\beta$ are the molar volumes for the α and β phases. The vertical unbroken lines give the equilibrium position of the miscibility gap; the molar volume of α at the miscibility gap (point P) is smaller than the molar volume of β at the gap (point Q). The average molar volume at composition X is given by $\overline{V}_{avg}$ on the tie line PQ. Shifting the miscibility gap toward β (to the position of the broken vertical lines) shifts the tie line to P'Q', and causes an increase in the average molar volume, to $\overline{V}'_{avg}$.

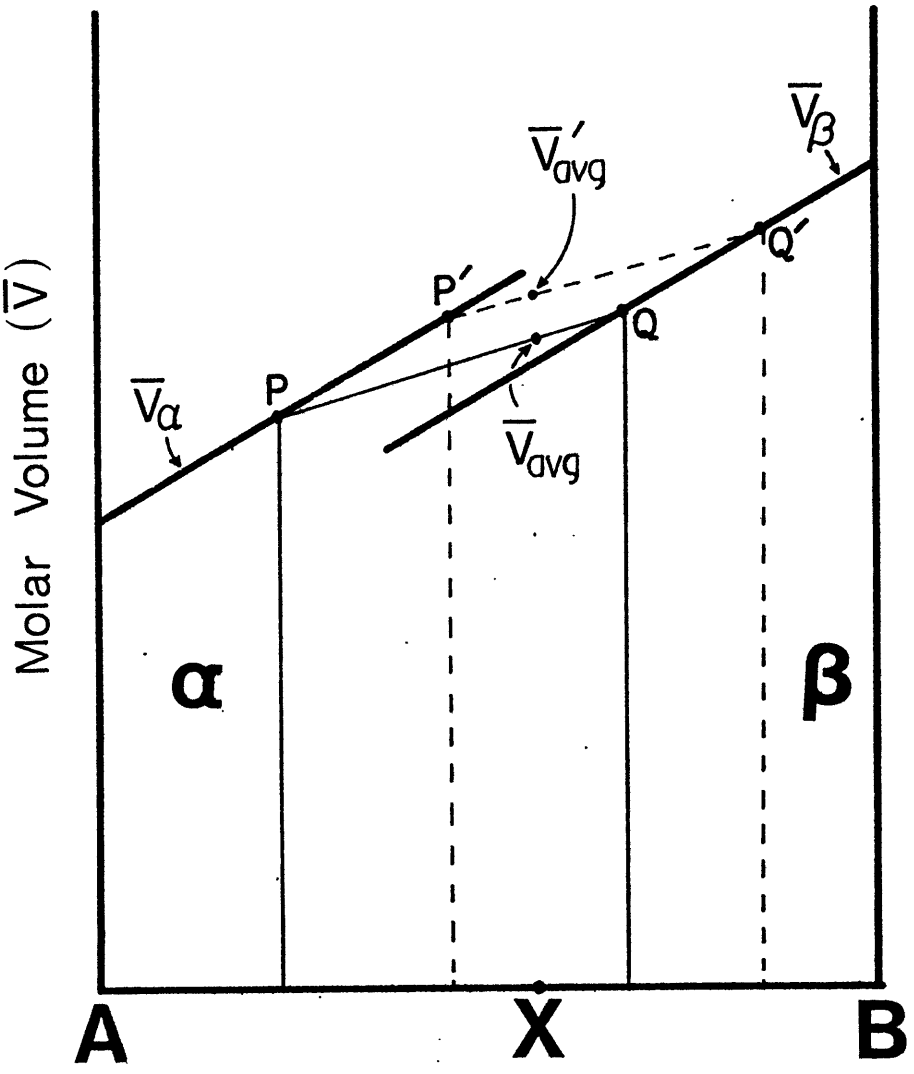
Molar Volume ($\overline{V}$)
$\overline{V}_\alpha$
$\overline{V}'_{avg}$
$\overline{V}_\beta$
P
P′
Q
Q′
$\overline{V}_{avg}$
α
β
A
X
B

Conclusions: primitive mineral and high pressure, temperature origins

It is concluded that: 1) There is no compelling evidence that the terrestrial Os-Ir-Ru alloys are unaltered chondritic material; 2) The conclusion of BB that nearly all terrestrial Os-Ir-Ru alloys are inert residues of partial melting, and not products of crystallization of melts, is tenuous, as most known bedrock occurrences of these minerals are in rocks not generally believed to be residues of partial melting; 3) "Refractory residues" of partial melting need not be primitive minerals; 4) The interpretation of the Port Orford alloy textures given by BB is non-unique; 5) The argument made by BB to infer the high-pressure Os-Ir-Ru phase diagram is incorrect (the molar volume data used in the argument are also questionable); as a consequence, the high pressure-high temperature origin proposed by BB is questionable.

IV-7: SUMMARY: PLATINUM GROUP MINERALS IN THE JOSEPHINE PERIDOTITE

It is concluded that the type 1 PGMs in the Josephine chromitites probably formed by precipitation from melts in the mantle, and the type 2 PGMs probably formed by reduction of type 1 laurites. Some of the Josephine placer PGMs may have been derived from PGM-bearing chromitites. It is plausible that some of the placer PGMs formed in the

Josephine peridotites during partial melting, but PGMs have not vet been found in the peridotites. There is no evidence that the Josephine chromitite PGMs, the Josephine placer PGMs, or any terrestrial PGMs are unaltered "primitive" minerals or formed in the region of the earth's core.

CHAPTER V: CONCLUSIONS AND SUGGESTIONS FOR ADDITIONAL STUDIES

This work provides new information on the abundances of noble metals in the mantle, and the behavior of noble metals during partial melting and subsequent formation of silicate and chromite accumulates. The conclusions of this work are summarized in section V-1. Some of the conclusions could be tested and amplified by studies outside the scope of the present work, and suggestions for future studies are made in section V-2.

V-1: CONCLUSIONS

Noble metal abundances in the primitive mantle

The abundances of Pd, Au, Pt, and Ir in the most fertile Ronda and Josephine peridotites are 0.75-1.5 x 10^{-2}x the abundances in C1 carbonaceous chondrites; these abundances are roughly in agreement with mantle estimates based on lherzolite nodules. It cannot be determined if the mantle noble metal abundances are too high for core-mantle equilibrium until the composition of the core is better known. If the core is dominantly metallic Fe-Ni, then the mantle noble metal abundances are probably too high for core-mantle equilibrium; however, if the core is oxygen-rich, the mantle noble metal abundances may be consistent with equilibrium.

Behavior of noble metals during partial melting

Partial melting produces a fractionation of the noble metals, such that Pd and Au, and possibly Pt, are enriched in the melt phase relative to Ir. It is not clear which phases control the behavior of the noble metals during partial melting. Sulfide is probably the major host of the noble metals in the mantle at temperatures below the solidus of the peridotite silicates, but with the onset of partial melting, sulfide is likely to dissolve into the silicate melt. The dissolution of mantle sulfide may result in the precipitation of refractory Ir alloys, while Pd and Au, which do not form refractory minerals, may dissolve into the silicate melt. Platinum may also dissolve into the silicate melt. Upon cooling of the partially melted peridotite, noble metal-bearing sulfides may reprecipitate from trapped silicate melts.

Noble metal contents of primitive mantle melts

The partial melts derived from the Ronda peridotites were probably picritic to basaltic in major element composition, and had average Pd, Au, and Pt contents of 19, 6, and 24 ppb, respectively. The Ir abundances of the melts are not well constrained, and may have ranged from 0-10 ppb. The Pd, Au, and Pt abundances of the Ronda melts are similar to the abundances found in gabbroic complexes and some continental basalts, but are much higher than the average abundances found in MORBs.

The Ronda mafic layers and the depletion of Pd and Au from partial melts

In the Ronda mafic layers, which are interpreted as successive accumulates of partial melts moving through the mantle, Pd and Au behaved as compatible elements. The compatible behavior of Pd and Au was probably the result of precipitation of sulfide along with the silicates which make up the mafic layers; precipitation of sulfide was probably the result of decreasing pressure and temperature, and the consequent decrease in sulfur solubility in the silicate melts. Sulfide precipitation rapidly depletes Pd and possibly Au from silicate melts, and may be the cause of the low average Pd and Au abundances found in many basalts, such as MORBs.

Origin of Ir-rich chromitites and the effect of chromite precipitation on noble metal fractionation

The positive Ir-Cr correlation in chromitites may result from the progressive depletion of Ir and Cr from partial melts undergoing fractional crystallization in the mantle. The precipitation of Ir-rich chromitites may be a major cause of the fractionation of Ir from Pd and Au in basalts.

Formation of platinum group minerals in the mantle

Platinum group minerals in the Josephine chromitites probably formed in the upper mantle, possibly by direct

precipitation from silicate-sulfide melts; some PGMs may have precipitated from trapped sulfide melts. The primary PGM assemblage of the chromitites formed at conditions of relatively high sulfur activity. Some of the primary platinum group sulfides were later reduced to alloys during conditions of low sulfur activity, possibly during serpentinization. It is likely that chromitites are the sources of some of the PGMs found in the placers of the Josephine Peridotite.

Platinum group minerals may form in ordinary mantle peridotites, perhaps at the point of sulfide depletion during partial melting. However, as of yet there are few confirmed reports of PGMs from ordinary mantle peridotites.

V-2: SUGGESTIONS FOR ADDITIONAL STUDIES

Noble metal abundances of primitive basalts

The noble metal abundances of the primitive Ronda partial melt, derived in this study, are only averages, and do not indicate the full range of melt noble metal abundances possible in primitive partial melts. In addition, the Ir abundance of the Ronda melt is very poorly constrained. An alternative approach to determining the noble metal abundances of primitive partial melts involves analysis of eruptive basalts which closely meet the criteria for primitive partial melts (criteria such as high Mg/Fe, MgO, NiO, Cr, etc.). Basalts suitable for analyses might be the Baffin Island picrites (Clarke, 1970), or "primitive" MORB glasses (Frey et al., 1974). Noble metal analyses of

these basalts would be very useful in constraining the effects of post-partial melting processes on the fractionation of noble metals.

Experimental noble metal paritioning studies

Experimental studies are needed to determine the partitioning of noble metals among silicate melts, sulfide melts, and silicate, oxide and metallic minerals at controlled oxygen and sulfur activities. Experimental partitioning studies would not only help resolve the roles of the different mantle phases in controlling the behavior of noble metals during partial melting and fractional crystallization, but would also aid in determining if the mantle noble metal abundances could reflect equilibrium with the earth's core. In addition, a determination of the solubility of Ir in chromite as a function of oxygen activity, would be useful in resolving the controversies over the relative importance of solid solution versus discrete Ir-rich PGMs in the formation of Ir-rich chromitites and in fractionation of Ir from basalts (e.g., Gijbels et al., 1974; Hertogen et al., 1980; Keays and Campbell, 1981). Studies on the solubility of Ir in sulfide and silicate melts, as a function of sulfur activity and at saturation with Ir-rich PGMs, would also be useful in resolving the controversy over the conditions of formation of Ir-rich PGMs in the mantle (e.g., Bird and Bassett, 1980).

Osmium isotopic studies

Osmium isotopic studies on the PGMs of the Josephine chromitites and Josephine placers would help resolve any possible link between the bedrock and placer assemblages, and would constrain the time of formation of the PGMs. Attempts were made in this study to determine the Os isotopic ratios in laurites from the Josephine chromitites by ion probe; these attempts were unsuccessful, perhaps due to the use of negative ion bombardment and the resultant low ion yield, and the small size of the laurites (5-10μ). The use of positive ion bombardment should improve the ion yield (Allegre and Luck, 1980), as should analysis of recently discovered larger laurite grains (15-30μ).

REFERENCES

Agiorgitis, B. and Wolf, R. (1978) Aspects of osmium, ruthenium and iridium contents in some Greek chromites. Chem. Geol. 23 267-272.

Ahmad, I., Ahmad, S. and Morris, D.F.C. (1977) Determination of noble metals in geological materials by radiochemical neutron-activation analysis. Analyst 102 17-24.

Allegre, C.J. and Luck, J.-M. (1980) Osmium isotopes as petrogenetic and geological tracers. Earth Plan. Sci. Letters 48 148-154.

Arculus, R.J. and Delano, J.W. (1981) Siderophile element abundances in the upper mantle: evidence for a sulfide signature and equilibrium with the core. Geochim. Cosmochim. Acta 45 1331-1343.

Atterer, M., Gedscholde, H., Glauner-Breitinger, G, Glauner, R. and others (1954) Gold. Gmelins Handbuch der Anorganischen Chemie, syst. no. 62, Verlag Chemie.

Baedecker, P.A. and Ehmann, W.D. (1965) The distribution of some noble metals in meteorites and natural materials. Geochim. Cosmochim. Acta 29 329-342.

Balling, J.M. (1965) The free energies of formation of platinum sulfide and ruthenium sulfide. Ph.D. Thesis Mass. Inst. Technology.

Banse, H., Genser, C., Koch, P., Muller, W., von Niedermuller, W., Polutoff, N., Scheider, T. and Thaler, L (1951) Platin. Gmelins Handbuch der Anorganischen Chemie, syst. no. 68, teil A, leif. 6, Verlag Chemie.

Beamish, F.E. and van Loon, J.C. (1972) Recent Advances in the Analytical Chemistry of the Noble Metals, Pergamon Press, Oxford.

Beamish, F.E. and van Loon, J.C. (1977) Analysis of Noble Metals: Overview and Selected Methods, Academic Press, New York.

Becker, R. and Agiorgitis, G. (1978) Iridium, osmium and palladium distribution in rocks of the Troodos Complex, Cyprus. Chem. Erde 37, 302-306.

Bergmann, H., Buschbeck, K.-C., Czack, G., Drechsler, A., Feicht, H., Flachsbart, I., Gagarin, R., Hoffman, H., Iwan-Hiherhaus, L., Keim, R., Rehfeld, K., Skchleitzer-Steinkopf, E., Slawisch, A., Trobisch-Raussendorf, U., Vetter, U., Wagner, J., Wendt, H. (1970) Ruthenium. Gmelins Handbuch der Anorganischen Chemie, Verlag Chemie.

Bird, J.M. and Bassett (1980) Evidence of a deep mantle history in terrestrial osmium-iridium-ruthenium alloys. Jour. Geophys. Res. 85, 5461-5470.

Bishop, F.C., Smith, J.V. and Dawson, J.B. (1975) Pentlandite-magnetite intergrowths in DeBeers spinel lherzolites: review of sulfides in nodules. Phys. Chem. of the Earth 9 323-337.

Blanchard, D.P., Rhodes, J.M., Dungan, M.A., Rodgers, K.V., Donaldson, C.H., Brannon, J.C., Jacobs, J.W., and Gibson, E.K. (1976) The chemistry and petrology of basalts from leg 37 of the Deep-Sea Drilling Project. Jour. Geophysical Research 81 4231-4246.

Blander, M., Fuchs, L.H., Horowitz, C., and Land, R. (1980) Primordial refractorv metal particles in the Allende meteorite. Geochim. Cosmochim. Acta 44 217-223.

Bliss, N.W. and MacLean, W.H. (1975) The paragenesis of zoned chromite from central Manitoba. Geochim. Cosmochim. Acata 39, 973-990.

Brett, R. and Bell, P.M. (1969) Melting relations in the Fe-rich portion of the system Fe-FeS at 30 kbar pressure. Earth Plan. Sci. Lett. 6 479-482.

Brooks, H.C. and Ramp, L. (1968) Gold and Silver in Oregon. Bull. 61 Oregon Dept. Geology Mineral Industries.

Burns, R.G. and Fyfe, W.S. (1966) Distribution of elements in geological processes. Chem. Geol. 1 49-56.

Cabri, L.J. (1972) The mineralogy of the platinum-group elements. Mineral Sci. and Engin. 4 3-29.

Cabri, L.J. (1976) Glossary of platinum-group minerals. Econ. Geol. 71 1476-1480.

Cabri, L.J. and Harris, D.C. (1975) Zoning in Os-Ir alloys and the geological and tectonic environment of the source rocks to the bulk Pt:Pt+Ir+Os ratio for placers. Canadian Mineral. 13 266-274.

Cabri, L.J. and LaFlamme, J.H. (1976) The mineralogy of the platinum-group elements from some copper-nickel deposits of the Sudbury area, Ontario. Econ. Geol. 71 1159-1195.

Carmichael, I.S.E., Turner, F.J. and Verhoogen, J. (1974) Igeneous Petrology McGraw-Hill, Inc. U.S.A.

Cassard, D., Nicolas, A., Rabinovitch, M., Moutte, J., LeBlanc, M., and Prinzhofer, A. (1981) Structural classification of chromite pods in southern New Caledonia. Econ. Geol. 76 805-831.

Chamberlain, J.A., McLeod, C.R., Traill, R.J., and Lachance, G.R. (1965) Native metals in the Muskox Intrusion, Canad. Jour. Earth Sci. 2 188-215.

Chang, P.-K., Yu, C.M., and Chiang, C.Y. (1973) Mineralogy and occurrence of the platinum-group elements in a chromium deposit in northwestern China. Geochimica 2 76-85.

Chou, C-L (1978) Fractionation of siderophile elements in the earth's upper mantle. Proc. Lunar Plan. Sci. Conf. 9th 219-230.

Chyi, L.L. and Crocket, J.H. (1976) Partition of platinum, palladium, iridium, and gold among co-existing minerals from the Deep Ore Zone, Strathcona Mine, Sudbury, Ontario. Econ. Geol. 71 1196-1205.

Clarke, D.B. (1970) Tertiary basalts from Baffin Bay: possible primary magmas from the mantle. Contr. Mineral. Petrol. 25 203-224.

Coish, R.A. and Church, W.R. (1979) Igneous geochemistry of mafic rocks in the Betts Cove ophiolite, Newfoundland. Contr. Min. Petrol., 70 29-39.

Constantinides, C.C. Kingston, G.A. and Fisher, P.C. (1980) The occurrence of platinum group minerals in the chromitites of the Kokkinorotsos chrome mine, Cyprus. Proceedings of the International Ophiolite Symposium, Cyprus, 1979, 93-101.

Cotton, F.A. and Wilkinson, F.R.S. (1972) Advanced Inorganic Chemistry. John Wiley and Sons, New York.

Cousins, C.A. and Kinlock, E.D. (1976) Some observations on textures and inclusions in alluvial platinoids. Econ. Geol. 71 1377-1398.

Craig, J.R. and Scott, S.D. (1974) Sulfide phase equilibria. In: Ribbe, P.H. (ed.) Sulfide Mineralogy. Mineral. Soc. Am. Short Course Notes, Vol. 1.

Crocket, J.H. (1969) Platinum metals. In: Wedepohl, K.H. (ed.) Handbook of Geochemistry Springer-Verlag.

Crocket, J.H. (1979) Platinum-group elements in mafic and ultramafic rocks: a survey. Canadian Mineralogist 17 391-402.

Crocket, J.H. and Chyi, L.L. (1972) Abundances of Pd, Ir, Os, and Au in an alpine ultramafic pluton. 24th International Geological Congress, Section 10. 202-209.

Crocket, J.H. and Teruta, Y. (1977) Palladium, iridium, and gold contents of mafic and ultramafic rocks drilled from the Mid-Atlantic Ridge, leg 37, Deep Sea Drilling Project. Canad. Jour. Earth Sci. 14 777-784.

Crocket, J.H., Keays, R.R. and Hsieh, S. (1967) Precious metal abundances in some carbonaceous and enstatite chondrites. Geochim. Cosmochim. Acta 31 1615-1623.

Crocket, J.H., Keays, R.R. and Hsieh, S. (1968) Determination of some precious metals by neutron activation analysis. Jour. Radioanalyt. Chem. 1 487-507.

Currie, L.A. (1968) Limits for qualitative detection and quantitative determination. Analyt. Chem. 40 586-593.

Das Sarma, B., Sen, B.N. and Chowdhury, A.N. (1965) Platinum and gold contents of granite G-1 and diabase W-1. Econ. Geol. 60 373.

Dick, H.J.B. (1974) Terrestrial nickel-iron from the Josephine Peridotite, its geologic occurrence, associations, and origin. Earth Plan. Sci. Lett. 24 291-298.

Dick, H.J.B. (1976) The origin and emplacement of the Josephine Peridotite of southwestern Oregon. Ph.D. Thesis, Yale University.

Dick, H.J.B. (1977) Partial melting in the Josephine Peridotite I, the effect on mineral composition and its consequence for geobarometry and geothermometry. Am. Jour. Sci. 277 801-832.

Dickey, J.S., Jr. (1970) Partial fusion products in alpine-type peridotites: Serrania de la Ronda and other examples. Miner. Soc. Am. Spec. Paper 3 33-49.

Dickey, J.S., Jr. (1975) A hypothesis of origin for podiform chromite deposits. Geochim. Cosmochim. Acta 39 1061-1074.

Diller, J.S. (1921) Chromite in the Klamath Mountains, California and Oregon. U.S. Geol. Survey Bull. 725 1-35.

Distler, V.V., Malevskiy, A.Yu., and Laputina, I.P. (1977) Distribution of platinoids between pyrrhotite and pentlandite in crystallization of a sulfide melt. Geochem. International v. 14, no. 6 30-40.

Eckstrand, O.R. (1975) The Dumont serpentinite: a model for control of nickeliferous opaque mineral assemblages by alteration reactions in ultramafic rocks. Econ. Geol. 70 183-201.

Ernst, W.G. and Piccardo, G.B. (1979) Petrogenesis of some Ligurian peridotites - I. Mineral and bulk-rock chemistry. Geochim. Cosmochim. Acta 43 219-237.

Fabries, J. (1979) Spinel-olivine geothermometry in peridotites from ultramafic complexes. Contrib. Mineral. Petrol. 69 329-336.

Feather, C.E. (1976) Mineralogy of platinum-group minerals in the Witwaterstrand, South Africa. Econ. Geol. 71 1399-1428.

Feigl. F. (1949) Chemistry of Specific, Selective, and Sensitive Reactions, Academic Press, New York.

Fitzgerald, R. (1973) Electron microprobe instrumentation. In Andersen, C.A. (ed.) Microprobe Analysis. John Wiley and Sons, New York.

Flanagan, F.J. (1976) 1972 compilation of data on U.S.G.S. standards, U.S.G.S. Prof. Paper 840 131-183.

Fleet, M.E., MacRae, N.D. and Herzberg, C.T. (1977) Partition of nickel between olivine and sulfide: a test for immiscible sulfide liquids. Contrib. Miner. Petrol. 65 191-197.

Fleetwood, M.J. (1968) Industrial applications II. In: Belk, J.A. and Davies, A.L. (eds.) Electron Microscopy and Microanalysis of Metals, Elsevier, Amsterdam.

Fominykh, V.G. and Khvostova, V.P. (1970) Platinum content of Ural dunite. Doklady Akad. Nauk SSSR 191 184-185 (translation; original title: O platinonosnosti dunitov Urala; 191 #2, 443-445).

Ford, R.J. (1981) Platinum-group minerals in Tasmania. Econ. Geol. 76 498-504.

Frey, F.A. (1982) Rare earth element abundances in upper mantle rocks. In preparation.

Frey, F.A., Bryan, W.B. and Thompson, G. (1974) Atlantic Ocean floor: geochemistry and petrology of basalts from legs 2 and 3 of the Deep-Sea Drilling Project. Jour. Geophys. Res. 79 5507-5527.

Frey, F.A. and Suen, C.-Y.J. (1982) The Ronda high temperature peridotite: geochemistry and petrogenesis. In preparation.

Fuchs, L.H. and Blander, M. (1980) Refractory metal particles in refractory inclusions in the Allende meteorite. Proc. Lunar Plan. Sci. Conf. 11th 929-944.

Gaudin, M.A. (1939) Principles of Mineral Dressing, McGraw-Hill, New York.

Genser, C., Kotowski, A., Schneider, T., and Polutoff, N. (1938) Platin. Gmelins Handbuch der Anorganischen Chemie, syst. no. 68, teil A, lief 1.

Genthe, F.A. (1853) On a probably new element with iridosimine and platinum from California. Am. Jour. Sci. Arts 2 246.

George, R.P., Jr. (1978) Structural petrology of the Olympus ultramafic complex in the Troodos ophiolite, Cyprus, Geol. Soc. Am. Bull. 89 845-865.

Gijbels, R. (1971) Determination of noble metals by neutron-activation analysis. Talanta 18 587-601.

Gijbels, R., Millard, H.T., Desborough, G.A., and Bartel, A.J. (1971) Neutron activation analysis for osmium, ruthenium, and iridium in some silicate rocks and rock-forming minerals. In: Brunfelt, A.O. and Steinnes, E. (eds.) Activation Analysis in Geochemistry and Cosmochemistry, NATO Advanced Study Institute.

Gijbels, R.H., Millard, H.T., Desborough, G.A., and Bartel, A.J. (1974) Osmium, ruthenium, iridium and uranium in silicates and chromite from the eastern Bushveld Complex, South Africa. Geochim. Cosmochim. Acta, 38 319-337.

Goetzel, C.G. (1949) Treatise on Powder Metallurgy Vol. I Technology of Metal Powders and Their Products, Interscience, New York.

El Goresy, A., Nagel, K. and Ramdohr, P. (1979) Spinel framboids and fremdlinge in Allende inclusions: Possible sequential markers in the early history of the solar system. Proc. Lunar Plan. Sci. Conf. 10th, 833-850.

El Goresy, A. and Ramdohr, P. (1978) Osmium depletion in an Allende inclusion: possible supernova material? Lunar Plan. Sci. 11th, 257-258.

Green, D.H. (1967) High-temperature peridotite intrusions. In: Wyllie, P.J. (ed.) Ultramafic and Related Rocks, Wiley, New York, 212-222.

Green, D.H. and Ringwood, A.E. (1967) The stability fields of aluminous pyroxene peridotite and garnet peridotite and their relevance in upper mantle structure. Earth Plan. Sci. Lett. 3 151-160.

Green, T.E., Law, S.L., and Campbell, W.J. (1970) Use of a selective ion exchange paper in x-ray spectrography and neutron activation. Application to the determination of gold. Analyt. Chem. 42 1749-1753.

Greenbaum, D. (1977) The chromitferous rocks of the Troodos Ophiolite Complex, Cyprus. Econ. Geol. 72 1175-1194.

Griffith, W.P. and Raub, C.J. (1980) Osmium, Supplement Vol. 1. Gmelins Handbuch der Anorganischen Chemie. Springer-Verlag, Berlin.

Griffith, W.P., Raub, C.J. and Raub, E. (1978) Iridium, Supplement Vol. 2. Gmelins Handbuch der Anorganischen Chemie. Springer-Verlag, Berlin.

Grimaldi, F. and Schnepfe, M. (1967) Determination of palladium in the parts per billion range in rocks. U.S. Geol. Sur. Prof. Paper 575-C C141--C144.

Grover, J.E., Lindsley, D.H., and Bence, A.E. (1980) Experimental phase relations of olivine vitrophyres from breccia 14321: The temperature- and pressure-dependence of Fe-Mg partitioning for olivine and liquid in a highlands melt-rock. Proc. Lunar Plan. Sci. Conf. 11th, 179-196.

Gulson, B.L. and Lovering, J.F. (1968) Rock analysis using the electron probe. Geochim. Cosmochim. Acta 32 119-122.

Haffty, J. and Riley, L.B. (1968) Determination of palladium, platinum, and rhodium in geological materials by fire assay and emission spectrography. Talanta 15 111-117.

Hagen, J.C. (1954) Some aspects of the geochemistry of platinum, palladium, and gold in igneous rocks with special reference to the Bushveld Complex, Transvaal. Ph.D. Thesis, M.I.T.

Haggerty, S.E. (1975) The chemistry and genesis of opaque minerals in kimberlites. Phys. Chem. of the Earth 9 295-308.

Hamaguchi, H., Kuroda, R., Tomure, K., Osawa, M., Watanabe, K. Onuma, N. Yasunage, T., Hosohara, K, and Endo, T. (1961) Values for trace elements in G-1 and W-1 with neutron activation analysis. Geochim. Cosmochim. Acta 23 296-299.

Harris, D.C. and Cabri, L.J. (1973) The nomenclature of the natural alloys of osmium, iridium and ruthenium based on new compositional data of alloys from world-wide occurrences. Canad. Mineral. 12 104-112.

Hartford, W.H. (1963) Chromium. In: Kilthoff, I.M. and Elving, P.J. (eds.), Treatise on Analytical Chemistry, Part II, vol. 8. Interscience, New York.

Harper, G.D. (1980) The Josephine Ophiolite - remains of a late Jurassic marginal basin in northwestern California. Geology 8 333-337.

Haughton, D.R., Roeder, P.L. and Skinner, B.J. (1974) Solubility of sulfur in mafic magmas. Econ. Geol. 69 451- .

Hemley, J.J., Montoya, J.W., Christ, C.L., and Hostetler, P.B. (1977) 277 322-351.

Hertogen, J., Janssens, M.-J., Palme, H., and Anders, E., (1980) Trace elements in ocean ridge basalt glasses: implications for fractionation during mantle evolution and petrogenesis. Geochim. Cosmochim. Acta 44 2125-2143.

Hiemstra, S.A. (1979) The role of collectors in the formation of the Bushveld Complex. Canad. Mineral. 17 469-482.

Hillebrand, W.F. and Lundell, G.E.F. (1953) Applied Inorganic Analysis, Second edition, John Wiley and Sons, New York.

Himmelberg, G.R. and Loney, R.A. (1973) Petrology of the Vulcan Peak alpine-type peridotite, southwestern Oregon, Geol. Soc. Am. Bull. 84 1585-1600.

Hoffman, E.L., Naldrett, A.J., van Loon, J.C., Hancock, R.G.V., and Manson, A. (1978) The determination of all the platinum group elements and gold in rocks and ore by neutron activation analysis after preconcentration by a nickel sulfide fire-assay technique on large samples. Analyt. Che. Acta 102 157-166.

Hullinger, F. 91968) Crystal chemistry of the chalcogenides and pnictides of the transition elements. In: Jorgensen, C.K. (ed.) Structure and Bonding 4 Springer-Verlag, New York.

Irvine, T.N. (1967) Chromian spinel as a petrogenetic indicator. Part 2. Petrologic applications. Canad. Jour. Earth Sci. 4 71-103.

Irvine, T.N. (1974) Petrology of the Duke Island Ultramafic Complex Southeastern Alaska, Geol. Soc. Am., Boulder.

Jagoutz, E., Palme, H., Baddenhausen, H., Blum, K., Cendales, M., Dreibus, G., Spettel, B., Lorenz, V., and Wanke, H. (1979) The abundance of major, minor, and trace elements in the earth's mantle as derived from primitive ultramafic nodules, Proc. Lunar Plan. Sci. Conf. 10th 2031-2050.

Jellinek, F. (1972) Sulfides, selenides, and tellurides of the transition elements. In: Sharp, D.W.A. (ed.) Inorganic Chem. Series One vol. 5, pt. 1, 339-396. MTP International Reviews of Science, Butterworths, Oxford.

Jones, J.H. and Drake, M.J. (1981) An experimental approach to core-mantle equilibrium. Abstract, EOS 62 1073-1074.

Juza, V.R. and Meyer, W. (1934) Beitrage zur systematischen Verwandtschafts-lehre. 59. Uber die Sulfide des Rutheniums. Z. Anorg. Chem. 213 273-282.

Katz, A. and Grossman, L. (1976) Intercalibration of 17 standard silicates for 14 elements by instrumental neutron activation analysis, U.S.G.S. Prof. Paper 840 49-57.

Keays, R.R. and Campbell, I.H. (1981) Precious metals in the Jimberlana intrusion, western Australia: implications for the genesis of platiniferous ores in layered intrusions. Econ. Geol. 76 1118-1141.

Keays, R.R. and Crocket, J.H. (1970) A study of precious metals in the Sudbury Nickel Irruptive ores. Econ. Geol. 65 438-450.

Kellogg, A.E. (1922) Platinum in the quartz veins of southwest Oregon. Engineering Mining Jour. 113 1000.

Kemp, J.F. (1902) The Geological Relations and Distribution of Platinum and Associated Metals, U.S. Geol. Survey, Washington.

Kimura, K., Lewis, R.S., and Anders, E. (1974) Distribution of gold and rhenium between nickel-iron and silicate melts; implications for abundance of siderophile elements on the Earth and Moon. Geochim. Cosmochim. Acta 38 683-701.

Knop, O., Huang, C.-H., Reid, K.I.G., Carlow, J.S., and Woodhams, F.W.D. (1976) Chalkogenides of the transition elements. X. X-ray, neutron, Mossbauer, and magnetic studies of pentlandite and the π phases π (Fe, Co, Ni, S), Co_8MS_8, and $Fe_4Ni_4MS_8$ (M=Ru, Rh, Pd). J. Solid State Chem., 16, 97-116.

Koch, P. and Banse, H. (1949) Platin. Gmels Handbuch der Anorgannischen Chemie, syst. no. 68, teil A., lief. 5.

Kubaschewski, O. and Evans, E.L. (1958) Metallurgical Thermochemistry, Pergamon Press, New York.

Kullerud, G. and Yund, R.A. (1962) The Ni-S system and related minerals. Jour. Petrology 3 126-175.

Kurat, G., Palme, H., Spettel, B., Baddenhausen, H., Hofmeister, H., Palme, C., Wanke, H. (1980) Geochemistry of ultramafic xenoliths from Kapfenstein, Austria: evidence for a variety of upper mantle proccesses, Geochim. Cosmochim. Acta 44 45-60.

Larson, H.R. and Elliott, J.F. (1967) The standard free energy of formation of certain sulfides of some transition elements and zinc. Trans. Meallurg. Soc. A.I.M.E. 239 1713-1720.

Lederer, C.M. and Shirley, V.S. (eds.) (1978) Table of Isotopes 7th Edition, John Wiley and Sons, New York.

Liebhafsky, H.A., Pfeiffer, H.G., Winslow, E.H., and Zemany, P.D. (1972) X-rays, Electrons, and Analytical Chemistry. John Wiley and Sons, New York.

Loney, R.A., Himmelburg, G.R. and Coleman, R.G. (1971) Structure and petrology of the alpine-type peridotite at Burro Mountain, California, U.S.A., Jour. Petrol. 12, 245-309.

Loomis, T.P. (1972a) Contact metamorphism of pelitic rocks by the Ronda ultramafic intrusion, southern Spain. Geol. Soc. Am. Bull. 83 2449-2474.

Loomis, T.P. (1972b) Diapiric emplacement of the Ronda high-temperature ultramafic intrusion, southern Spain, Geol. Soc. Am. Bull. 83 2475-2496.

Lundeen, M.T. (1978) Emplacement of the Ronda peridotite, Sierra Bermeja, Spain. Geol. Soc. Am. Bull. 89 172-180.

MacLean, W.H. (1969) Liquidus phase relations in the FeS-FeO-Fe_3O_4-SiO_2 system, and their application in geology. Econ. Geol. 64 865-884.

Malevskiy, A. Yu., Laputina, I.P. and Distler, V.V. (1977) Behavior of the platinum-group metals during crystallization of pyrrhotite from a sulfide melt. Geochem. International, v. 14, no. 5 177-184.

Marhenke, E.R.R. and Sandell, E.B. (1963) Spectrophotometric determination of traces of palladium after coprecipitation with tellurium. Analyt. chem. Acta 28 259-263.

Masson, D.L. (1953) Small Scale Placer Mining, State College of Washington, Pullman, Washington.

Medaris, L.G., Jr. (1972) High pressure peridotites in southwestern Oregon. Geol. Soc. Am. Bull. 83 41-58.

Mertie, J.B. (1969) Economic geology of the platinum metals. U.S. Geol. Survey Prof. Paper 630.

Mitchell, R.H. and Keays, R.R. (1979) Palladium, gold and iridium in mantle minerals: implications for models of magma genesis. Abstract, I.U.G.G., Canberra.

Mitchell, R.H. and Keays, R.R. (1981) Abundance and distribution of gold, palladium and iridium in some spinel and garnet lherzolites: implications for the nature and origin of precious metal, sulfur-rich intergranular components in the upper mantle. Geochim. Cosmochim. Acta 45 2425-2442.

Miyagi, M. and Wayman, C.M. (1966) Martensitic transformations in iron-iridium alloys. Trans. Metallurg. Soc. A.I.M.E. 236 806-811.

Mo, X.-X., Stebbins, J.F. and Carmichael, I.S.E. (1981) The partial molar volume of Fe_2O_3 in silicate liquids and the pressure dependence of oxygen fugacity. Abstract, EOS 62 1065.

Morgan, J.W., Wandless, G.A., Petrie, R.K., and Irving, A.J. (1980) Composition of the earth's upper mantle - I. Siderophile trace elements in ultramafic nodules. Tectonophysics 75 47-67.

Muan, A. (1975) Phase relations in chromium oxide-containing systems at elevated temperatures. Geochim. Cosmochim. Acta 39 791-802.

Muller, O. and Roy, R. (1969) Synthesis and crystal structure of Mg_2PtO_4 and Zn_2PtO_4, Mater. Res. Bull. 4, 39-43.

Muller, O. and Roy, R. (1974) The Major Ternary Structural Families, Springer-Verlag.

Murray, C.G. (1972) Zoned ultramafic complexes of the Alaskan type: feeder pipes of andesitic volcanoes. Geolog. Soc. Am. Memoir 132, 313-335.

Mysen, B.O. and Popp, R.K. (1980) Solubility of sulfur in $CaMgSi_2O_6$ and $NaAlSi_3O_8$ melts at high pressure and temperature with controlled f_{O2} and F_{S2}. Am. Jour. Sci. 280 78-92.

Nadkarni, R.A. and Morrison, G.H. (1974) Determination of the noble metals in geological materials by neutron activation analysis. Analyt. Chem. 46 232-236.

Naldrett, A.J. (1973) Nickel sulphide deposits - their classification and genesis, with special emphasis on deposits of volcanic association. Trans. Can. Inst. Mining Met. 76 183-201.

Naldrett, A.J. and Cabri, L.J. (1976) Ultramafic and related mafic rocks: their classification and genesis with special reference to the concentration of nickel sulfides and platinum-group elements, Econ. Geol. 71 1131-1158.

Naldrett, A.J. and Duke, J.M. (1980) Platinum metals in magmatic sulfide ores. Science 208 1417-1424.

Noddack, I. and Noddack. W. (1931) Die geochemie des Rheniums. Z. physikal chem. 154 207-244.

Noddack, W., Noddack, I., and Bohnstedt, U. (1940) Die Teilungskoeffizienten der Schwermetalle zwischen Eisensulfid und Eisen. I. Z. Anorganische Chemie 244 252.

Obata, M. (1977) Petrology and petrogenesis of the Ronda high-temperature peridotite intrusion, southern Spain. Ph.D. Thesis, M.I.T.

Obata, M. (1980) The Ronda Peridotite: garnet-, spinel-, and plagioclase-lherzolite facies and the P-T trajectories of a high-temperature mantle intrusion, Jour. Petrology 21 533-572.

Oregon Dept. of Geol. and Min. Industries (1942) Oregon Metal Mines Handbook, Bull. 14-C, vol. II, sec. I, 134-135.

Orueta, D. (1917) Estudio geolgico y petrografico de la Serania de Ronda. Mem. Inst. Geol. Espana, 567.

Page, N.J., Johnson, M.G., Haffty, J., and Ramp, L. (1975) Occurrence of platinum group metals in ultramafic rocks of the Medford-Coos Bay 2° quadrangles, southwestern Oregon, U.S.G.S. Miscellaneous Field Studies Map, MF-694.

Page, N.J., Myers, J.S., Haffty, J., Simon, F.O. and Aruscavage, P.J. (1980) Platinum, palladium, and rhodium in the Fiskenasset Complex, southwestern Greenland. Econ. Geol. 75 907-915.

Page, N.J., Rowe, J.J. and Haffty, J. (1976) Platinum metals in the Stillwater Complex, Montana. Econ. Geol. 71 1352-1363.

Palache, C., Berman, H., and Frondel, C. (1944) The System of Mineralogy of James Dwight Dana and Edward Salisbury Dana, Vol. I, Element, Sulfides, Sulfosalts, Oxides. John Wiley and Sons, New York.

Palme, H. and Wlotzka, F. (1976) A metal particle from a Ca, Al-rich inclusion from the meteoriite Allende, and the condensation of refractory siderophile elements. Earth Plan. Sci. Letters 33 45-60.

Pardee, J.T. (1934) Beach Placers of the Oregon Coast, U.S. Geol. Survey Circular 8.

Paul, D.K., Crocket, J.H., and Nixon, P.H. (1979) Abundances of palladium, iridium and gold in kimberlites and associated nodules. In: Boyd, F.R. and Meyer, H.O.A. Proc. 2nd Int. Kimerlite Conf. Vol. 1 272-279.

Peele, R. and Church, J.A. (eds.) (1945) Mining Engineer's Handbook, John Wiley and Sons, New York.

Pehlke, R.D., Mazandarany, F.N., and Radzilowski, R.H. (1975) Solid electrolyte emf cell determination of the standard free energy of Cr_2O_3 and applications to chromium-bearing mineral systems. Geochim. Cosmochim. Acta, 39, 833-845.

Rajamani, V. and Naldrett, A.J. (1978) Partitioning of Fe, Co, Ni, and Cu between sulfide liquid and basaltic melts and the composition of Ni-Cu sulfide deposits. Econ. Geol. 73 82-93.

Ramdohr, P. (1980) The Ore Minerals and their Intergrowth, Pergamon Press, New York.

Ramp, L. (1961) Chromite in Southwestern Oregon, Bull. 52 Oregon Dept. Geol. Mineral Industries.

Raub, C.J. and Raub, E. (1978) Iridium, Supplement Vol. 1, Gmelins Handbuch der Anorganischen Chemie, Springer-Verlag, Berlin.

Raub, E. (1964) Die Ruthenium-Irdium-Legierungen. Z. Metallk. 55 316-319.

Raub, E. and Plate, W. (1961) Die Eisen-Ruthenium-Legierungen. Z. Metallk. 51, 477-481.

Razin, L.V. (1976) Geologic and genetic features of forsterite dunites and their platinum-group mineralization. Econ. Geol. 71 1371-1376.

Reed, S.J.B. (1975) Electron Microprobe Analysis, Cambridge University Press.

Reiswig, R.D. and Dickinson, J.M. (1964) The osmium-iridium equilibrium diagram. Trans. Metallurg. Soc. A.I.M.E. 230 469-472.

Ringwood, A.E. (1975) The Composition and Petrology of the Earth's Mantle, McGraw-Hill, New York.

Ringwood, A.E. (1977) Composition of the core and implications for the origin of the earth, Geochem. Jour. 11 111-135.

Rodden, C.J. (ed.) (1950) Analytical Chemistry of the Manhattan Project, McGraw-Hill, New York.

Roeder, P.L., Campbell, I.H. and Jamieson, H.E. (1979) A re-evaluation of the olivine-spinel geothermometer, Contrib. Mineral. Petrol. 68 325-334.

Roeder, P.L. and Emslie, R.F. (1970) Olivine liquid equilibrium, Contr. Mineral. Petro. 29 275-289.

Rosenfeld, J.L. and Chase, A.B. (1961) Pressure and temperature of crystallization from elastic effects around solid inclusions in minerals? Am. Jour. Sci. 259 519-541.

Rostoker, W. and Dvorak, J.R. (1965) Interpretation of Metallographic Structures, Academic Press, New York.

Rowe, J.J. and Simon, F.O. (1971) Determination of palladium and platinum in geological materials by neutron activation analysis after fire-assay preconcentration. Talanta 18 121-125.

Sack, R.O., Carmichael, I.S.E., Rivers, M., and Ghiorso, M.S. (1980) Ferric-ferrous equilibria in natural silicate liquids at 1 bar. Contrib. Mineral. Petrol. 75 369-376.

Sato, M. (1978) Oxygen fugacity of basaltic magmas and the role of gas-forming elements. Geophys. Res. Lett. 5 447-449.

Shannon, R.D. and Prewitt, C.T. (1969) Effective ionic radii in oxides and fluorides. Acta Cryst. B25 925-946.

Sharp, W.E. (1969) Melting curves of sphalerite, galena, and pyrrhotite and the decomposition curve of pyrite between 30 and 65 kilobars. Jour. Geophys. Res. 74 1645-1652.

Shaw, D.M. (1970) Trace element fractionation during anatexis. Geochim. Cosmochim. Acta, 34 237-243.

Shcherbakov, Y.G. and Perezhogin (1964) Geochemistry of gold, Geochem. International 489-496.

Shilo, N.A., Razin, L.V., and Chubarov, V.M. (1980) The mineralogy of platinum elements genetically related to the alpine-type hyperbasites from the northwestern part of the Asiatic branch of the Pacific tectonic region. In: Proceedings of the 11th Congress of International Mineral. Assoc., 172-184, Nauka, Moscow.

Shima, H. and Naldrett, A.J. (1975) Solubility of sulfur in an ultramafic melt and the relevance of the system Fe-S-O. Econ. Geol. 70 960-967.

Silliman, B. (1873) Platinum and iridosmine, Amer. Jour. Sci. Arts, series 3, v. 6, 132-133.

Simmons, G. and Richter, D. (1976) Microcracks in rocks. In: Strens, R.G.J. (ed.), The Physics and Chemistry of Minerals and Rocks, 117-118.

Skinner, B.J., Luce, F.D., Dill, J.A., Ellis, D.E., Hagan, H.A., Lewis, D.M., Odell, D.A., Sverjensky, D.A., and Williams, N. (1976) Phase relations in the ternary portions of the system Pt-Pd-Fe-As-S. Econ. Geol. 71 1469-1475.

Snetsinger, K.G. (1971) Erlichmanite (OsS_2), a new mineral. Amer. Mineral. 56 1501-1506.

Snetsinger, K.G. (1974) A further occurrence of rutheniridosmine. Canad. Mineral., 12 426.

Stanton, R.L. (1972) Ore Petrology, McGraw-Hill, New York.

Stolper, E., Walker, D., and Hays, J.F. (1981) Melt segregation from partially molten source regions: the importance of melt density and source size region. J. Geophys. Res. 86, 6261-6271.

Suen, C.-Y.J. (1978) Geochemistry of peridotites and associated mafic rocks, Ronda Ultramafic Complex, Spain, Ph.D. thesis, M.I.T.

Sun, S.S., Nesbitt, R.W., and Sharaskin, A.Y. (1979) Geochemical characteristics of mid-ocean ridge basalts. Earth Plan. Sci. Lett. 44 119-138.

Sutton, J.R. (1921) Inclusions in diamond from South Africa, Mineral. Mag., 19 208-210.

Taggart, A.F. (1945) Handbook of Mineral Dressings of Ores and Industrial Minerals, John Wiley and Sons, Inc., New York.

Taylor, H.P., Jr. and Noble, J.A. (1969) Origin of magnetite in the zoned ultramafic complexes of southeastern Alaska. In: Wilson, H.D.B. (ed.), Magmatic Ore Deposits, 209-230, Econ. Geol. Monograph no. 4.

Thayer, T.P. (1969) Gravity differentiation and magmatic re-emplacement of podiform chromite deposits. In: Wilson, H.D.B. (ed.), Magmatic Ore Deposits, Econ. Geol. Mono. 4, 932-946.

Thayer, T.P. (1970) Chromite segregations as petrogenetic indicators. Geol. Soc. S. Africa Spec. Publ. 1 380-390.

Twenhofel, W.H. (1943) Origin of the Black Sands of the Coast of Southwest Oregon, Bulletin 24, Oregon Dept. of Geol. and Mineral Indus.

Uhlig, H.H. (1948) The Corrosion Handbook, Electrochemical Soc., New York.

Urashima, Y. (1974) Ruthenium, a new mineral from Horokanai, Hokkaido, Japan, Mineral. Jour. 7 438-444.

Vermaak, C.F. and Hendriks (1976) A review of the mineralogy of the Merensky Reef, with specific reference to new data on the precious metal mineralogy. Econ. Geol. 71, 1244-1269.

Vincent, E.A. and Crocket, J.H. (1960) Studies in the geochemistry of gold - I. the distribution of gold in rocks and minerals of the Skaergaard intrusion, east Greenland, Geochim. Cosmochim. Acta 18 130-142.

Waff, H.S. and Holdren, G.R., Jr. (1977) The nature of grain boundaries in dunite xenoliths: implications for magma transport in refractory upper mantle material. Geol. Soc. Am. Abstracts with Programs 9 1214.

Walsh, T.J. and Hausman, E.A. (1963) The platinum metals. In: Kolthoff, I.M. and Elving, P.J. (eds.), Treatise on Analytical Chemistry, Part II, vol. 8, Interscience, New York.

Wark, D.A. and Lovering, J.F. (1976) Refractory/platinum metal grains in Allende calcium-aluminum-rich clasts (CARCs): possible exotic presolar material? Lunar Sci. Conf. 7th, 912-914.

Weast, R.C. (ed.) (1978) CRC Handbook of Chemistry and Physics, 59th Edition, CRC Press.

Wells, F.G., Hotz, P.E. and Cater, F.W., Jr. (1949) Preliminary Description of the Geology of the Kerby Quadrangle, Oregon, Bull. 40 Oregon Dept. Geology Mineral Industries.

Winchell, A.N. (1914) Petrology and mineral resources of Jackson and Josephine Counties, Oregon. In: The Mineral Resources of Oregon, Oregon Bureau of Mines and Geology.

Woehler (1869) The occurrence of laurite and diamonds in the native platinum of Oregon (a communication to C.F. Chandler), Amer. Jour. Sci. Arts 48 441-442.

Wold, A. (1971) Platinum metal chalcogenides, In: Rao, U.V. (ed.) Platinum Group Metals and Compounds, Amer. Chem. Soc., Washington, D.C.

Wolf, R. and Agiorgitis, D. (1978) On an unusual platinum element enrichment in chromites fromn Skyros Island, Greece, N. Jb. Miner. Mh. 1 39-41.

Yu, T. and Chou, H. (1979) Ruarsite, a new mineral. Science Bulletin (Peoples Republic of China), 24 310-316.

APPENDIX A: Derivation of the Trapped Melt Equation

Definitions:

F' is the weight fraction of the rock which is melted.

F is the weight fraction of the rock which is removed as melt.

C_l is the concentration of the trace element in the melt.

C_p is the concentration of the trace element in the parent.

C_R' is the concentration of the trace element in the unmelted solid residue.

C_R is the concentration of the trace element in the unmelted residue plus the trapped melt (F'-F).

From mass balance:

$$C_p = C_l F' + C_R' (1-F') \text{ and } C_p = C_l F + C_R (1-F)$$

eliminating C_l,

$$\frac{C_p - C_R' (1-F')}{F'} = \frac{C_p - C_R (1-F)}{F}$$

re-arranging,

$$\frac{C_R}{C_p} = \frac{F'-F + (F-FF') C_R'/C_p}{F' - FF'}.$$

APPENDIX B: Change in Volume on Forming Type 2 Alloys, and the Observed Porosities of Type 2 Alloys

In chapter IV it was hypothesized that the type 2 platinum group alloys formed by removal of sulfur from type 1 platinum group sulfides,* with subsequent addition of Fe and Ni. Such a process should lead to a change in volume for the PGM, and in most cases, the volume should decrease. A decrease in volume could be manifest either by development of a spongy, porous texture (as during commercial reduction of Fe_3O_4 to Fe; Goetzel, 1949), or by shrinkage of the PGM inclusion away from the surrounding chromite, or by both processes.

The change in volume associated with the loss of sulfur and addition of Fe and Ni can be calculated, given the assumptions:

1) The masses of Ru, Os, Ir, and Pt are conserved during the conversion of the sulfide to the alloy.

2) The precursor sulfide contains very little Fe+Ni (this assumption is good if the precursor sulfide is thought to be laurite).

3) The densities of the precursor sulfide and resultant alloy are known.

---

* An analogous hypothesis could be made for the formation of some type 2 PGMs by removal of arsenic from a type 1 arsenide (i.e., sperrylite, $PtAs_2$).

4) The weight fractions of sulfur in the sulfide, and Fe+Ni in the alloys are known.

Let:

V_{ALL} = the volume of the resultant alloy

V_{SUL} = the volume of the precursor sulfide

M_{ALL} = the mass of the alloy

M_{SUL} = the mass of the sulfide

ρALL = the density of the alloy

ρSUL = the density of the sulfide

W^{Fe}_{ALL} = the weight fraction of Fe+Ni; in the alloy

W^{S}_{SUL} = the weight fraction of S in the sulfide

The mass of Ru + Os + Ir + Pt in the sulfide is:

$$M_{SUL} - M_{SUL}\, W^{S}_{SUL}$$

The mass of Ru + Os + Ir + Pt in the alloy is:

$$M_{ALL} - M_{ALL}\, W^{Fe}_{ALL}$$

From assumption (1),

$$M_{SUL} - M_{SUL}\, W^{S}_{SUL} = M_{ALL} - M_{ALL}\, W^{Fe}_{ALL}, \text{ or}$$

$$M_{ALL}\,(1 - W^{Fe}_{ALL}) = M_{SUL}\,(1 - W^{S}_{SUL}) \tag{B-1}$$

From the definition of density,

$$M_{ALL} = \rho_{ALL}\, V_{ALL},\ M_{SUL} = \rho_{SUL}\, V_{SUL} \tag{B-2}$$

Combining (B-1) and (B-2),

$$\frac{V_{ALL}}{V_{SUL}} = \frac{\rho_{SUL}}{\rho_{ALL}} \frac{(1-W^{S}_{SUL})}{(1-W^{Fe}_{ALL})}$$

The fractional decrease in volume informing the alloy from the sulfide is:

$$\frac{\Delta V}{V_{SUL}} = \frac{(V_{SUL} - V_{ALL})}{V_{SUL}} = 1 - \frac{V_{ALL}}{V_{SUL}}$$

hence:

$$\frac{\Delta V}{V_{SUL}} = 1 - \frac{\rho_{SUL}}{\rho_{ALL}} \frac{(1 - W^{S}_{SUL})}{(1 - W^{Fe}_{ALL})} \tag{B-3}$$

In order to calculate $\Delta V/V_{SUL}$ from equation B-3, the composition of the alloy is obtained by microprobe analysis; hence W^{Fe}_{ALL} is obtained directly. W^{S}_{SUL} is calculated by assuming a stoichiometry for the sulfide. The densities of the sulfide and alloy can be estimated by interpolation in table B-1.

As an example, the volume change associated with forming the alloy pictured in figures IV-2a and b, from laurite, is calculated below. The analysis of this alloy in weight fractions is (from table IV-3, analysis #7):

Ru	Os	Ir	Pt	Fe	Ni	TOTAL
0.330	0.172	0.118	0.020	0.343	0.032	1.015

The analysis is normalized to total 1.000:

0.325	0.169	0.116	0.020	0.338	0.032	1.000

hence $W^{Fe}_{ALL} = 0.370$. In order to estimate the density of the alloy, the analysis is converted to mole fractions:

Ru	Os	Ir	Pt	Fe	Ni	TOTAL
0.282	0.078	0.053	.009	0.531	0.047	1.000

The small amount of Ni is treated as Fe in subsequent calculations; i.e., the mole fraction of Fe is taken as

0.578. Similarly, Pt and Ir are treated as Os, and the formula for the alloy is written:

$$(Ru_{0.668}\ Os_{0.332})_{0.422}\ Fe_{0.578}$$

The density of this alloy is approximated by:

$$\rho_{ALL} \approx 0.668 \cdot \rho(Ru_{0.422}\ Fe_{0.578}) + 0.322 \cdot \rho(Os_{0.422}\ Fe_{0.578})$$

The densities of the Ru-Fe and Os-Fe alloys are interpolated from table B-1 to be 10.72 and 16.73, respectively, and ρ_{ALL} is approximately 12.72. By a similar calculation, the density of the precursor laurite ($Ru_{0.668}\ Os_{0.185}\ Ir_{0.126}\ Pt_{0.021}\ S_{2.00}$) is estimated to be 7.32. From stoichiometry, W^S_{SUL} for the laurite is 0.328.

Hence, $\Delta V/V_{SUL}$ is estimated to be:

$$1 - \frac{7.32}{12.72}\ \frac{(1 - .328)}{(1 - .360)} = 0.396$$

or nearly 40% of the original volume. Judging by figure IV-2b, the alloy is roughly 25% void spaces, which could account for most of the volume loss. It is possible that the space now occupied by the magnetite-ferrit-chromite surrounding the alloy was once occupied by laurite, and hence may account for the remainder of the volume change.

Some type 2 PGMs might form with little or no change in volume; an Fe- and Ni-rich Pt alloy from Salt Rock (analysis #11, table IV-3) may provide such an example.

this alloy has several type 2 characteristics, such as an association with radial cracks, high Fe+Ni content, and porosity; however, the porosity is only a few percent of the alloy volume, and the alloy shows no sign of shrinkage. If the precursor PGM is assumed to be sperrylite ($PtAs_2$), the calculated volume decrease is ca. 2.5%, in accord with the observed porosity.

Table B-1: Densities of Platinum Group Compounds

X = mole fraction

ρ in g/cm^3

Ru-Fe[a]

X_{Ru}	ρ
0.0	7.87
0.0	8.16
0.092	8.40
0.11	8.49
0.14	8.74
0.234	9.28
0.30	9.60
1.0	12.41

Os-Fe[b]

X_{Os}	ρ
0.0	7.87
0.2	11.45
0.4	14.33
1.0	22.42

Pt-Fe[c]

X_{Pt}	ρ
0.0	7.87
0.264	11.95
0.50	15.23
0.70	17.57
1.00	21.45

$(Ru,Os)S_2$[b]

X_{Os}	ρ
0.0	6.21
0.5	7.88
1.0	9.57

$PtAs_2$[d]

ρ = 10.78

The density of IrS_2 is assumed equal to that of OsS_2.

a) From x-ray data in Raub and Plate (1961).

b) From x-ray data in Griffith and Raub (1980).

c) From x-ray and pyncometric data in Banse et al. (1951).

d) From x-ray data in Weast (1978).

ACKNOWLEDGEMENTS

Light breaks where no sun shines.

- Dylan Thomas

I gratefully acknowledge the moral support of my wife and parents through 5 1/2 difficult years. I also acknowledge the efforts of my examining committee toward producing an almost readable manuscript. Especially, I would thank my advisor, Fred Frey, for pushing me down the road to completion, and for enlightening me about the structure and purpose of Science.

Financial support for the author was provided by research and teaching assistantships in the Department of Earth and Planetary Sciences at MIT, and by fellowships from the MIT Minerals Institute. Funds for neutron irradiation were provided by the MIT II Reactor. Field work for this study was supported by a Geological Society of America Penrose award, and the MIT Minerals Institute provided funds for glassware and supplies.

Many people provided the author with important instruction and technical assistance. Henry Dick introduced the author to field work in the Josephine Peridotite, and provided many of the samples analyzed in this study; samples from the Ronda Ultramafic Complex were taken from the collections of C.J. Suen, M. Obata, and J.S. Dickey. Professor M.G. Simmons of MIT and K. Motylewski of the Smithsonian Astrophysical Observatory performed wizardry with SEMs, and my wife Christine assisted with radiochemical analyses and drafting.

Fran Doughty typed and re-typed all 1,723.4 versions of the manuscript.

Finally, I would like to thank anyone else I may have forgotten.